Copyright Warning & Restrictions

The copyright law of the United States (Title 17, United States Code) governs the making of photocopies or other reproductions of copyrighted material.

Under certain conditions specified in the law, libraries and archives are authorized to furnish a photocopy or other reproduction. One of these specified conditions is that the photocopy or reproduction is not to be "used for any purpose other than private study, scholarship, or research." If a, user makes a request for, or later uses, a photocopy or reproduction for purposes in excess of "fair use" that user may be liable for copyright infringement,

This institution reserves the right to refuse to accept a copying order if, in its judgment, fulfillment of the order would involve violation of copyright law.

Please Note: The author retains the copyright while the New Jersey Institute of Technology reserves the right to distribute this thesis or dissertation

Printing note: If you do not wish to print this page, then select "Pages from: first page # to: last page #" on the print dialog screen

NJIT
New Jersey's Science & Technology University

The Van Houten library has removed some of the personal information and all signatures from the approval page and biographical sketches of theses and dissertations in order to protect the identity of NJIT graduates and faculty.

INFORMATION TO USERS

This material was produced from a microfilm copy of the original document. While the most advanced technological means to photograph and reproduce this document have been used, the quality is heavily dependent upon the quality of the original submitted.

The following explanation of techniques is provided to help you understand markings or patterns which may appear on this reproduction.

1. The sign or "target" for pages apparently lacking from the document photographed is "Missing Page(s)". If it was possible to obtain the missing page(s) or section, they are spliced into the film along with adjacent pages. This may have necessitated cutting thru an image and duplicating adjacent pages to insure you complete continuity.

2. When an image on the film is obliterated with a large round black mark, it is an indication that the photographer suspected that the copy may have moved during exposure and thus cause a blurred image. You will find a good image of the page in the adjacent frame.

3. When a map, drawing or chart, etc., was part of the material being photographed the photographer followed a definite method in "sectioning" the material. It is customary to begin photoing at the upper left hand corner of a large sheet and to continue photoing from left to right in equal sections with a small overlap. If necessary, sectioning is continued again — beginning below the first row and continuing on until complete.

4. The majority of users indicate that the textual content is of greatest value, however, a somewhat higher quality reproduction could be made from "photographs" if essential to the understanding of the dissertation. Silver prints of "photographs" may be ordered at additional charge by writing the Order Department, giving the catalog number, title, author and specific pages you wish reproduced.

5. PLEASE NOTE: Some pages may have indistinct print. Filmed as received.

Xerox University Microfilms

300 North Zeeb Road
Ann Arbor, Michigan 48106

75-24,623

RUSSO, Onofrio Louis, n.d.
AN INVESTIGATION OF THE OPTICAL ABSORPTION PROPERTIES OF SILICON AS RELATED TO ITS ELECTRICAL CONDUCTIVITY.

New Jersey Institute of Technology, D.Eng.Sc., 1975
Engineering, general

Xerox University Microfilms, Ann Arbor, Michigan 48106

AN INVESTIGATION OF THE OPTICAL ABSORPTION PROPERTIES OF SILICON AS RELATED TO ITS ELECTRICAL CONDUCTIVITY

BY

ONOFRIO LOUIS RUSSO

A DISSERTATION

PRESENTED IN PARTIAL FULFILLMENT OF

THE REQUIREMENTS FOR THE DEGREE

OF

DOCTOR OF ENGINEERING SCIENCE

AT

NEW JERSEY INSTITUTE OF TECHNOLOGY

This dissertation is to be used only with due regard to the rights of the author. Bibliographical references may be noted, but passages must not be copied without permission of the College and without credit being given in subsequent written or published work.

Newark, New Jersey

1975

APPROVAL OF DISSERTATION

AN INVESTIGATION OF THE OPTICAL ABSORPTION PROPERTIES OF SILICON AS RELATED TO ITS ELECTRICAL CONDUCTIVITY

BY

ONOFRIO LOUIS RUSSO

FOR

DEPARTMENT OF ELECTRICAL ENGINEERING

NEW JERSEY INSTITUTE OF TECHNOLOGY

BY

FACULTY COMMITTEE

APPROVED: ______________________________ Chairman

____

____

____

NEWARK, NEW JERSEY

JUNE, 1975

ABSTRACT

The purpose of this study is to demonstrate the feasibility of obtaining the electrical conductivity of band gap semiconductors, by considering the absorption of radiation in the visible region. The experimental evidence confirmed predictions that the conductivities of the silicon samples are related to the horizontal displacement of energy in the absorption curves. The material used in this study was p-doped silicon, although the approach should be valid in general for either elemental or compound semiconductors.

The absorption coefficient for silicon was measured in the radiation region between 2.0 and 3.0 ev. This region above the indirect band gap (≈ 1.1 ev) is where the absorption coefficient is significant (order of 10^5 cm^{-1}), consequently, a reflectance method was considered most appropriate to measure the absorption. Measurements were made on p-doped silicon wafers differing by four orders of magnitude. The nominal values of the resistivities as determined by four point probe measurements were from 0.005 ohm-cm to 50 ohm-cm.

Maxwell's equations are applied for a plane electromagnetic wave propagating in an absorbing, homogeneous, linear medium. The resulting solutions lead to expressions for the real refractive index, n_r, and the extinction coefficient, k. The amount of absorption of radiation in the medium is defined in terms of the absorption

coefficient, α, which is directly proportional to k and inversely proportional to the wavelength, λ.

The value for k as a function of wavelength was measured using a non-normal incidence reflectance method in which the pseudo-polarizing angle was measured. A Bausch and Lomb Grating Monochromator and a Tungsten light source was used for the monochromatic source ($\pm 1\mathring{A}$ at the 50% intensity points). The incident monochromatic light beam was collimated, chopped mechanically by a chopper wheel to produce 3600 HZ, and then reflected from a silicon wafer. The wafer was mounted on a turn-table designed so that the reflected and incident angles were equal to better then five minutes of arc. The reflected light which was elliptically polarized was measured by a photomultiplier assembly. The amplitude of the reflected components in and normal to the plane of incidence was determined by a good grade of polarizer mounted before the photomultiplier entrace slit. Expressions are given which show that only the polarizing angle, θ_p, and the amplitude ratio of reflected components, are necessary to determine k and n_r.

Two theoretical models were assumed in an effort to fit the experimental data. The first attempt was on a semi-classical model in which the charge carriers were considered to be bound elastically with damping to account for dissipation due to collisions. The model, through a proper choice of the damping constants is found to be a reasonable fit to the absorption curve, but only for the region

from 2.0 to 2.5 ev.

The quantum mechanical approach was, as expected, by far the better of the two models chosen. The experimental absorption coefficient curve had the same general shape as the ideal quantum mechanical curve, but higher by an order of magnitude. This discrepancy is explained by the presence of a surface oxide layer and the fact that the quantum mechanical curve was based on an ideal semiconductor.

The absorption coefficient is found to vary as the square of the radiation energy in excess of the indirect band gap, for the entire region between 2.0 and 3.0 ev. There was no evidence that the absorption process was due to direct transitions, even for energies near 3.0 ev. Expressions are derived which indicate that the ratio of two low frequency electrical conductivities are dependent on the effective band shrinkage due to doping and the Fermi level shift. The conductivity σ_2 can be determined by comparing its absorption curve with that of a known σ_1. This is realized by using the horizontal energy displacement between the two curves, ΔE_d, in the derived expression.

Further data taken on clean (etched surfaces) silicon wafers did indicate that direct transitions occurred consistently at 2.48 ev.

ACKNOWLEDGEMENTS

The author is indebted to Dr. K. Sohn, Dr. R. Cornely, Dr. R. McMillan and Dr. M. Natapoff for their encouragement and helpful suggestions.

The author also wishes to thank Dr. J. Pankove of the RCA Laboratories, Princeton and Dr. I. Lefkowitz, City University of New York for their comments and very stimulating discussions.

TABLE OF CONTENTS

CHAPTER PAGE

1. Introduction 1
   1.1 General 1
   1.2 Historical Background 11

2. Theory 15
   2.1 Absorption of Electromagnetic Radiation in Matter .
      (a) Maxwell's equations for electromagnetic waves in semiconductors. 15
      (b) Absorption coefficient and its relationship to the optical constants 18
   2.2 Semi-Classical Model of Absorption of Radiation for Elemental Semiconductors. 22
      (a) General description. 22
      (b) Free carrier absorption. 31
   2.3 Ideal Quantum Mechanical Model for Absorption . . . 32
      (a) Introduction 32
      (b) General absorption formalism 38
      (c) Direct transitions 40
      (d) Indirect transitions 41
   2.4 Actual Quantum Mechanical Absorption. 42
   2.5 Conductivity Determination from Absorption Characteristics 44
      (a) Optical constants of an absorbing medium . . . 44

CHAPTER PAGE

(b) Effect of a surface film on the optical constants. 51

(c) Effect due to band shrinkage and the Fermi level shift. 57

3. Experimental Method. 70

3.1 Apparatus and Method. 70

3.2 Precision of Measurement. 72

3.3 Effect of Photon Flux 77

4. Results. 80

4.1 Comparison of Absorption Models 80

4.2 Dependence of Absorption on Radiation Energy. 89

4.3 Low Frequency Conductivity. 92

5. Discussion 99

6. Conclusion 114

References 116

Appendix A 121

Appendix B 124

LIST OF FIGURES

FIGURE	TITLE	PAGE
1.	Direct Transitions	34
2.	Indirect Transitions	35
3.	Energy Band Diagram for Silicon	37
4.	Reflected and Refracted Wave Vectors	45
5.	Theoretical Reflectance Curves	52
6.	Multiple Reflections in Non-Absorbing Layer	53
7.	Reflectance as a Function of Dielectric Thickness	58
8.	Reflectance as a Function of Metallic Thickness	59
9.	Flat Energy Band Approximation for Silicon	62
10.	Energy Band Comparison	68
11.	Apparatus	71
12.	Effect of Angle of Incidence on Wave Vectors	73
13.	Instrumentation	73
14.	Effect of Surface Film on Measurement of Angle	76
15.	Semi-Classical and Measured Absorption Coefficients	87
16.	Semi-Classical and Measured Refractive Indices	88
17.	Experimental and Quantum Mechanical Absorption Coefficients	90
18.	Absorption Characteristics of Silicon Above the Indirect Gap	93
19.	Absorption Characteristics for Heavily Doped Silicon	95
20.	Absorption as a Function of Energy	97

LIST OF TABLES

TABLE	TITLE	PAGE
1.	Experimental Results	81
2.	Semi-Classical Results	83
3.	Quantum Mechanical Results for Indirect Transitions	84
4.	Quantum Mechanical Results for Direct Transitions	85
5.	Effect of a Surface Layer	109

CHAPTER 1

INTRODUCTION

1.1 General

The purpose of this thesis is to demonstrate that the electrical conductivity of band gap semiconductor materials such as silicon can be determined from its optical contants. The optical constants, namely the real refractive index and the extinction coefficient are a consequence of a complex propagation velocity which is assumed for a plane electromagnetic wave traveling in the medium. A complex propagation velocity is necessary in order to describe the absorption of energy which is inherent in lossy materials.

The effort in the study has essentially been confined to the determination of the electrical conductivity of silicon at radiation wavelengths in the visible spectrum (400-700 nm). An expression for the optical constants is obtained classically using Maxwell's equations for a plane wave propagating in an isotropic, homogeneous, linear medium. It is assumed that any deviations from isotropy and homogeneity will be small and not affect the results. The linearity is satisfied because the field strength of the radiation used for the investigation is small ($E \approx 1$ v-cm^{-1}) compared to values of the electric field in the outermost parts of the atoms where the field is smallest ($E \approx 10^8$v-cm^{-1}). Linearity is here defined as the

condition whereby the properties of the material are independent of the magnitude of the source of excitation.

The optical constants used to determine the electrical conductivity in the visible frequency range are the values measured by a method which will be described in detail in Chapter 2. The real refractive index and the absorption coefficient are determined by measuring the state of polarization in a beam of monochromatic light reflected from a silicon wafer. It is apparent that the technique avoids the use of a physical contact and so has the advantage of eliminating contact potentials and contact resistances which are ever present in any direct contact measuring method.

The justification for the undertaking of this study can best be realized by considering the importance of electrical conductivity measurements for semiconductors and the methods currently used to make these measurements. These methods become difficult to implement when the measurements are made at very low temperatures or at high temperatures. There are at present three basic measurement techniques used to determine the electrical conductivity of semiconductors.

The first is the conventional method where a known current passes through two conductors in contact with the semiconductor surface and the resulting voltage measured across two inner contacts. The method has been successfully employed in determining the conductivity, initially by Pearson and Bardeen [1] and later by Morin and Maita [2].

The current contacts for the samples were applied by the electrolytic deposition of rhodium (Pearson and Bardeen) or by bonding through gold plate with Sb-doped gold wire (Morin and Maita). The voltage contacts are a known distance apart and are made by rhodium pressure contacts. Successful results were obtained by both teams because of the care exercised in the preparation of the samples and the fact that the size and geometric shape imposed no restrictions on the measurement. In general, however, there are several disadvantages to this method:

1. The voltage pressure contacts between a conductor probe and a semiconductor has been shown to result in a contact resistance [3] also called a constriction resistance which is dependent on the contact force and the resistivity of the higher resistivity materials.
2. There also exists minority carrier injection at one of the current carrying contacts which if large enough can effect the potential between the voltage contacts [4]. Injection is present whenever a conductor which if in contact with an n-type semiconductor is made positive with respect to the semiconductor. A detailed discussion of carrier injection is given by Shockley [5].
3. Perhaps the major disadvantage of this method is that metal-semiconductor contacts are usually rectifying in nature [6-8]. A complete picture of a rectifying contact and be obtained only if the surface properties of the semiconductor is also considered. The symmetry and periodicity of the energy band in the bulk of the material is not valid at the surface and this results in allowable

surface energy states for electron energies which normally lie in the forbidden gap. The surface layer, about several lattice constants in thickness (≈10Å), however, is small compared to the mean free path of the carriers.

Surface states with energies in the forbidden band are called Tamm levels and were first considered by Tamm [9]. The theory relating the surface states and its effects on metal-semiconductor contacts was introduced by Bardeen [10-13] in 1947, and experimental evidence on the existence of surface states has been given by Shockley and Pearson [14]. Prior to this time, the semiconductor surface was considered to be electrically neutral and a surface charge existed only when a contact is made between the metal and the semiconductor. This was partly explained by the fact that the materials have different work functions.

The surface properties of semiconductors significantly affect the carrier lifetime and it has been shown experimentally that the hole lifetime increases with temperature for both germanium [15] and silicon [16]. The increased lifetime results in an increased diffusion length which affect the carrier concentration at the contacts when current flows through the semiconductor. The typical room temperature values of L_p are about .02 cm for Silicon and .06 cm for germanium and can vary by better than an order of magnitude for temperature variations of about 50°C from room temperature. The increase for silicon being more pronounced than that for germanium.

The second and perhaps most widely used method is the four point probe technique. This method consists of four sharp needle probes which are placed a fixed distance apart on the flat surface of the material to be measured. A current flows through the outer probes and the voltage is measured across the inner probes. The technique in this method is to keep the probe spacing dimensions small which can ordinarily lead to serious measurement difficulties if care is not taken. The effects of increased carrier concentration at the contacts due to carrier injection is significant when the dimensions are small, because the excess concentration of minority carriers will affect the potential of other contacts resulting in an enhanced conductivity. This injection, however, is prevented or very significantly reduced by good contact which can be accomplished by mechanically lapping the surface on which the probes rest.

The four point probe method which eliminates the disadvantage of metal-semiconductor rectifying contacts and minority carrier injection, also permits measurement of resistivity in samples having a wide variety of sizes and geometric shapes, including small volumes which may be imbedded in a larger semiconductor volume such as an n region. The four point probe method applied to a semi-infinite volume of semiconductor material, for measurements of the semiconductor when the boundaries are conductors and non-conductors has been presented in detail by Valdes [17].

The method, although the most popular, suffers from the disadvantage that measurements for a given conductivity depend on the shape and upon the material on which the semiconductor is lying. The true resistivity value is obtained by an appropriate correction factor which varies with the shape, size and materials adjacent to the boundaries [17].

The third method, although not as popular as the four point probe is commonly used and is a three point technique, in which the potential of the reverse breakdown voltage of the metal-semiconduct point (rectifying contact is measured. The method consists of three probes, two of which are current probes and the other a potential probe which measures the voltage across the depletion layer. A typical application for the three point probe would be in the measurement of an n-type epitaxial layer which is grown on an n+ substrate. The n+ substrate has in general, a much lower resistivity than the n epitaxial layer, so that the major portion of the current flow which is through the substrate results in a substantial potential across the depletion layer. The resistivity of the n layer is determined by increasing the reverse voltage until a voltage breakdown occurs. The breakdown which is a non-destructive avalanche effect depends on the material to be measured, the composition of the points, and the point contact pressure. An expression for the variation of breakdown voltage as a function of resistivity together with the results for the commonly

used Osmium points on n type silicon found by a least sqares computer analysis is available [18]. It has been shown that the depletion width which increases with reverse voltage must be less than the width of the n layer, otherwise the breakdown will be a function of the thickness [19-21].

The basic advantage that the three point probe has over the four point probe is that it is independent of the sample geometry provided that the potential probe is at a distance greater than the depletion width from the reverse biased contact. However, some aspects of this method which are not desirable, include a restricted resistivity range of about one order of magnitude [18-22] (0.1 to 1.0 ohm-cm) and the necessity of a calibration curve. The calibration curve is obtained by measuring the breakdown voltage of non-epitaxial chemically polished samples of known resistivity. This calibration curve of breakdown voltage vs. resistivity is then used to measure the resistivity of epitaxial layers. Also, the three point probe measurement is dependent on probe characteristics such as point material, point radius, point loading and probe spacing.

All of the three contact methods have the advantage that the measurements yield the d.c. or low frequency conductivity directly whereas the new method considered in this thesis will result in an optical conductivity. It will be shown that there is a relationship between the optical conductivity (measured in the visible range of 400-700 nm)

and the value of the low frequency conductivity thereby making this method particularly desirable and unique.

A brief review of the remaining chapters of this thesis will now be presented in an attempt to show a relationship between the various parts of this work. Chapter 2 will consist of the theory necessary to develop the relationship between the optical conductivity as obtained by the optical constants and the low frequency conductivity as determined by the mobility and majority carrier density. Expressions for the optical constants will first be obtained by considering a complex propagation constant in Maxwell's Equations. The Fresnel relationships between the radiation incident on the semiconductor surface and the state of polarization of the reflected waves results in the expressions which determine the optical constants in terms of parameters which are measured experimentally. The electric polarization caused by the displacement of the electrons in the material from their rest positions as caused by the incident radiation field is considered next. This is necessary for rapidly varying fields such as optical fields where the effect of this electric dipole moment is not negligible and does contribute to the electric displacement vector. A solution to the linear differential equation for conditions in which the electric polarization is not negligible is investigated for real resonances which are realized analytically by taking damping conditions into account. The results at the resonant frequency are oscillations of finite amplitude, a consequence of the

introduction of the damping factor. The Clausius-Mossotti relationship is then considered and the resulting expressions for the real refractive index and the extinction coefficients are obtained. These coefficients determine the optical conductivity theoretically which is then compared with the optical conductivity measured by the procedure explained in Chapter 3.

It is found experimentally that the real refractive index agrees favorably with the results obtained by the analytical expression whereas the absorption coefficients determined from measured data deviates somewhat from the values obtained by the analytical expression. This is resolved, however, by the consideration of the band theory of semiconductors, in particular the role played by carriers in making transitions from the valence band to the conduction band caused by the radiation field. The band gap of silicon of about 1.1 ev is less than the photon energies in the visible region which are approximately in the range of 2-3 ev. The findings of this study shows that the measured absorption coefficient at optical frequencies is consistent with theoretical preditions as determined by a treatment of quantum mechanical principles as applied to interband transitions. The theoretical predictions dictate that the absorption coefficient should vary essentially as the square of the photon energy for energies above but near the indirect band gap (1.1 ev) and as the square root of the photon energies near the direct band (2.6 ev).

The experimental procedure described in Chapter 3 essentially is a method using monochromatic radiation in the visible range in a narow collimated beam which is incident on the semiconductor surface. The reflected beam is polarized and preferentially normal to the plane of incidence when the incident radiation angle is at the polarization angle. The semiconductor sample is rotated so that the incident radiation angle can be changed and the reflected radiation observed. The measured angle for which the reflected wave vector (measured as an intensity) normal to the incident plane is a minimum is the polarization angle also called the Brewster Angle. This measured polarization angle and the values of the intensities of both the reflected components parallel and normal to the incident plane are used to determine the refractive index and the absorption coefficient. The procedure is repeated at different wavelengths between 2 and 3 ev and also for semiconductor wafers of different resistivities.

The theoretical and experimental results are included in Chapter 4. The measured values of the index of refraction, absorption coefficient and optical conductivities are shown graphically as a function of photon energy and compared with the expressions for these parameters derived by the phenomenological model using the Clausius-Mossotti relation and the expressions for the absorption coefficient as determined by the Quantum mechanical model. It is shown here that the expressions for the absorption coefficient agrees with the Quantum mechanical model.

The plot in the region between the indirect and direct band gap shows that the absorption coefficient varies as the photon energy raised to a power between one half and two. It is not the aim of this thesis, however, to determine the exact empirical relationship which exists in this region for this would necessitate considerable more data taken over a wider range of wavelengths extending into the infra-red and ultraviolet. The optical region was chosen because of its desirability for instrumentation and convenience for measurement.

The optical conductivity shown to be related to the low frequency conductivity is then compared for different nominal values of low frequency conductivity as measured by a four point probe.

A comparison between the theoretical and experimental results is given in Chapter 4, and a discussion of the results in Chapter 5.

1.2 Historical Background

The classical theory of optical properties of solids which is based on Maxwell's Equations yields the extinction coefficient, k, and the refractive index with its dependence on frequency but does not give an explanation for the frequency dependence. When the frequency is in the optical range, the wavelength of the radiation is only several orders of magnitude greater than the atomic distances. Consequently, an atomic model is necessary in an attempt to explain the results obtained experimentally.

The theory developed by Lorentz [23], in 1880, indicated that a

simple atomic model can account for this frequency dependence. The model assumes that electrons in the material are bound elastically to their equilibrium positions and are also subject to a damping force which is proportional to the velocity. A similar theory developed by Drude [24] and Zener [25] was based on the assumption that the electrons are free and included only a damping term. This theory is most applicable to the case of metals where there are as many free electrons as there are atoms, whereas the Lorentz theory is more general and a better model for semiconductors.

Measurements of the optical parameters for layers of various materials immersed in a medium have been obtained by determining the reflectance at normal incidence [27-29]. The values for germanium was measured in the visible region by O'Bryan [30] using a reflection method not at normal incidence, but his values disagree with the results of Brattain and Briggs [31] who measured transmission through a thin evaporated layer, with the results of other reflectance techniques by Archer [32] and with those obtained by Philip and Taft [33-34]. Results for intrinsic optical absorption in both germanium and silicon were reported by Dash and Newman [35]. The experimental procedure used by Dash and Newman [35] for single crystal material required accurate measurement of the thickness samples which were in the order of about 10 micron, and the measurement of the radiation which was absorbed in transmission. The data taken only for the absorption coefficient was

for wavelengths in excess of 6300 Å.

Archer [32] measured the optical constants for germanium in the range of 3600 Å to 7000 Å and used a non-normal reflectance technique [36] in which it was shown that the optical constants were not dependent on the angle of incidence as had been reported previously [37]. He also showed that the effect of an oxide film of 10 Å would cause a variation from 2% to 30% for the extinction coefficient k and of 0.6% to 5% in the value of the refractive index n.

Thin films which exist on substrates which are in general absorbing are difficult to analyze and approximation techniques are commonly used. The solution to these types of problems are realized by the use of graphical methods. When the film is very thick and absorption appreciable so that multiple reflections are minimized, then standard techniques for measurement on bulk materials may be used [28-29].

Schumann et al [38] measured the optical constants of silicon in the infra-red by using a spectro-photometer modified so as to measure both the reflectance and transmittance at normal incidence. The values for the refractive index n and the extinction coefficient k are measured for carrier concentrations ranging from 10^{15} cm^{-3} to 10^{19} cm^{-3} and for wavelengths extending from 2.5 um to 40 um. The data is then compared to calculations obtained from a theoretical

model [39] which assumes semiclassical free carrier absorption. The data appears to agree with the theoretical model for short wavelengths but deviates substantially at the longer wavelengths.

Measurements to determine the carrier concentrations of silicon [40] using an infra-red He-Ne (3.391 um) Laser as a polarized light source have been made for n type and p type silicon and compared with plasma resonance. The method consists of infra-red radiation which is polarized in the plane of incidence and a detector which measures the reflected radiation so as to determine the polarizing angle which occurs when the reflected wave vector is a minimum.

The values of n and k may be used to calculate the real and imaginary parts of the dielectric constant at any wavelength. The values of the real and imaginary part of the dielectric constant are not independent. The Kramers-Kronig [41-42] relation shows that if n and k are known for all frequencies, the real and imaginary parts of the dielectric constant can be determined at any frequency. This has essentially also been done by Bode [43] and this method to obtain the optical constant has been used by Robinson [44].

CHAPTER 2

THEORY

2.1 Absorption of Electromagnetic Radiation in Matter

(a) Maxwell's equations for electromagnetic waves in semiconductors. The optical properties of semiconductors in general are characterized by a relatively high reflectivity and high absorption of visible radiation. The transmission of wavelengths in this region is small and difficult to detect experimentally unless the material has a thickness of about a wavelength of the radiation. It is therefore more advantageous to obtain the optical properties of semiconductors by a reflectance technique when the frequency of radiation is in the visible range. The optical properties of materials are represented by two constants, namely, the refractive index, n_r, and the extinction coefficient, k.

The electric field of a plane electromagnetic wave of frequency propagating in the position x direction with a velocity v is given by

$$E = E_o \, \varepsilon^{\, i2\pi\nu \, (t - x/v)} \qquad (1)$$

Consider that the velocity of propagation of the wave in a medium is in general

$$v = c/n' \qquad (2)$$

where n' is the complex index of refraction given by the optical

constants n_r and k so that

$$n' = n_r - ik \tag{3}$$

Considering that the radiation is propagating through a homogeneous sample having a permeability μ_a, a permittivity E_a, and a conductivity σ , it is possible to find n_r and k as a function of μ_a, E_a, σ and ν

Using Maxwell's equations for a plane electromagnetic wave in the medium

$$\nabla \cdot D = \rho \tag{4}$$

$$\nabla \cdot B = 0 \tag{5}$$

$$\nabla \times E = -\frac{\partial B}{\partial t} \tag{6}$$

$$\nabla \times H = J + \frac{\partial D}{\partial t} \tag{7}$$

and assuming that the semiconductor is an uncharged homogeneous isotropic and linear medium, then in the charge free region

$$\nabla \cdot D = 0 \tag{8}$$

$$\nabla \cdot E = 0 \tag{9}$$

Taking the curl of (6) and for a linear medium substituting $\mu_a H$ for B

$$\nabla \times (\nabla \times E) = -\frac{\partial}{\partial t} (\nabla \times \mu_a H) \tag{10}$$

Using (7) and (10), substituting $\varepsilon_a E$ for D, $\mu_r \mu_v = \mu_a$, $\varepsilon\varepsilon_o$ for ε_a and the fact that for any vector

$$\nabla \times (\nabla \times E) = \nabla (\nabla \cdot E) - \nabla^2 E \tag{11}$$

then if $\mu_v \varepsilon_o$ is replaced by C^{-2}

$$\nabla^2 E - \frac{\mu_r \varepsilon}{C^2} \frac{\partial^2 E}{\partial t^2} - \mu_r \mu_v \frac{\partial J}{\partial t} = 0 \tag{12}$$

where C is the speed of light, μ is the relative permeability, μ_o is the permeability of free space, ε is the dielectric constant and ε_o is the permittivity of free space. The value of the relative permeability $\mu = 1$ for semiconductors when the excitation frequency is in the visible region. Therefore, the linearity condition assumed which replaces $\mu_a H$ for B is satisfied. The other condition of linearity is to show that J can be replaced by σE. This condition is satisfied in metals where the linear range is large, that is to say, that the range of current densities where $J = \sigma E$ is large. It was indicated theoretically by W. Shockley [45] in 1951, that departures from Ohm's Law for semiconductor is more likely than in metals when subjected to a large electric field. Shockley [45] showed that

$$\left(\frac{\mu_o}{\mu} \right)^4 - \left(\frac{\mu_o}{\mu} \right)^2 = \frac{3\pi}{32} \left(\frac{\mu_o E}{u} \right)^2 \tag{13}$$

where μ is the mobility in an electric field E, μ_o is the small field mobility and u is the velocity of sound in the material.

The variation of μ with the electric field was verified experimentally for n-type germanium by Arthur, Gibson and Granville [46] and the variation was found to agree reasonably well with equation (13). They found that there were observable departures in the mobility in fields as low as 10^3 volt/cm.

The condition necessary for μ to be independent of the electric

field is from equation (13)

$$E << \frac{u}{\mu_o} \tag{14}$$

The smallest value that the right hand side of equation (13) can have is when μ_o is a maximum. This is true for lightly doped silicon when both the minority and majority carriers are significant in determining the mobility. The electron drift mobility μ_n in both n-type and p-type materials is larger than the hole mobility μ_p in both materials, although the ratio of μ_n/μ_p is smaller as the doping increases [47-48]. Selecting μ_n = 1500 cm^2-volt-sec for high resistivity material ($\rho > 50$ ohm-cm) and assuming $u = 5 \times 10^5$ cm/sec for the velocity of sound in silicon, it is found that the value of E must be less than 330 volt-cm^{-1}.

The intensity of the light to be used in the experiment is at a level low enough so that $E << 330$ volt-cm^{-1}. Therefore the mobility and consequently also the conductivity will be assumed to be independent of the electric field. Thus equation (12) becomes

$$\nabla^2 E - \frac{\varepsilon}{C^2}\frac{\partial^2 E}{\partial t^2} - \mu_v \sigma \frac{\partial E}{\partial t} = 0 \tag{15}$$

(b) <u>Absorption coefficient and its relationship to the optical constant.</u> The absorption coefficient can in general be determined by considering how the radiation intensity changes in the medium. This can be found by knowing the value of k which is in turn related to n_r. Therefore, using equations (1) and (15) gives

$$\frac{1}{v^2} = \frac{\varepsilon}{C^2} - i\,\frac{\mu_v \sigma}{2\pi\nu} \tag{16}$$

and from equations (2) and (3)

$$\frac{1}{v^2} = \frac{n_r^2 - k^2}{C^2} - i\,\frac{2n_r k}{C^2} \tag{17}$$

Therefore, equating reals and imaginaries

$$n_r^2 - k^2 = \varepsilon \tag{18}$$

and

$$n_r k = \frac{\mu_v C}{4\pi\nu} \tag{19}$$

Using (18) and (19) and solving for n_r and k gives

$$n_r^2 = \frac{\varepsilon}{2} \quad 1 + [\, 1 + (\frac{\sigma}{2\pi\varepsilon_a\nu})^2 \,]^{1/2} \tag{20}$$

and

$$k^2 = \frac{\varepsilon}{2} \quad [\, 1 + (\, \frac{\sigma}{2\pi\varepsilon_a\nu} \,)^2 \,]^{1/2} - 1 \tag{21}$$

Since $\varepsilon_a = \varepsilon\varepsilon_o$, $\varepsilon_o = \frac{1}{36 \times 10^9}$ farad/meter, $c = 3 \times 10^8$ m/s

and

$$\nu = c/\lambda \tag{22}$$

where λ is the radiation wavelength, then

$$n_r^2 = \frac{\varepsilon}{2} \quad 1 + [\, 1 + (\, \frac{60\sigma\lambda}{\varepsilon} \,)^2 \,]^{1/2} \tag{23}$$

and

$$k^2 = \frac{\varepsilon}{2} \quad [\, 1 + (\, \frac{60\sigma\lambda}{\varepsilon} \,)^2 \,]^{1/2} - 1 \tag{24}$$

where n_r, k, σ and E are all dependent on λ. Also, using the value of C and $\mu_v = 4\pi \times 10^{-7}$ henry/meter, gives using equation (19)

$$\sigma = \frac{n_r k}{30\lambda} \tag{25}$$

The value of the extinction coefficient, k, is related to the absorption constant, α, by considering the available volume power density at a distance x in the material which is due to an incident electric field at the surface. Using (1)

$$\frac{p\ (x)}{p\ (o)} = \frac{\sigma E^2\ (x)}{\sigma E^2\ (o)} = \varepsilon^{-\frac{4\pi\nu k}{C}x} \tag{26}$$

and defining

$$\alpha = \frac{4\pi\nu k}{C} \tag{27}$$

then

$$\frac{p\ (x)}{p\ (o)} = \varepsilon^{-\alpha x} \tag{28}$$

The application of Maxwell's equations for a plane wave propagating in a semiconductor medium has led to the expression for the conductivity given by equation (25). The frequency dependent conductivity given by this expression is called the optical conductivity when the wavelength of the radiation field is in or near the visible spectrum. This value of σ is in general different than the low frequency conductivity σ_o.

The expression for σ_o is determined by considering

$$J_o = \sigma_o E_o \tag{29}$$

and the concept that the current density, J_o, due to the electric field, E_o, is in general determined by two types of carriers which for semiconductors are the electrons and the holes, therefore

$$J_o = q \langle v_e \rangle n + q \langle v_p \rangle p \tag{30}$$

where n is the electron density, p is the hole density, $\langle v_e \rangle$ is the average electron drift velocity, $\langle v_p \rangle$ is the average hole drift velocity, and q, the electronic charge.

The acceleration of both the electrons and holes due to a constant electric field will cause a constant acceleration. The average velocities of both electrons and holes can be expressed as

$$\langle v_e \rangle = \frac{qE_o}{m_e^*} \tau e \tag{31}$$

and

$$\langle v_h \rangle = \frac{qE_o}{m_h^*} \tau h \tag{32}$$

where m_e^* is the electron effective mass, m_h^* is the hole effective mass, τe and τh are electron and hole lifetime respectively.

Using equations (29), (30), (31) and (32)

$$\sigma_o = \frac{nq^2\tau e}{m_e^*} + \frac{pq^2\tau h}{m_h^*} \tag{33}$$

where σ_o as obtained in equation (33) is a well known result.

2.2 Semi-Classical Model of Absorption of Radiation for Elemental Semiconductors

(a) General description. The expression for the conductivity, σ, given by (25) will be used to determine a conductivity by using values of n_r and k measured at a particular value of the wavelength, λ. In addition, the measured value of σ will also be compared to a theoretical wavelength dependent value of σ. Theoretical values for n_r and k using (23) and (24), however, can not be obtained explicitly unless both ε and σ are specified. Expressions for n_r and k which will be independent of ε and σ, will be obtained by considering what appears to be a reasonable theoretical model. The model describes the physical propertities of the medium in terms of constants which can be specified.

All clear transparent materials have normal dispersion characteristics in the visible region. Normal dispersion is the condition whereby the refractive index of a material decreases as the wavelength is increased. The normal dispersion properties of gases was first explained by Cauchy [49, 50] in which the refractive index n_r was shown to be dependent on the wavelength, λ, by

$$n_r = A + B/\lambda^2 + C/\lambda^4 + \ldots\ldots \tag{34}$$

It is usually only necessary to retain the first two terms which gives reasonable agreement with experiment in the visible region, but is not satisfactory in the infra-red region. It is in the cross-over region, where for transparent materials, that the refractive index undergoes an anomalous dispersion. The value of n falls off more rapidly than indicated by (34) until the radiation approaches an absorption band where it is almost entirely absorbed. The refractive index then increases and reaches a peak as the wavelength is increased. A further increase in wavelength results in a decrease in both the refractive index and the absorption coefficient. The absorption band is dependent on the physical properties of the materials and is in general not limited to any particular portion of the frequency spectrum. The peak value of n_r in the anomalous dispersion curve for the semiconductor silicon has been found to be in the visible spectrum at a wavelength of about 4000 Å (3.3 ev) [33] and at about 6000 Å (2.1 ev) for germanium [34].

Clearly, the Cauchy expression which is valid in only a limited normal dispersion region is not applicable for materials such as silicon which exhibit an anomalous dispersion in the visible region. A model which will lead to an appropriate expression for n_r and k as a function of wavelength can be realized by considering that the charge carriers in a substance are bound elastically to the atoms and are caused to vibrate by the exciting electric field of the radiation. Then the restoring force that bounds the electron to its equilibrium position can be considered to be proportional to its displacement.

Damping is also essential in considering an appropriate model because it is necessary to account for the dissipation of energy caused by collisions between carriers and atoms and the emission of radiation due to the vibrating electrons.

The elemental semiconductors such as silicon do not exhibit polar characteristics, that is, they do not in general have a resultant electric dipole moment in the absence of an external electric field. The electric dipole moment in elemental semiconductors is generated when a displacement between the nuclei and electrons is caused by an electric field. Consider that this dipole moment p is given by

$$\vec{p} = \alpha_p \vec{E}' \tag{35}$$

where α_p is the polarizability and E' is the effective electric field in the material acting on the particles. The total electric moment per unit volume P due to N atoms per unit volume is

$$\vec{P} = N\alpha\vec{E}' \tag{36}$$

The expressions for the electric field, E', given by

$$\vec{E}' = \vec{E} + \frac{\vec{P}}{3\varepsilon_o} \tag{37}$$

and for the dielectric constant ε',

$$\varepsilon' = 1 + \frac{P}{\varepsilon_o E} \tag{38}$$

which when used with (36) gives the polarizability α_p as

$$\alpha_p = \frac{3\varepsilon_o}{N} \frac{\varepsilon' - 1}{\varepsilon' + 2} \tag{39}$$

Equation (39) is the Clausius-Mossotti relation.[51,52]. Ordinarily replacing ε' by n_r^2gives the Lorentz-Lorenz conditions [53,54] whereas in this study it will be assumed that ε' be replaced by n'^2 so that

$$\alpha_p = \frac{3\varepsilon_o}{N} \frac{n'^2 - 1}{n'^2 + 2} \tag{40}$$

where ε' is considered to be complex in general. It follows from (16) that ε' can be represented by

$$\varepsilon' = \varepsilon - i \frac{\sigma\lambda}{2\pi} \frac{\mu_v}{\varepsilon_o} \tag{41}$$

Assuming that the carriers of charge, q, are acted on by a Lorentz force, $\vec{F}$, where

$$\vec{F} = q (\vec{E}' + \vec{v} \times \vec{B}) \tag{42}$$

and if the contribution due to the magnetic field can be neglected, then

$$\vec{F} = q\vec{E}' \tag{43}$$

Equation (43) is a valid approximation for a semiconductor because the velocities of the carriers in a non-degenerate semiconductor can be considered to essentially have a maxwellian distribution.

Consequently, the average energy of the carriers at room temperature is small resulting in a carrier velocity which is small when compared to the speed of light.

The differential equation which describes the motion of the electron when subjected to an electric field E' is

$$m^* \frac{d^2\vec{y}}{dt^2} + g\frac{d\vec{y}}{dt} + a\vec{y} = q\vec{E}' \tag{44}$$

where m* is the effective mass of the carrier, g is the damping constant and a the elastic constant. If the electric field of angular frequency, ω, producing a dipole in the medium is given by

$$\vec{E}' = \vec{E}_o' e^{i\omega t} \tag{45}$$

then the solution to equation (44) becomes

$$\vec{y} = \frac{q\vec{E}'}{m^* (\omega_o^2 - \omega^2) + i\omega g} \tag{46}$$

where ω_o is given by

$$\omega_o^2 = \frac{a}{m^*} \tag{47}$$

Realizing that each electron contributes a dipole moment $\vec{p}$ such that

$$\vec{p} = q\vec{y} \tag{48}$$

then using (48), (35) and (36) gives the polarizability

$$\alpha_p = \frac{q^2}{m^* (\omega_o^{\,2} - \omega^2) + i\omega g} \tag{49}$$

and an appropriate expression in terms of the complex refractive index, n', can be obtained by the use of (40) and (49) so that

$$\frac{n'^2-1}{n'^2+2} = \frac{Nq^2}{3\varepsilon_o m^* \omega_o^{\,2}} \; \frac{1}{1 - (\frac{\omega}{\omega_o})^2 + i(\frac{g}{m^*\omega_o})\,(\frac{\omega}{\omega_o})} \tag{50}$$

when the low frequency conductivity is given by

$$\sigma_o = \frac{Nq^2\tau}{m^*} \tag{51}$$

where τ is the mean free time and also called the relaxation time, then (50) can be expressed in terms of the low frequency conductivity.

The value of the conductivity σ_o is found by considering the limit of equation (5) as the frequency approaches zero. Because it is known that k approaches zero rapidly as ω decreases then

$$\sigma_o = 3\varepsilon_o \tau \omega_o^{\,2} \, \frac{n_{ro}^{\,2}-1}{n_{ro}^{\,2}+2} \tag{52}$$

where n_{ro} is the low frequency refractive index.

Defining ψ_o by

$$\psi_o \equiv \frac{n_{ro}{}^2-1}{n_{ro}{}^2+2} \tag{53}$$

So that from equation (50) becomes

$$\frac{n'^2-1}{n'^2+2} = \frac{\psi_o}{1-(\frac{\omega}{\omega_o})^2 + i\,(\frac{g}{m^*\omega_o})\,(\frac{\omega}{\omega_o})} \tag{54}$$

and solving for n'^2

$$n'^2 = \frac{1 + 2\,\psi_o - (\frac{\omega}{\omega_o})^2 + i2\delta\,(\frac{\omega}{\omega_o})}{1-\psi_o - (\frac{\omega}{\omega_o})^2 + i2\delta\,(\frac{\omega}{\omega_o})} \tag{55}$$

where a new damping constant δ is defined as

$$\delta = \frac{g}{2m^*\omega_o} \tag{56}$$

Because the energy of the radiation is proportional to the frequency, an expression for n' as a function of the photon energy can be obtained from equation

$$n'^2 = \frac{1 + 2\psi_o - (\frac{E}{E_o})^2 + i2\delta\,(\frac{E}{E_o})}{1-\psi_o - (\frac{E}{E_o})^2 + i2\delta\,(\frac{E}{E_o})} \tag{57}$$

Using equations (3) and (57) and equating real and imaginary terms yields

$$n_r^2 + k^2 = \frac{[1 + 2\psi_o - (\frac{E}{E_o})^2][1 - \psi_o - (\frac{E}{E_o})^2] + (2\delta)^2 (\frac{E}{E_o})^2}{[1 - \psi_o - (\frac{E}{E_o})^2]^2 + (2\delta)^2 (\frac{E}{E_o})^2} \quad (58)$$

$$n_r k = \frac{3\delta\psi_o (\frac{E}{E_o})}{[1 - \psi_o - (\frac{E}{E_o})^2]^2 + (2\delta)^2 (\frac{E}{E_o})^2} \quad (59)$$

The experimental data yields values of n_r and k for photon energies between 2 and 3 ev. Inspection of equations (58) and (59) shows that the values of n_r and k both measured at two different wavelengths will determine E_o and δ which will completely specify n_r and k in terms of only determined coefficients and the photon energy. Therefore, a theoretical expression for the optical conductivity based on the assumed physical model can be obtained and compared with the optical conductivity determined by equation (25). The values of n_r and k used in equation (25) will be the measured values. This comparison will be considered in detail in Chapter 4.

It can be seen from equation (52), that the conductivity σ_o can be determined if the relaxation time τ is also known. A relationship for the relaxation time of polar molecules in liquids as given by Debye [55] for an assumed complex polarizability is

$$\alpha_d = \frac{\alpha_{do}}{1 - i\omega\tau_d} \quad (60)$$

where α_{do} is the static polarizability and τ_d is the dielectric relaxation time. The polarizability given by equation (49) of this study, however, is not of the same type of relaxation behavior because of a resonance condition. Rewriting equation (49) gives

$$\alpha_p = \frac{\frac{q}{m^*\omega_o^2}}{1 - (\frac{\omega}{\omega_o})^2 + i\omega\tau_r} \tag{61}$$

and by the use of (47) and (56) τ_r is given by

$$\tau_r \cong \frac{g}{m^*\omega_o^2} = \frac{2\delta}{\omega_o} \tag{62}$$

and τ_r defined as the recovery time is the time interval necessary for the disturbed system to revert to its initial equilibrium condition. Although the recovery time is not defined in the same way as the relaxation time, there does appear to be a relationship between the two.

Experimentally, the values of k in the optical range for silicon will be shown by this study to vary considerably for different values of doping whereas the refractive index remain relatively independent of doping. An increase in the impurity concentration leads to a less ideal crystal structure and so an increase in the damping constant δ. A relationship which exists between a variation in k and a variation

in δ can be obtained by differentiating (59).

The theoretical model proposed by the expression given in equation (44) which may be valid in certain regions should not be expected to account for the complete absorption spectrum of band gap semiconductors especially for radiation energies near the band gap. The model, however, for conditions under which the elastic constant is negligible and only a damping term is considered does account for free carrier absorption.

(b) Free carrier absorption. When the frequency of the excitation is lower than the band gap of the semiconductor, then quantum mechanically interband transitions are not possible and the value of α as determined by the Drude theory of free carrier absorption [56] is given by

$$\alpha_{fc} = \frac{q^2 N \quad \tau_f}{n_r m^* c \varepsilon_o \ (1 + \omega^2 \tau_f{}^2)} \tag{63}$$

where τ_f is the relaxation time given by

$$\tau_f = \frac{m^*}{g} \tag{64}$$

For $\omega\tau_f >> 1$, the absorption coefficient, α has been observed for p-type silicon to obey the λ^2 law very well [57]. However, the relationship is no longer valid for energies near and above the band edges where (63) predicts a decreasing α with frequency whereas

experimentally the value of α increases with frequency in this range.

2.3 Ideal Quantum Mechanical Model for Absorption

(a) Introduction. Absorption of electromagnetic radiation in the optical region for semiconductors can be divided into four basic groups:

1. Free carrier absorption by either electrons or holes.
2. Fundamental absorption due to transitions of electrons from the valence to the conduction band.
3. Absorption due to lattice and impurity scattering and that caused by the excitation of band carriers.
4. Absorption due to transitions of electrons between trapping levels which exist within the forbidden energy gap.

The absorption indicated by group 4 is very significant in real semiconductors but is very difficult to analyze in detail because of the complexity of the trapping structure within the band gap. It will, therefore, not be considered in this study. Absorption of radiation by the processes of groups 1 and 3 have already been discussed with the exception of impurity scattering which becomes important only at low temperatures. The most important absorption process, however, particularly at the band edge is the fundamental absorption process. When the wavelength of the incident radiation is large enough so that electrons can not be excited from the valence to the conduction band,

then the interaction between the carriers and the radiation field can be treated by using classical electromagnetic theory as has already been done. However, if the radiation is such that its energy is greater than the energy gap of the semiconductor, then the absorption coefficient does increase very rapidly as has been observed experimentally. This fundamental absorption takes place when the energy of a photon is greater than the band gap. However, there are two basic types of transitions by which an electron can be excited to the conduction band; a direct transition and an indirect transition. A direct transition is one in which the electron which is excited to the valence band by only the absorption of a photon conserves the crystal momentum. This is indicated on an energy E versus wavevector k_c diagram by vertical transitions in which the wavevector k_c for the conduction band is the same as the wavevector k_c for the valence band. For silicon this transition is more probable for k_c=o although other values of k can also cause direct transitions. In general, the energy of the photon is given by

$$h\nu = E_f - E_i \tag{65}$$

where E_f is the final electron energy and E_i is the initial electron energy. This type of transition is shown in figure 1. An indirect transition is also possible and this occurs when energy is supplied

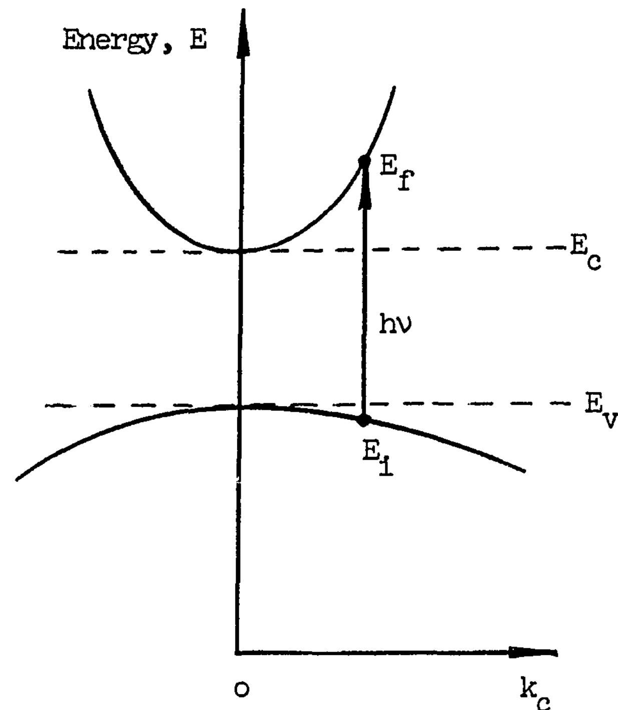

Figure 1.—Direct Transitions between the initial state of an electron in the valence band, E_i, and the final state in the conduction band, E_f. The quantity k_c is related to the crystal momentum, P, by $P = hk_c$.

Note: The behavior of an electron in a periodic potential of a crystal lattice was first considered by F. Block†. The quantity k is not proportional to the momentum of the electron, p, which is not constant in a periodic potential. The quantity, P, the crystal momentum is a constant of the motion of the electron and is equal to the real momentum, p, only when the potential is a constant.

† F. Block, Z. Phys. (1928), 52, 555.

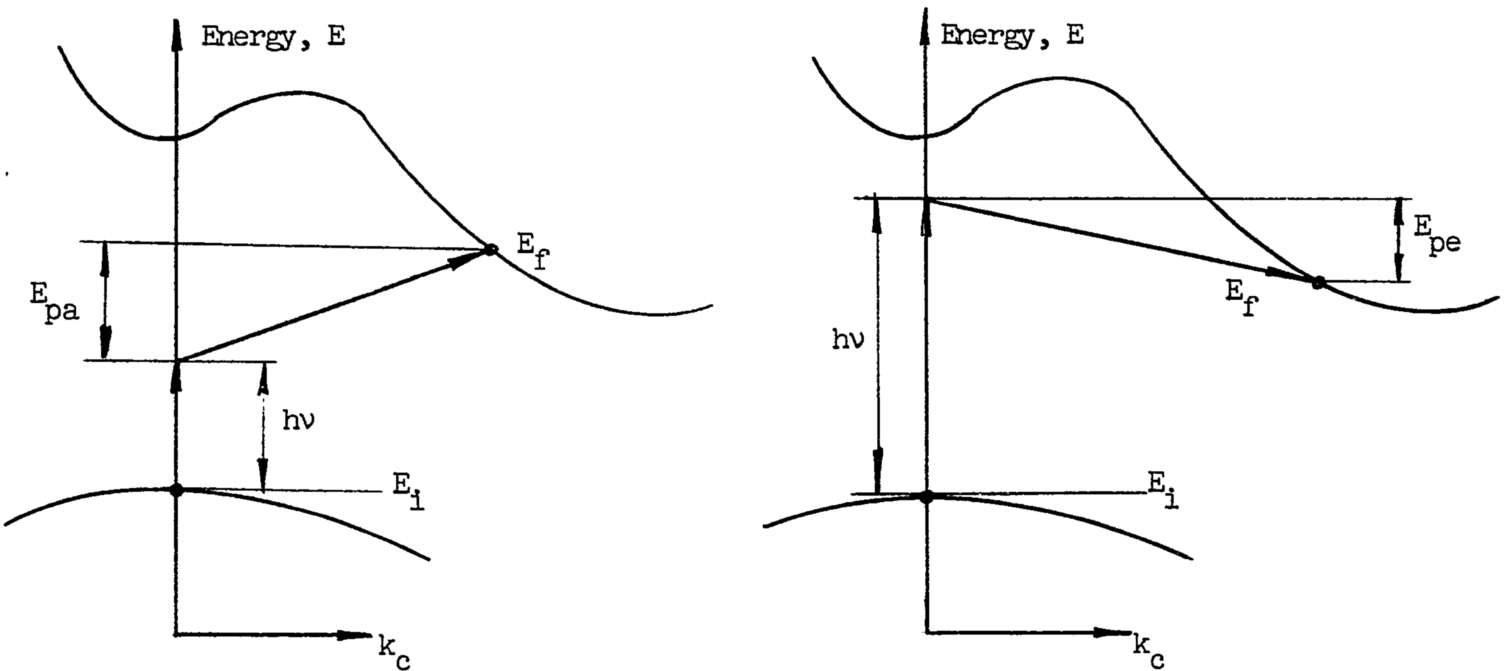

Figure 2.—Indirect Transitions for electrons in the valence band which are excited to the conduction band by (a) the absorption of a phonon and (b) the emission of a phonon.

or absorbed by the lattice vibrations when a photon is absorbed by the electron. The transitions are then non-vertical and involves both a change in energy and momentum so that either an absorption of emission of a phonon is necessary in order to conserve the momentum or the crystal. The phonon absorption energy E_{pa} and the phonon emission energy E_{pe} necessary for the indirect transition are given by equations (66) and (67) respectively and the process is shown in figure 2.

$$E_{pa} = E_f - E_i - h\nu \qquad (66)$$

$$E_{pe} = h\nu - (E_f - E_i) \qquad (67)$$

The calculation of energy bands in solids have been sucessfully obtained for germanium and silicon by Herman [58] and Cardona and Pollack [59]. Herman [60] indicated theoretically that a minimum for silicon should occur at $k_c = o$ and another along the [100] direction. Experimental evidence appears to confirm that the theoretical calculations are valid [61]. An energy band structure for silicon in which only two energy levels for each band are shown is illustrated in figure 3. The bands shown in figure 3 indicate that both the valence and conduction bands are doubly degenerate at $k_c = (000)$. The degeneracy as related to energy bands is defined as the condition which exists when the minima or maxima of bands occur for the same value of k. The effective mass of a carrier in these bands is in

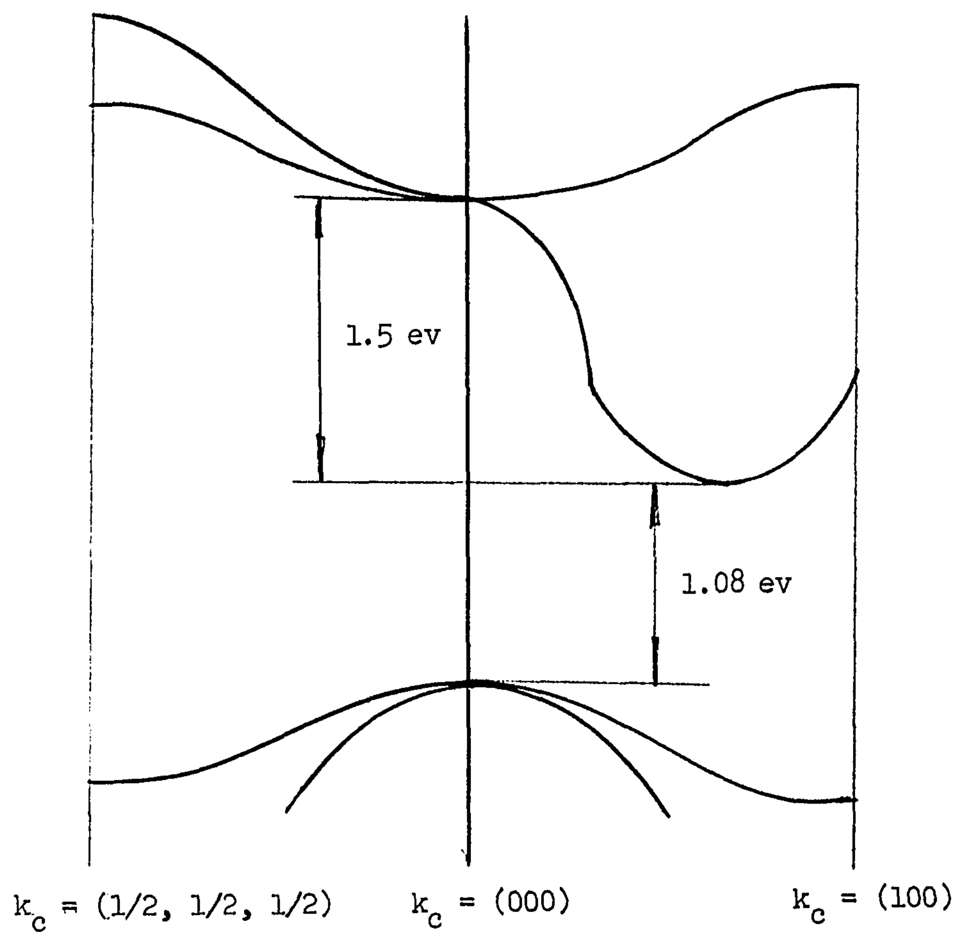

Figure 3.—The energy band diagram for silicon showing only two energy levels in each band.

general dependent on the energy band. The effective mass, m^* is defined as

$$m^* = \frac{h^2}{\frac{d^2E}{dk_c^{\,2}}} \tag{68}$$

So that the energy bands with greater curvature will result in effective masses which are lighter than those bands which exhibit a gradual energy change. The electron and hole effective masses are determined experimentally by a cyclotron resonance method. The method was suggested by Dorfman [62], by Dingle [63] and by Shockley [64] and applied experimentally by Dresselhaus, Kip and Kittel [65]. The results of cyclotron resonance yield defferent effective masses for holes in the valence band and different effective electron masses in the conduction band. However, in this study for purposes of clarity, an average effective mass will be used for each carrier.

(b) General absorption formalism. The process by which electrons make transitions across the energy gap is a quantum effect and is explained by wave mechanics. When the methods of perturbation theory are used, it is imperative that the interaction term in the Hamiltonian formalism be small so that if H is the Hamiltonian then

$$H = H_o + H_{jk} \tag{69}$$

then $H_{jk} << H_o$ where H_o is the ideal Hamiltonian whose solutions are well known and H_{jk} is the term involving the interaction. Under these conditions and assuming H_{jk} is time dependent, the transition rate from state j to state k as given by first order time dependent perturbation theory and commonly referred to as Fermi's Gold Rule Number 2 [66] is

$$w = \frac{2\pi}{h} | H_{jk} |^2 \frac{dn}{dE} \tag{70}$$

where w is the transition rate which is in units of $m^{-3} - s^{-1}$ and $\frac{dn}{dE}$ is the energy density of final states.

When the transitions are caused by the interaction of an electromagnetic wave with an electron, the interaction term in the Hamiltonian as given by the matrix element H_{jk} is

$$H_{jk} = \frac{q\vec{E}}{2\pi m^* \nu} \cdot pe^{-i\vec{K}\cdot\vec{r}} \tag{71}$$

where $\vec{K}$ is the wave vector of the radiation field and p the momentum operator of the electron.

The absorption coefficient α is the quantity which determines the energy removed per unit time per unit volume from a radiation beam of unit intensity. From the relationship

$$dI = - I\alpha dx \tag{72}$$

where I is the intensity which is the energy density times the flow velocity, then

$$\alpha = \frac{h\nu w}{(\frac{1}{2}\varepsilon_a E^2)\ \frac{c}{n'}} \tag{73}$$

So that using (18), (70) and (73)

$$\alpha = \frac{2n'h\nu}{\varepsilon_o\ (n_r^{\ 2} - k^2)\ cE^2}\ \frac{2\pi}{h}\ |H_{jk}|^2\ \frac{dn}{dE} \tag{74}$$

where the units of α are in m^{-1}.

(c) Direct transitions. If the assumption is made that all of j states are filled and all the k states empty, then the expression for α when the wave vector of the radiation $\vec{K}$ is small compared to the wave vector k_1 of the electron is given [67] for direct allowed transitions ($k_c = o$) by

$$\alpha_{da} = \frac{q^2\ (2m_r*)^{3/2}\ n'}{\pi\ (n_r^{\ 2} - k^2)\ \varepsilon_o c m^* h^2}\ (h\nu - E_{gd})^{1/2} \tag{75}$$

where m_r* is the reduced mass of the electron-hole pair and E_{gd} the direct energy gap.

When quantum mechanical selection rules forbid direct transitions at $k_c = o$ but does allow them for $k \neq o$, then the absorption is given

by [68] is

$$\alpha_{df} = \frac{A_f \ (h\nu - E_{gd})^{3/2}}{h\nu} \tag{76}$$

(d) Indirect transitions. Transitions which take place by the absorption of a photon and the emission or absorption of a phonon at the same time are called indirect transitions. Second order perturbation theory necessary to determine the absorption coefficient was used for the indirect transition and expressions for α were obtained [69]. The expression for α when k_{cv} (k_c in the valence band) is different from k_{cc} (k_c in the conduction band) was shown [70] to be for phonon absorption

$$\alpha_a = \frac{A \ (h\nu - E_g + E_p)^2}{e^{Ep/Kt} - 1} \quad \text{when } h\nu > E_g - E_p \tag{77}$$

$$= \quad o \quad \text{when} \quad \leq E_g - E_p$$

and for phonon emission by

$$\alpha_e = \frac{A \ (h\nu - E_g - E_p)^2}{1 - e^{-Ep/Kt}} \quad \text{when } h\nu > E + E_p \tag{78}$$

$$= \quad o \quad \text{when } h\nu \leq E + E_p$$

The absorption coefficient α_i is the sum of these two coefficient so that

$$\alpha_i = \alpha_a + \alpha_e \tag{79}$$

Indirect transitions may take place also when $k_{cv} = k_{cc}$, then the transition is called a forbidden transition and the absorption coefficient α_{af} is given by

$$\alpha_{af} = \frac{B\ (h\nu - E_g + E_p)^3}{e^{Ep/Kt} - 1} \tag{80}$$

2.4 Actual Quantum Mechanical Absorption

The absorption coefficients determined for direct and indirect transitions were based on the assumption that the states in the valence band are filled and the conduction states empty,so that transitions between these states are permissible. A situation can exist where some of the states in the conduction band become occupied or in the valence band become empty. This condition can exist in some materials which are highly doped allowing the Fermi level to move into the conduction or valence band. This degenerate condition decreases the number of available final states to a degree that photon transitions to these states is not possible resulting in an absorption coefficient which decreases with the carrier concentration. This

anomalous absorption has been observed in InSb by Tanenbaum and Briggs [71] and explained by Burstein [72] and Moss [73]. It will be shown in this study that this process does not occur for silicon. For indirect band gap semiconductors such as silicon it is possible that scattering processes in which the absorption coefficient increases with carrier concentration can occur by electron-electron scattering [74], [75] or by impurity scattering [76]. Results for As-doped germanium [77] show that the absorption does increase with carrier concentration and that

$$\alpha = AN\,(h\nu - E_{gi} - \delta_F)^2 \qquad (81)$$

where A is a constant, N is the number of carriers (scatterers) and δ_F, the penetration of the Fermi level in the band. Heavy doping of the indirect gap semiconductors can also result in an effective shrinkage of the direct and indirect band gaps [78].

This study will show that the value of α will vary as the energy raised to a power between one and two. This absorption coefficient and consequently the optical conductivity is not enhanced by the production of electron-hole pairs caused by the radiation (see section 3.3). The increase in carriers due to the energy and intensity of the radiation is small compared to the nominal carrier density due to the dopants so that the conductivity is not increased because of a photoconductive effect.

2.5 Conductivity Determination from Absorption Characteristics

(a) Optical constants of an absorbing medium. The relationships which express the reflection and transmission of light at the boundary between two media are determined by applying the boundary conditions to the solutions of Maxwell's equations. These boundary conditions require that tangential component of the electric and magnetic field vectors be continuous at the boundary of the two media.

When the electromagnetic radiation is considered to be a plane wave and the angle of incidence of the ray θ in medium n_o reflects from the surface as shown in figure 4, the Fresnel coefficients are known to be

$$s_s = \frac{R_s}{E_s} = \frac{n_o \text{Cos}\,\theta - n' \text{Cos}\,\theta'}{n_o \text{Cos}\,\theta + n' \text{Cos}\,\theta'} \tag{82}$$

$$s_p = \frac{R_p}{E_p} = \frac{n_o \text{Cos}\,\theta' - n' \text{Cos}\,\theta}{n_o \text{Cos}\,\theta' + n' \text{Cos}\,\theta} \tag{83}$$

$$t_s = \frac{E_s'}{E_s} = \frac{2\, n_o \text{Cos}\,\theta}{n_o \text{Cos}\,\theta + n' \text{Cos}\,\theta'} \tag{84}$$

$$t_p = \frac{E_p'}{E_p} = \frac{2\, n_o \text{Cos}\,\theta'}{n_o \text{Cos}\,\theta' + n' \text{Cos}\,\theta} \tag{85}$$

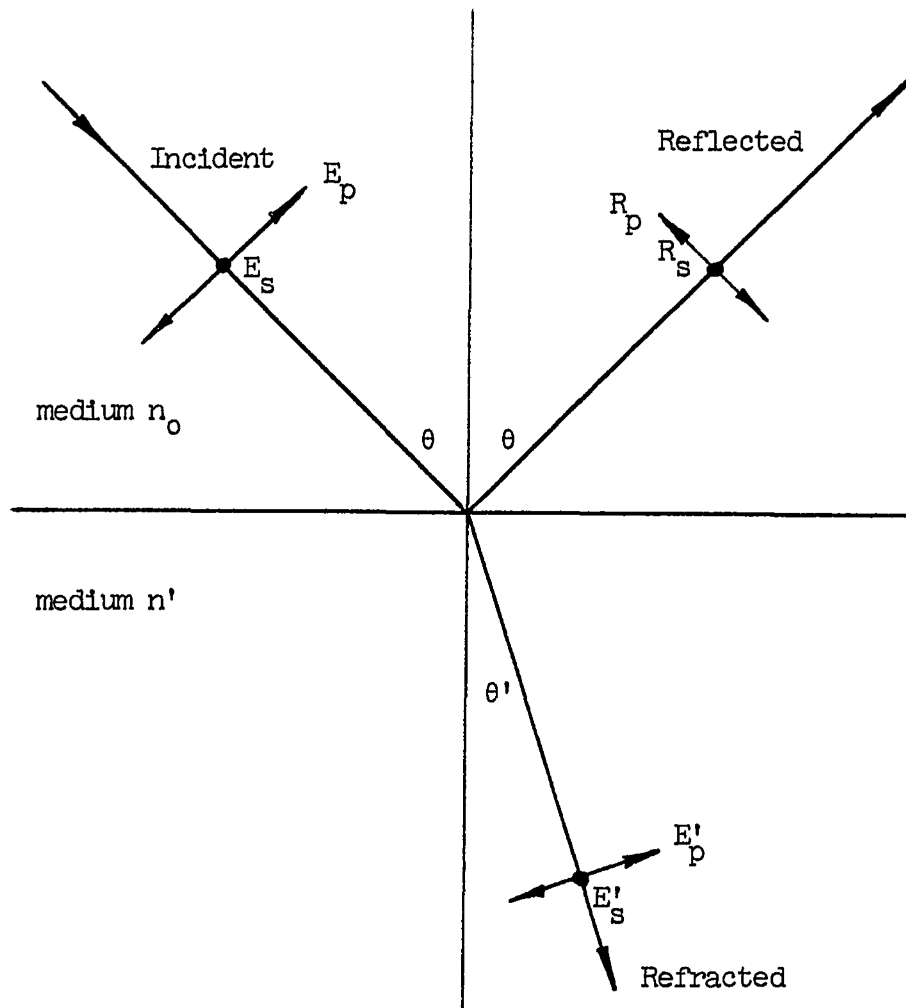

Figure 4.—Reflected and refracted wave vectors for an incident wave. The subscript s refers to electric vectors normal to the plane of incidence and the subscript p for electric vectors in the plane of incidence.

When Snell's law is used together with equations (82) through (85), they become

$$s_s = \frac{R_s}{E_s} = \frac{\text{Sin}\ (\theta' - \theta)}{\text{Sin}\ (\theta' + \theta)} \tag{86}$$

$$s_p = \frac{R_p}{E_p} = \frac{\tan\ (\theta - \theta')}{\tan\ (\theta + \theta')} \tag{87}$$

$$t_s = \frac{E_s'}{E_s} = \frac{2\ \text{Sin}\ \theta'\ \text{Cos}\ \theta}{\text{Sin}\ (\theta + \theta')} \tag{88}$$

$$t_p = \frac{E_p'}{E_p} = \frac{2\ \text{Sin}\ \theta'\ \text{Cos}\ \theta}{\text{Sin}\ (\theta + \theta')\ \text{Cos}\ (\theta - \theta')} \tag{89}$$

Where E_p, R_p, and E_p' are the wave vectors amplitudes polarized parallel to the plane of incidence and E_s, R_s, and E_s' are the amplitudes polarized normal to the incidence plane.

Equations (86) through (89) are valid for real angles only if the refractive index of medium n' is real which is true only for lossless materials such as dielectrics. In general however, n is complex such as is the case for the elemental semiconductor.

When n is real, then the Fresnel coefficient given by (83) and (87) goes to zero at an angle θ given by 90 - θ'. Under this condition,

the angle called the polarizing or Brewster angle, θ_B, becomes

$$\theta_B = \tan \frac{n'}{n_o} \quad (90)$$

The reflectances as given by

$$r_s = \frac{|R_s|^2}{|E_s|^2} \quad (91)$$

$$r_p = \frac{|R_p|^2}{|E_p|^2} \quad (92)$$

show that r_s is a monotonic increasing function of θ approaching unity at $\theta = 90°$ and approaching r_o at $\theta = 0°$, where

$$r_o = \left(\frac{n' - n_o}{n' + n_o}\right)^2 \quad (93)$$

The value of r_p approaches the same values as r_s but is not monotonic. It decreases to zero at the polarizing angle when the refractive indices n' and n_o are real.

When the refractive index n' is complex, then the relationship given by Snell's law no longer yields an angle of refraction but becomes using (3) for n'

$$\text{Sin } \theta' = \frac{n_o \text{ Sin } \theta}{n_r - i k} \tag{94}$$

so that Sin θ' now becomes a complex quantity and only becomes an angle of refraction for the special case in which $\theta = \theta' = 0$ which occurs at normal incidence.

Using (86) and (87) and letting the radiation be polarized so that $E_p = E_s$, then

$$\frac{R_p}{R_s} = - \frac{\text{Cos } (\theta + \theta')}{\text{Cos } (\theta - \theta')} \tag{95}$$

Because (95) is a complex quantity, it can be written as

$$\frac{R_p}{R_s} = \rho e^{i\gamma} \tag{96}$$

where ρ is the ratio of the real amplitudes of R_p and R_s and γ is the phase difference between these components. Using equations (95) and (96)

$$\frac{1 + \rho e^{i\gamma}}{1 - \rho e^{i\gamma}} = \frac{\text{Sin } \theta \text{ Sin } \theta'}{\text{Cos } \theta \text{ Cos } \theta'} \tag{97}$$

and using (94) and (97)

$$\frac{1 + \rho e^{i\gamma}}{1 - \rho e^{i\gamma}} = \frac{\text{Sin } \theta \tan \theta}{\left[\left(\frac{n_r - ik}{n_o}\right)^2 - \text{Sin}^2 \theta \right]^{1/2}} \tag{98}$$

The angle of incidence θ for which the phase difference is 90° occurs at the principal angle of incidence, which when $n_r^2 + k^2 >> 1$, is very nearly at the angle where R_p is minimum [79]. The angle corresponding to this minimum is called the pseudo-polarizing angle, θ_p, and using (98) and letting $n_o = 1$ for air

$$\frac{1 + i\rho}{1 - i\rho} = \frac{\text{Sin } \theta_p \tan \theta_p}{[(n_r - ik)^2 - \text{Sin}^2 \theta_p]^{1/2}} \tag{99}$$

When (99) is multiplied by the complex conjugate expression given by

$$\frac{1 - i\rho}{1 + i\rho} = \frac{\text{Sin } \theta_p \tan \theta_p}{[(n_r + ik)^2 - \text{Sin}^2 \theta_p]^{1/2}} \tag{100}$$

then the angle θ_p can be found using (99) and (100) by

$$\text{Sin}^4 \theta_p \tan^4 \theta_p = (n_r^2 + k^2)^2 - 2 (n_r^2 - k^2) \text{Sin}^2\theta_p + \text{Sin}^4\theta_p \tag{101}$$

In the visible radiation region, the refractive index for silicon is about four and the extinction coefficient is about unity, so that when

$n_r^2 + k^2 \gg 1$, equation (101) becomes

$$\sin \theta_p \tan \theta_p = (n_r^2 + k^2)^{1/2} \tag{102}$$

This result could also have been obtained by neglecting $\sin^2\theta$ in (100). Then using (98) and its complex conjugate, omitting the $\sin^2\theta$ term, defining K as

$$K = {}^{k}/n_r \tag{103}$$

and ρ as

$$\rho = \frac{R_{pa}}{R_{sa}} = \tan \psi \tag{104}$$

where the subscript a indicates the real amplitude, then the values for K and n are found to be

$$K = \tan 2\psi_p \tag{105}$$

and

$$n_r = \sin \theta_p \tan \theta_p \cos 2\psi_p \tag{106}$$

where ψ_p is the condition which exists when $\theta = \theta_p$.

Therefore, in order to determine the values of n_r and k, it is only necessary to know the psuedo-polarizing angle θ_p and the amplitudes of the reflected waves R_{pa} and R_{ps}.

Figure 5 shows the theoretical reflectance curves for $n_r = 3.5$ and $k = 1$. The curves are obtained by using equations (82), (83), (91), (92) and (94). The angle, θ at which r_p is minimum is the pseudo-polarizing angle θ_p. The curve for r_p shows that the reflectance does not go to zero at the polarizing angle when the extinction coefficient k is not zero.

(b) Effect of a surface film on the optical constants. The results obtained for the reflection and transmission coefficients of a single layer can be applied in a situation in which the layer is bounded on either side by semi-infinite layers. The incident beam is considered to undergo multiple reflections in the thin film will be assumed to be non-absorbing and have a thickness, d. This is illustrated in figure 6 in which the incident ray, E, is of unit amplitude. Then the resultant reflected amplitude can be shown to be [80]

$$R = \frac{s_1 + s_2 e^{-2iz}}{1 + s_1 s_2 e^{-2iz}} \tag{107}$$

where

$$s_1 = \frac{R_1}{E} \tag{108}$$

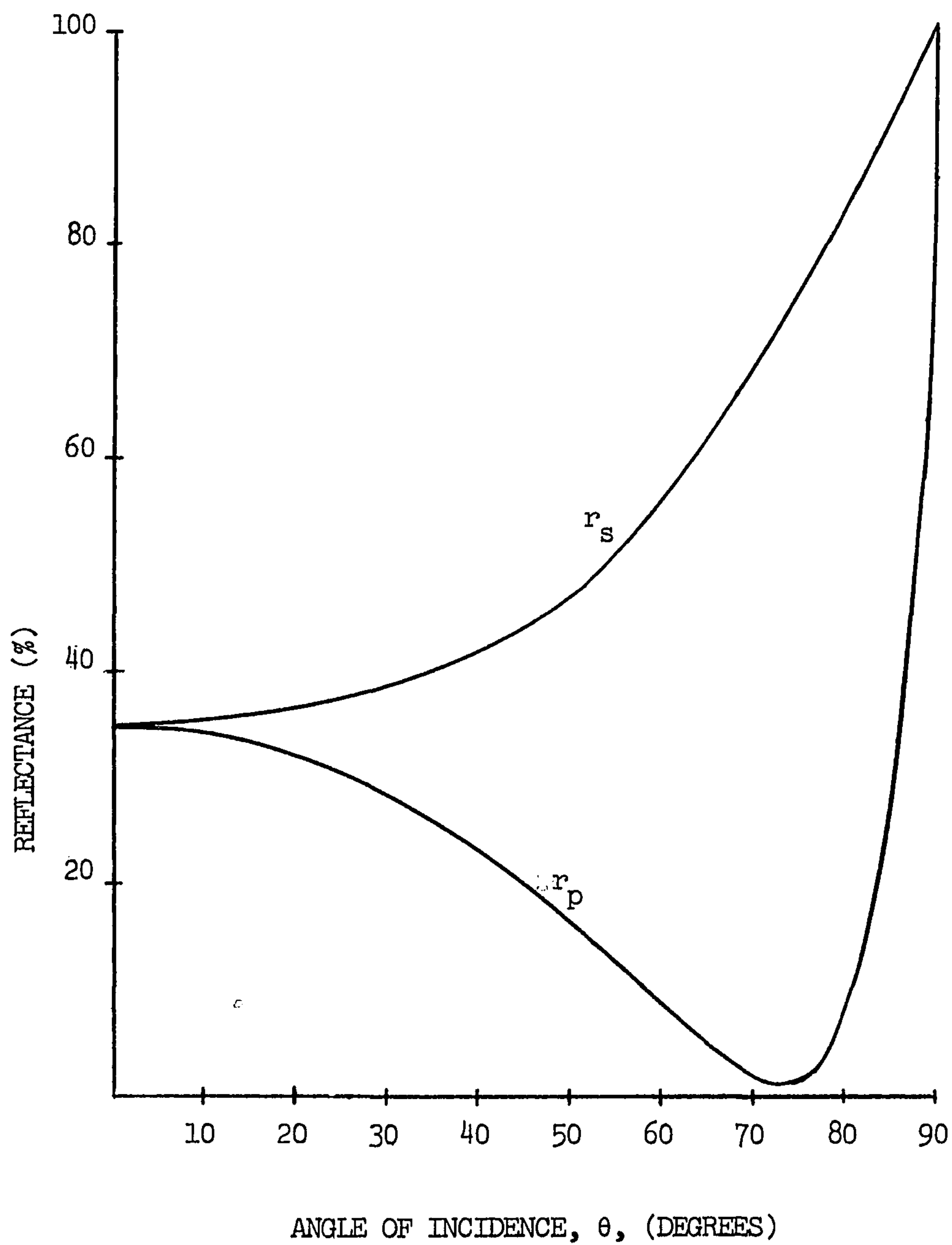

Figure 5.—Theoretical reflectance curves for $n_r = 3.5$ and $k = 1$.

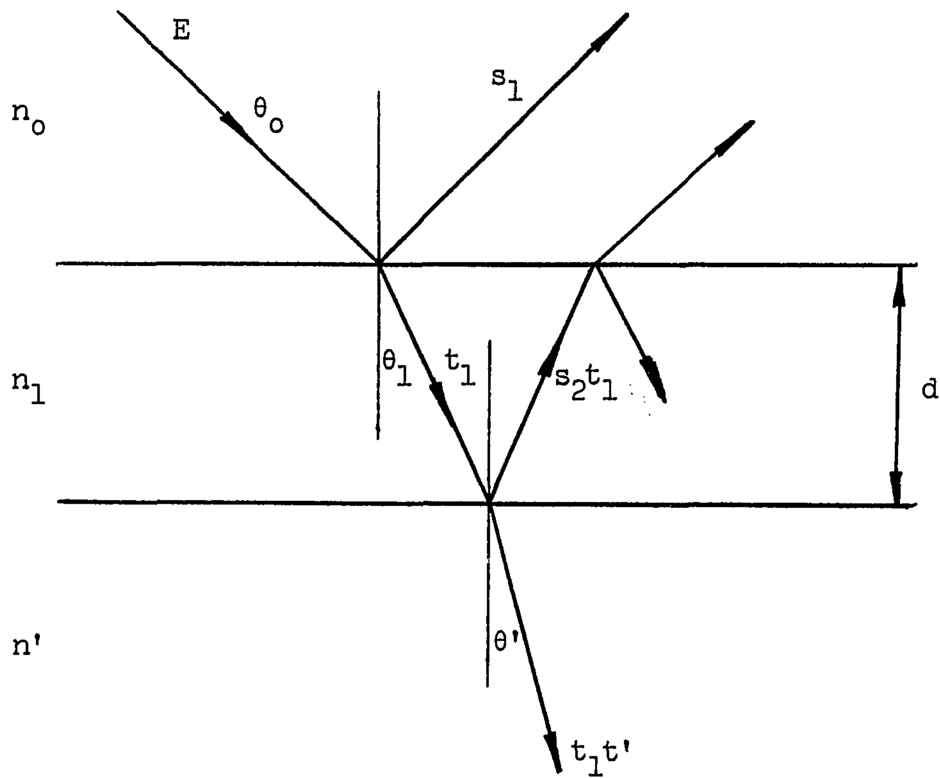

Figure 6.—Multiple reflections in a non-absorbing layer of thickness, d, and refractive index, n_1.

$$s_2 = \frac{R_2}{T_1} \tag{109}$$

$$z = \frac{2\pi n_1 d}{\lambda} \cos \theta_1 \tag{110}$$

and from energy considerations the reflectance as a ratio of reflected energy to the incident energy is obtained by considering that the flow of energy associated with the propagation of an electromagnetic wave is represented by the Poynting vector as

$$\vec{P} = \vec{E} \times \vec{H} \tag{111}$$

and requiring that the energy in the magnetic and electric fields be equal, the power or intensity is given by

$$P = n_x |E|^2 \tag{112}$$

where n_x is the refractive index of the medium in which the wave is traveling. The absolute value of n_x is used if it is complex.

The reflectance r is then defined as the ratio of the reflected intensity to the incident intensity so that

$$r = \frac{|R|^2}{|E|^2} \tag{113}$$

where R and E are the magnitudes or amplitudes of the reflected and incident fields respectively. Therefore

$$r = \left(\frac{R}{E}\right) \left(\frac{R^*}{E}\right) \tag{114}$$

which becomes, if E = 1

$$r = R\,R^* \tag{115}$$

where the value R^* represents the complex conjugate. The expression for the reflectance of the component parallel to plane of incidence is accordingly

$$r_p = \frac{S_{1p}\,S_{1p}^* + S_{1p}^*\,S_{2p}\,e^{-2iz} + S_{1p}\,S_{2p}^*\,e^{2iz} + S_{2p}\,S_{2p}^*}{1 + S_{1p}\,S_{2p}\,S_{1p}^*\,S_{2p}^* + S_{1p}\,S_{2p}\,e^{-2iz} + S_{1p}^*\,S_{2p}^*\,e^{2iz}} \tag{116}$$

and an expression for the component normal to the plane of incidence r_s, can be obtained by substituting the subscript s for p. Adapting equation (83) so that it is consistent with the conditions shown in figure 6, then

$$S_{1p} = \frac{n_o \operatorname{Cos}\theta_1 - n_1 \operatorname{Cos}\theta_o}{n_o \operatorname{Cos}\theta_1 + n_1 \operatorname{Cos}\theta_o} \tag{117}$$

and

$$S_{2p} = \frac{n_1 \text{ Cos } \theta' - n' \text{ Cos } \theta_1}{n_1 \text{ Cos } \theta' + n' \text{ Cos } \theta_1} \tag{118}$$

The value of n_o and n_1 are real because they represent media which are considered to be lossless. The value for n', however is complex so that (116) can be written as

$$r_p = \frac{S_{1p}{}^2 + S_{1p} (S_{2p} e^{-2iz} + S_{2p}{}^* e^{2iz}) + S_{2p} S_{2p}{}^*}{1 + S_{1p} (S_{2p} e^{-2iz} + S_{2p}{}^* e^{2iz}) + S_{1p}{}^2 S_{2p} S_{2p}{}^*} \tag{119}$$

Because S_{2p} is in general complex, it can be given as

$$S_{2p} = a + ib \tag{120}$$

and if (120) and its complex conjugate $S_{2p}{}^*$ are substituted in (119), then

$$r_p = \frac{S_{1p}{}^2 + 2 S_{1p} (a \text{ Cos } 2z + b \text{ Sin } 2z) + (a^2 + b^2)}{1 + 2 S_{1p} (a \text{ Cos } 2z + b \text{ Sin } 2z) + S_{1p}{}^2 (a^2 + b^2)} \tag{121}$$

The reflectance due to the medium n' when there is no surface layer is obtained from (121) and (110) using a value d = 0. This reflectance, r_{po} is then

$$r_p = \frac{S_{1p}^{\ 2} + 2\ a\ S_{1p} + (a^2 + b^2)}{1 + 2\ a\ S_{1p} + S_{1p}^{\ 2}\ (a^2 + b^2)} \tag{122}$$

The reflectance is also r_{po} whenever the value of d satisfies

$$Z = \frac{4\ n_1\ d\ \text{Cos}\ \theta_1}{\lambda} \quad \text{when } Z = 0,\ 1,\ 2,\ \ldots . \tag{123}$$

The reflectance, r given by equation (113) has been determined for a dielectric film as a function of its optical thickness when the film is on a material which has refractive indices smaller and greater than the film [81]. Results for a metallic film on a dielectric where the extinction coefficient was varied so as to change the absorption of the metallic film are also available [82]. The results are shown in figures 7 and 8.

(c) Effect due to band shrinkage and the Fermi level shift. The absorption of radiation in semiconductors is known to depend on the carrier density [74] - [76]. The carrier density of semiconductor materials is usually difficult to calculate unless some simplifying assumptions are made, however it can be obtained empirically with reasonable accuracy. Semiconductors which are doped result in a shift in Fermi level and an effective shrinkage of the band gap, although the effective band shrinkage is more noticeable for heavily doped materials [78]. The band shrinkage and the Fermi level shift are both

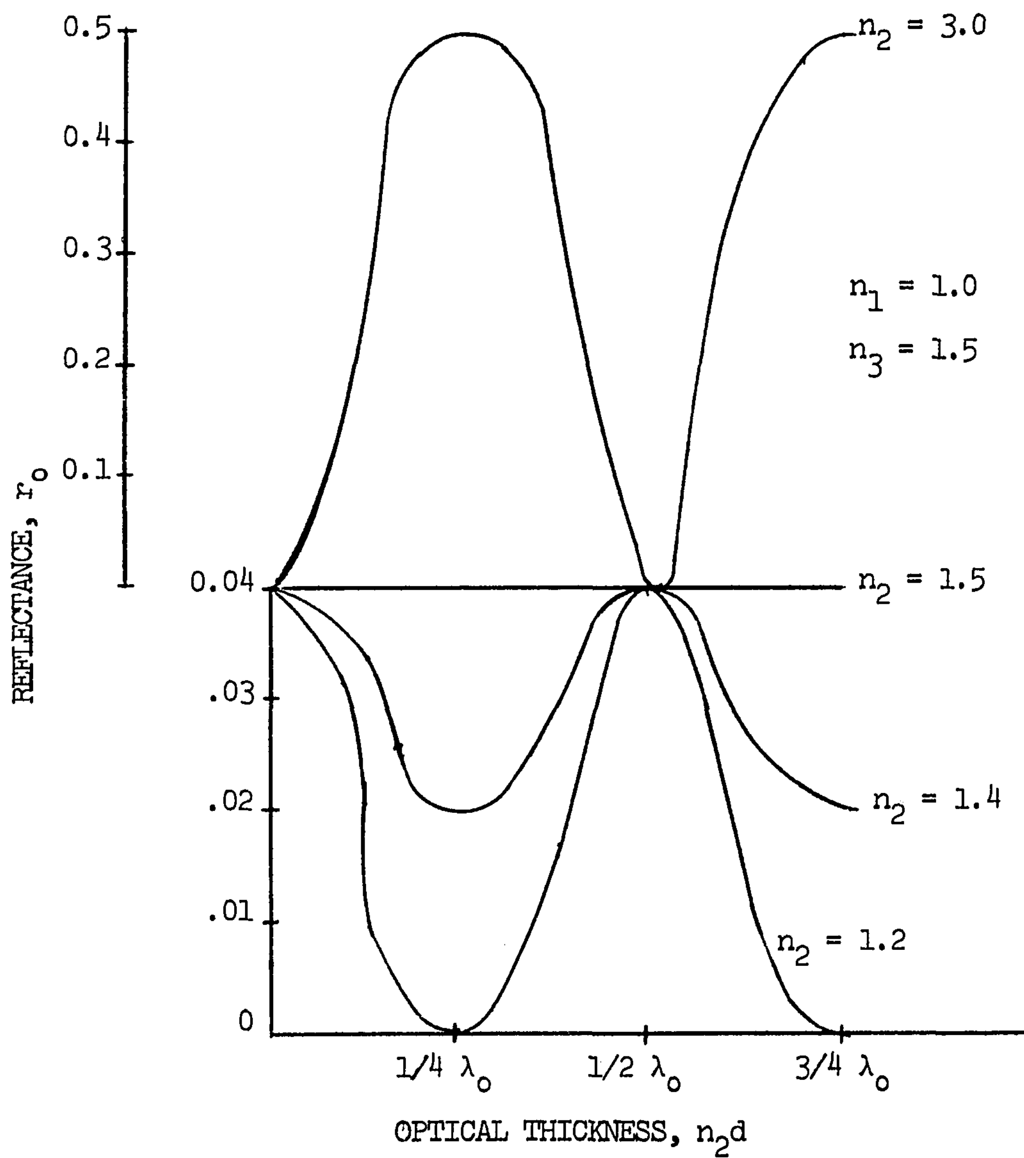

Figure 7.—Reflectance at normal incidence of a dielectric film as a function of its optical thickness (After Messner, [81]).

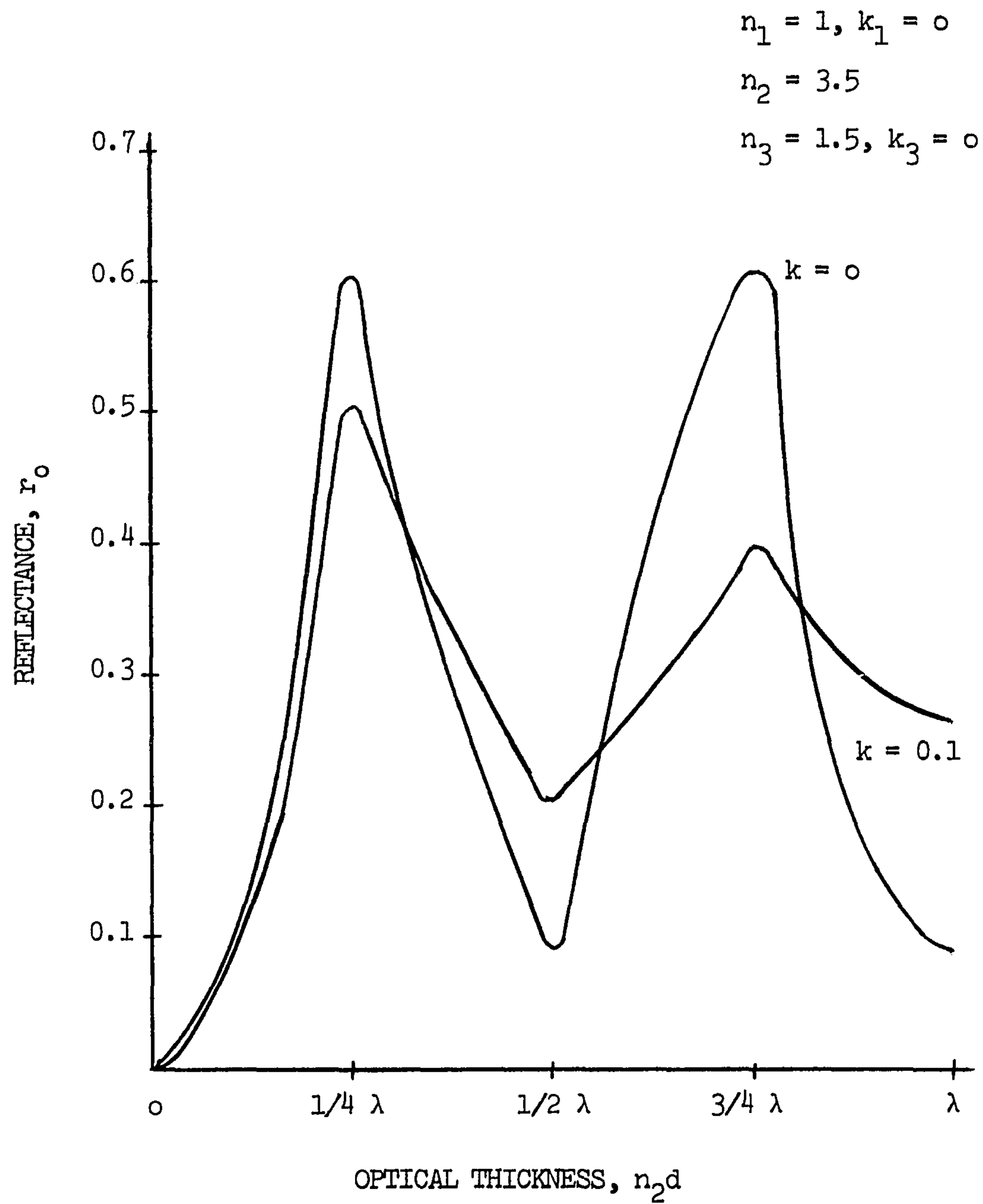

Figure 8.—Reflectance at normal incidence for a metallic film with extinction coefficient, k (After Hammer, [82]).

responsible for the increase in the carrier density so that values for these quantities, if known, can determine the carrier density. It can be shown that an expression can be obtained in which the combined effect of both band shrinkage and Fermi level shift is used to obtain the carrier density, and consequently, the low frequency conductivity.

The Fermi level, E_f, of a semiconductor which is non-degenerate, lies between the valence and the conduction bands. When the semiconductor is intrinsic, the Fermi level lies very nearly in the center of the forbidden gap and is independent of temperature. When the material is doped with impurities, the Fermi level is displaced from the center of the band and moves toward the gap center as the temperature increases. A semiconductor material which is doped with acceptor atoms becomes p-type with an acceptor level lying very near the valence band. The concentration of acceptor atoms at the acceptor level which are ionized determines the shift in the Fermi level from the center of the forbidden gap. The acceptor level is readily ionized at room temperature by electrons which are excited from the valence band. The small energy gap between the highest valence band level and the acceptor level allows a large increase in the number of negative ions and in the number of holes. The process of recombination is such that the number of corresponding free electrons decrease when the holes increase.

The shift in the Fermi level, ΔE for p-type material is shown in

figure 9(a) for an assumed flat band in the vicinity of the indirect band gap. The shift is given by

$$\Delta E = E_{fi} - E_f \tag{124}$$

where the intrinsic energy of the Fermi level is given by E_{fi}, and the Fermi level of the p-type material by E_f.

The hole density, p, for p-type material is obtained by

$$p = \int_{E_{veb}}^{E_{ve}} S\,(E)\ \ f_p\,(E)\ \ dE \tag{125}$$

where the density of states for holes is given by S (E) and the hole Fermi factor is given by $f_p(E)$. An expression by $f_p(E)$ is given in terms of the Fermi factor, F(E), by

$$f_p(E) = 1 - f\,(E) \tag{126}$$

and f(E) by

$$f\,(E) = [1 + e^{(E - E_f)/kt}]^{-1} \tag{127}$$

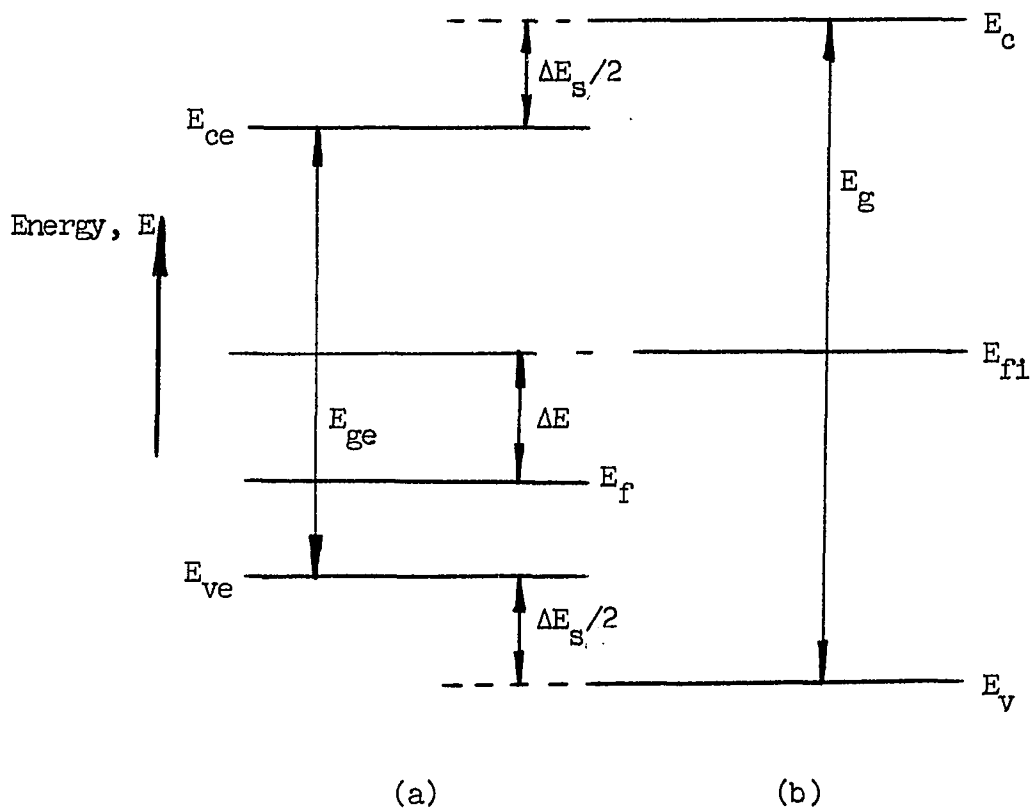

Figure 9.—(a) Energy level diagram for a p-doped semiconductor where E_{ge} is the effective band gap due to energy band shrinkage E_s.

(b) Energy level diagram for an intrinsic semiconductor.

Then the general expression for the hole density in p-type material at a given temperature can be shown to be, in terms of a constant c' and energy, as

$$p = \int_{o}^{\infty} \frac{c'\ E^{1/2}\ e^{(E - E_{fi})/kt}\ e^{\Delta E/kt}\ dE}{1 + e^{(E - E_{fi})/kt}\ e^{\Delta E/kt}} \qquad (128)$$

where the upper limit E_{ve} was chosen to be the reference level, zero. The bottom of the valence band, E_{vbe}, was chosen as infinity, because the integral converges very rapidly in the valence band region. When it is assumed that the semiconductor is non-degenerate, then the factor in the integral

$$e^{(E - E_{fi})/kt}\ e^{\Delta E/kt} << 1 \qquad (129)$$

and the expression for p, therefore becomes

$$p = \int_{o}^{\infty} c'\ E^{1/2}\ e^{(E - E_{fi})/kt}\ e^{\Delta E/kt}\ dE \qquad (130)$$

Under the same conditions of non-degeneracy it can also be shown that the effective intrinsic hole density p_{ie} can be given by

$$p_{ie} = \int_{o}^{\infty} c' \, E^{1/2} \, e^{(E - E_{fi})/kt} \, dE \qquad (131)$$

Both expressions (130) and (131) are valid for silicon which has an indirect band gap of about 1.1 ev when intrinsic. The Fermi level for intrinsic silicon, therefore can shift 0.55 ev before becoming degenerate. The actual values, however, are somewhat less than those indicated, because as shown in figure 9(a), there is a certain amount of band shrinkage when the semiconductor is doped. Using both (130) and (131), the hole density for the doped material, p, becomes

$$p = p_{ie} \, e^{\Delta E/kt} \qquad (132)$$

The diagram in figure 9(b) shows the band gap, Eg, for an intrinsic material. The value of the intrinsic hole density p_i is known to depend on the band gap by

$$p_i = c_1 \, e^{-Eg/2kt} \qquad (133)$$

where c_1 is a constant.

The effective intrinsic hole density, p_{ie}, is then given by

$$p_{ie} = c_1 e^{-(E_g - \Delta E_s)/2kt} \quad (134)$$

The hole density, p, can then be obtained by using (132), (133) and (134) so that

$$p = p_i e^{\Delta E_a/kt} \quad (135)$$

where

$$\Delta E_a = \Delta E + \Delta E_{s/2} \quad (136)$$

The expression for p in (135) is valid only when the condition expressed by (129) is valid. When the material is very highly doped, the Fermi level enters the valence band making the material degenerate. The value of p for degenerate materials can only be obtained by evaluating the integral in (128) by numerical techniques.

The relationship between the low frequency conductivity as given by equation (33) and the energy shift ΔE_a, can be obtained by considering two silicon samples of conductivities σ_1 and σ_2. The corresponding values of ΔE_{a1} and ΔE_{a2} will then be given for σ_1 and σ_2

$$\Delta E_{a1} = \Delta E_1 + \Delta E_{s1}/2 \quad (137)$$

and

$$\Delta E_{a2} = \Delta E_2 + \Delta E_{s2}/2 \tag{138}$$

From equation (33)

$$\sigma_k = q\,(\mu_{pk}\, p_k + \mu_{nk}\, n_k) \tag{139}$$

and by using (135) for p-type materials, the ratio of the two conductivities becomes

$$\frac{\sigma_2}{\sigma_1} = \frac{\mu_{p2}\, n_{i2}\, e^{\Delta E_{a2/kt}} + \mu_{n2}\, n_2}{\mu_{p1}\, n_{i1}\, e^{\Delta E_{a1/kt}} + \mu_{n1}\, n_1} \tag{140}$$

When the materials are doped sufficiently so that the minority carriers are negligible, then, because $n_{i1} = n_{i2}$ since both samples are silicon

$$\frac{\sigma_2}{\sigma_1} = \frac{\mu_{p2}}{\mu_{p1}}\, e^{\Delta E_d/kt} \tag{141}$$

where ΔE_d is given by

$$\Delta E_d = \Delta E_{a2} - \Delta E_{a1} \tag{142}$$

A plot of radiation energy versus the absorption coefficient will result in two curves separated by a fixed energy value ΔE_d. If one of the samples has a known conductivity, then the other can be obtained by equation (141) or in general by equation (140).

The energy bands for different samples of silicon as indicated in figure 10 are assumed to be flat only for purposes of illustration. It is shown that the band shrinkage increases with doping as does the Fermi level shift. The Fermi level for the intrinsic material is known to lie almost in the center of the band, so that

$$E_f = \frac{E_c + E_v}{2} \tag{143}$$

whereas. the Fermi level for a p-doped material can be given by

$$E_{fk} = E_f - \Delta E_k \tag{144}$$

The valence and conduction bands for the p-material will then become respectively,

$$E_{vk} = E_v + \Delta E_{sk}/2 \tag{145}$$

and

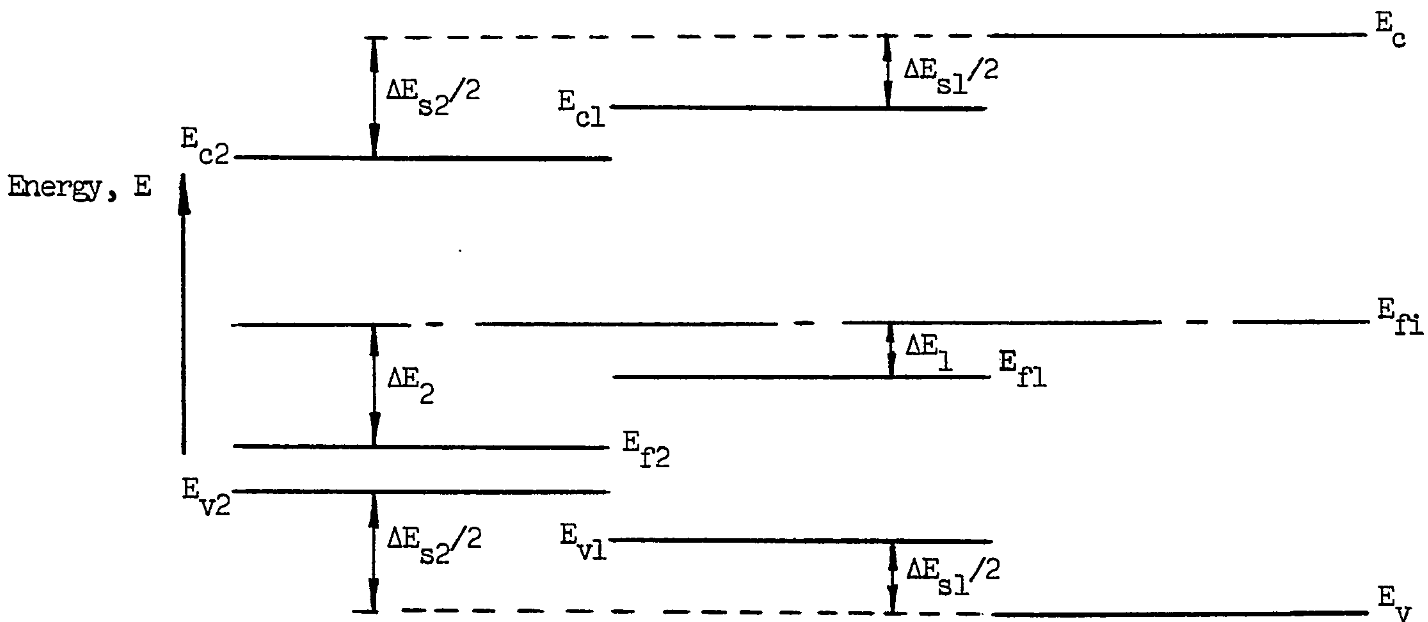

Figure 10.—Comparison of the energy bands for intrinsic silicon (Fermi level, E_{fi}), and two p-doped samples. The sample denoted by the index 2 is more highly doped than that of index 1.

$$E_{ck} = E_c - \Delta E_{sk}/2 \quad (146)$$

From equation (144), it is apparent that

$$\Delta E_2 - \Delta E_1 = E_{f1} - E_{f2} \quad (147)$$

Then, using (137), (138) and (142)

$$\Delta E_d = E_{f1} - E_{f1} + 1/2\ (\Delta E_{s2} - \Delta E_{s1}) \quad (148)$$

A relationship does exist between the Fermi level and the band shrinkage but the relationship is not relevant to this discussion. The relationship given by (148) indicates that the energy shift ΔE_d depends on Fermi level difference and the band shrinkage difference. The shift, E_d will be measured as a displacement between two absorption curves, one in which the conductivity is known. Equation (141) then determines the low frequency conductivity σ_2 when the low frequency conductivity σ_1 is known.

The expression for a degenerate condition is derived in Appendix A and is applied to measurements made on a highly doped wafer in Appendix B.

CHAPTER 3

EXPERIMENTAL METHOD

3.1 Apparatus and Method

The method used to determine the optical constants n_r and k is by a non-normal reflectance technique shown in figure 11. The monochromator shown is a Bausch and Lomb unit which contains a tungsten light source and a grating so that the wavelength can be varied from 2000 Å to 7000 Å. The bandwidth for the resulting wavelength at the exit port can be varied so that narrow bands corresponding to 1 Å at 50% intensity are feasible. This monochromatic light then passes through slits in a chopper wheel producing light pulses at a rate of 3.6 KHZ with a duty cycle of about 30%. The lens constructed collimator is then used to produce a narrow parallel beam of light which is incident on the semiconductor sample. The narrow parallel beam is collimated normal to the plane of incidence, where the plane of incidence is the plane which contains the diagram of figure 11. The narrow collimated beam of light then reflects from the semiconductor sample. After the radiation is reflected, it becomes polarized so that the reflected electric wave vector parallel, R_p to the plane of incidence, is in general less than the reflected electric wave vector normal, R_s, to the plane of incidence. The value of R_p for a lossless sample is zero when the incidence angle, θ, ($90 - \alpha$ in figure 11) is at the polarizing angle, θ_p. When the sample is absorbing such as is the case for metals and semiconductors, then the value of R_p is a non-zero minimum at θ_p. The polarizer, which is an Ealing type in which polaroid is

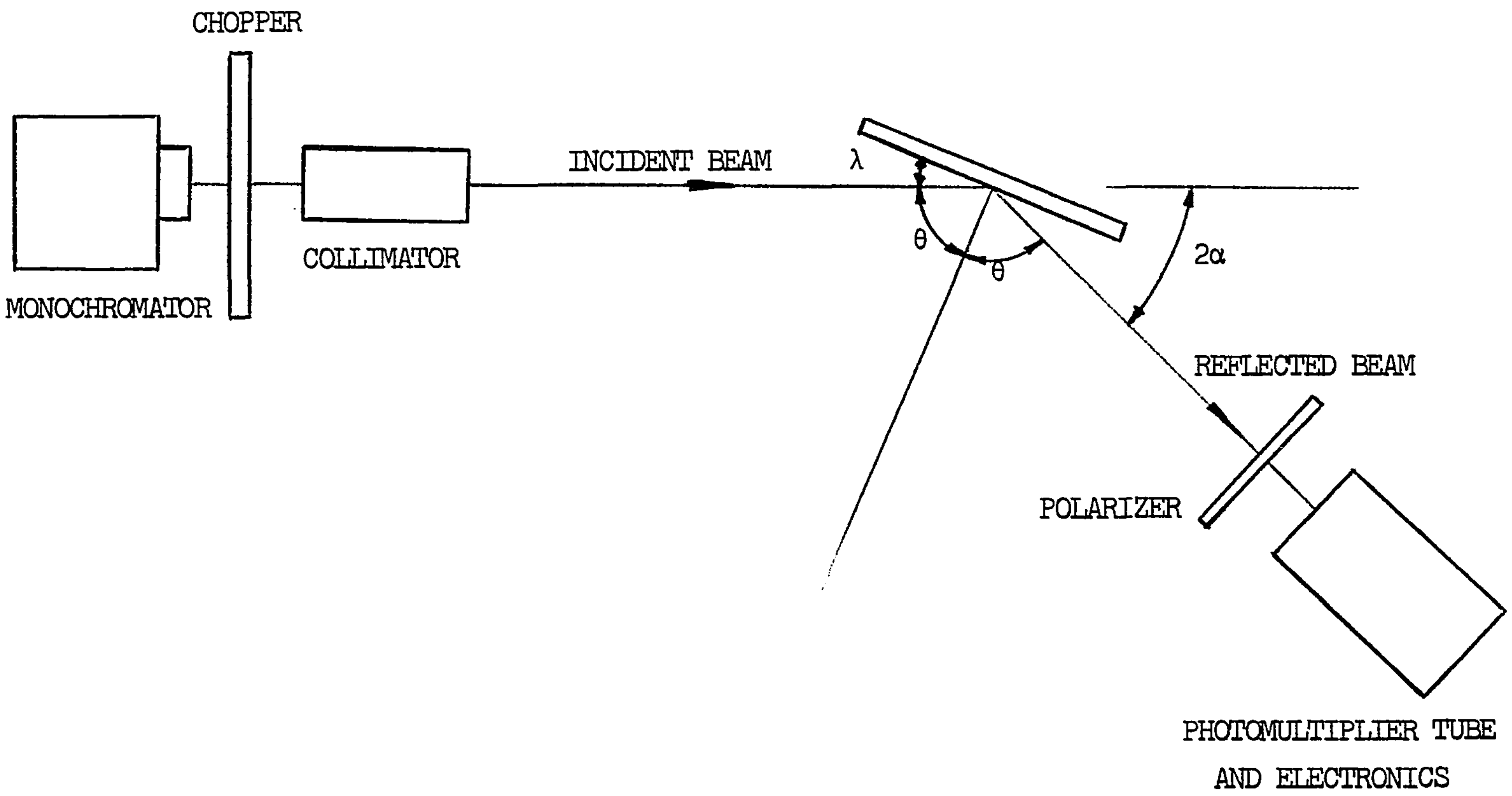

Figure 11

sandwiched between two glass disks, is mounted so that it can be rotated to orient its transmission axis parallel and normal to the plane of incidence. The polarizer used was of high quality (the quality measured by transmission axes results in a transmission intensity of 10^{-5}%) so that only the component parallel to the transmission axis can be transmitted. An illustration of the reflected wave vectors and the transmission of the wave vectors for different angles of incidence θ when the sample is absorbing is shown in figure 12. The photomultiplier tube an RCA type and associated electronics as shown in figure 13 is used to measure the intensity of wave vectors R_p and R_s. These values of intensities are measured as voltages are proportional to the square of the amplitudes of R_p and R_s.

The semiconductor sample is mounted on a spectrometer turntable with a specially designed leveling platform and accurate gear train assembly with only a few seconds of arc of backlash. The gear train assembly is necessary so that when the sample rotates at an angle α with respect to the incident beam, the polarizer and photomultiplier assembly rotate through an angle of 2α thereby maintaining that the photomultiplier is at the angle of reflection.

3.2 Precision of Measurement

The reflected light reaches the photomultiplier face through a slit 1/16" in width cut in a mask which covers the tube face. The width of the collimated reflected beam is adjusted so that it is only slightly less than the slit width. The photomultiplier is mounted so

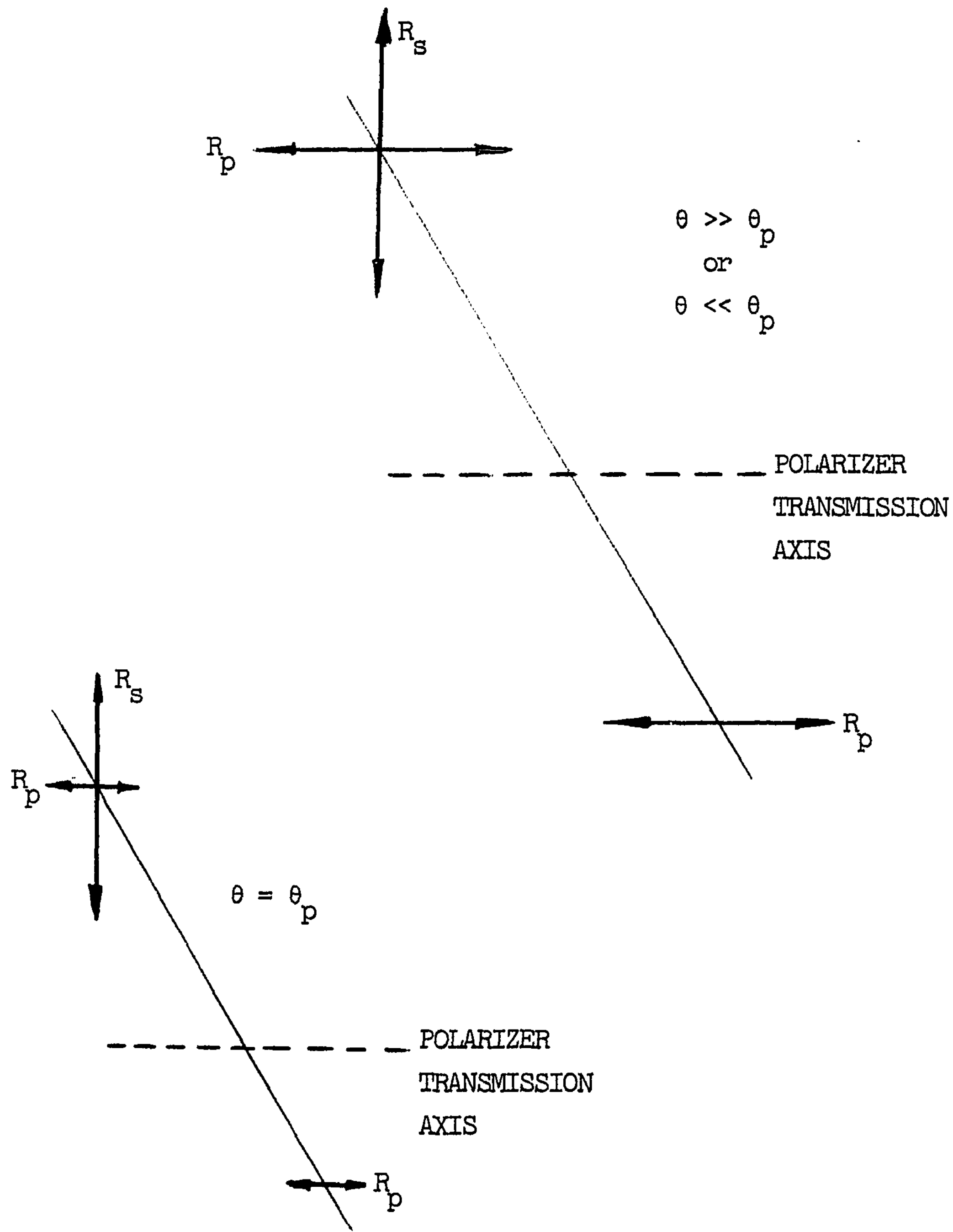

Figure 12

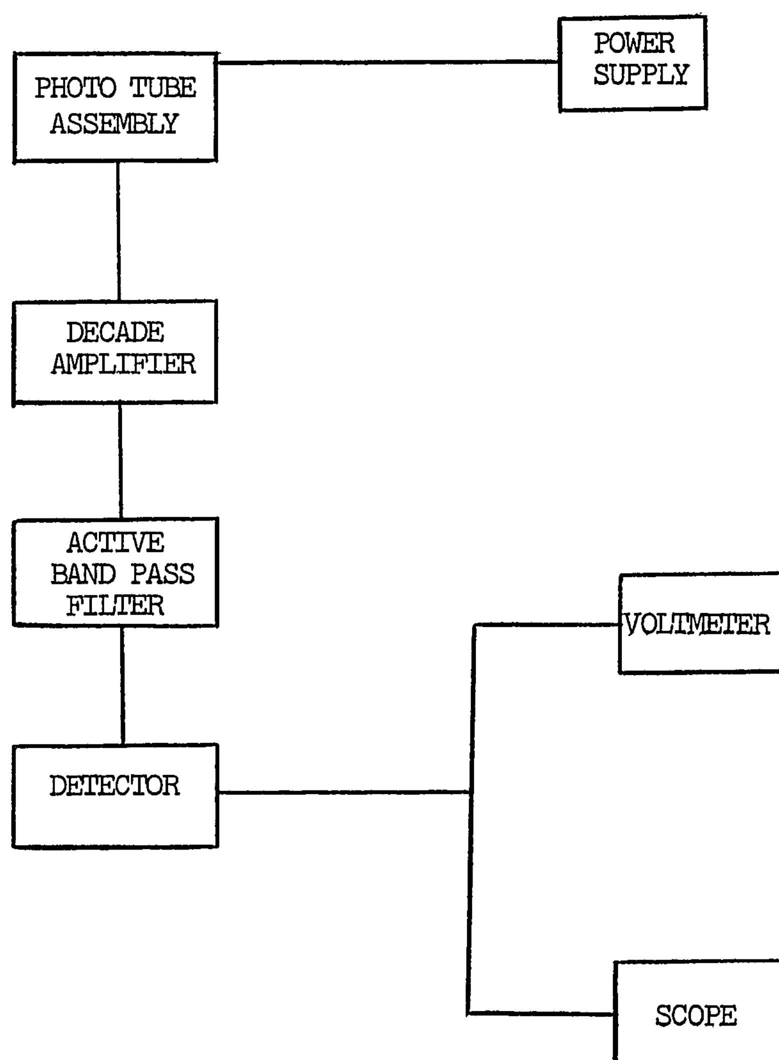

Figure 13

that its face is about four feet from the point of reflection on the semiconductor sample. Therefore, a deviation of one minute of arc results in a variation of about one sixteenth of an inch in the beam falling on the mask. This variation can be discerned visually by an observer under dark room conditions. The reading of the turntable of the spectrometer is calibrated so that it can read to thirty seconds of arc which is within the deviation that can be observed. The observation which can not be made much better than one minute of arc thereby limits the accuracy to this value.

It is also necessary to establish that the presence of an oxide layer on the silicon sample will not adversely affect the measurement. The sample of refractive index n_2 will be considered to be coated with a silicon dioxide layer of index n_1 and thickness d as shown in figure 14(a). The incident ray is shown as A and the reflected ray from the oxide surface as o, whereas the ray c is due to reflection from the silicon surface. Then the angle of deviation θ between the rays o and c as shown in figure 14(b) is found to be

$$\theta = \frac{dn_o}{Rn_1} \frac{2 \operatorname{Sin} \alpha \operatorname{Cos} \alpha}{1 - \left(\frac{n_o}{n_1}\right)^2 \operatorname{Sin}^2 \alpha} \qquad (149)$$

where R is the distance from the semiconductor sample to the detector.

The maximum deviation for θ occurs upon differentiating (124) when

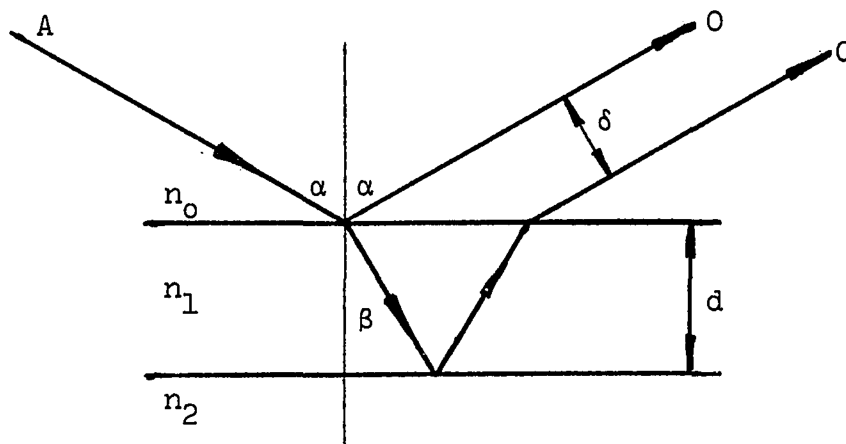

(a)

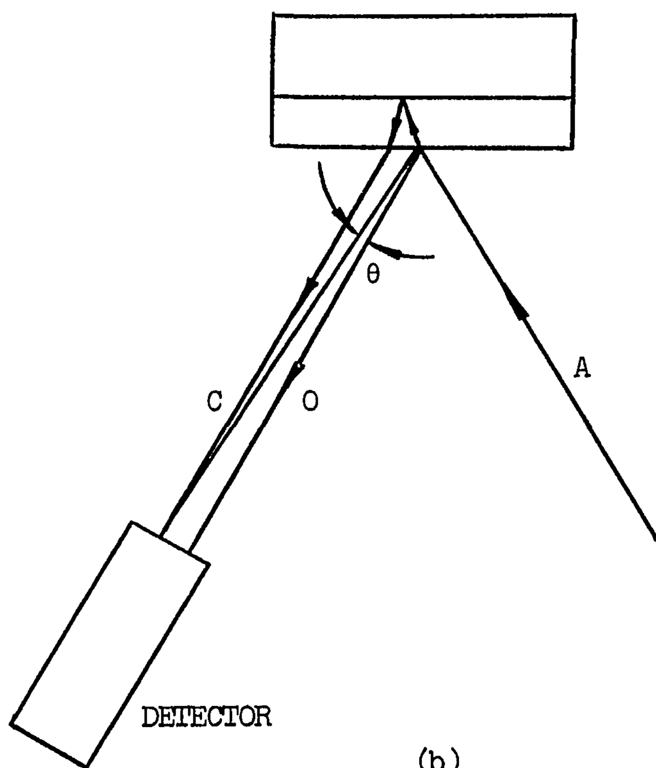

(b)

Figure 14

$$\mathrm{Sin}^2\,\alpha = \left(\frac{n_1}{n_o}\right)^2 \pm \left(\frac{n_1}{n_o}\right)\left[\left(\frac{n_1}{n_o}\right)^2 - 1\right]^{1/2} \tag{150}$$

and if $n_1 = 1.5$ and $n_o = 1$, then

$$\theta_{max} = .76\,\frac{d}{R} \tag{151}$$

So that when R is large as it is in this experiment ($\simeq$ 4 feet) and d $\simeq$ 20 Å then the value of θ_{max} is well within the limits of resolution of the experimental equipment.

3.3 Effect of Photon Flux

It is essential to show that the light flux which is used to make the conductivity measurements will not result in a large photo-conductive effect. The maximum number of electron-hole pairs produced by the photon flux will be shown to be small compared to the population density of the majority carriers. Therefore the true electrical conductivity will be measured and not an increased conductivity which may be caused by the measurement if a large number of pairs were produced.

The power density p(x) in a beam of electromagnetic radiation is given in terms of p(o) by equation (26). The available power density after propagating a distance x through the medium is represented by p(x) and the radiation incident at the surface by p(o).

If M is considered to be the number of photons absorbed per unit time, then it is true that

$$d\,p(x) = -E\,dM \tag{152}$$

Differentiating (26) and using (152) to obtain an integral equation so that

$$\int_{o}^{M} dM' = \frac{4\pi k}{\lambda}\,\frac{p(o)}{E}\int_{o}^{d} e^{\frac{-4\pi k}{\lambda}}\,dx \tag{153}$$

The value of d is chosen so that it is the reciprocal of the absorption coefficient. From equation (27) it is apparent that the exponent in equation (153) is the absorption coefficient, so that the resulting expression for M becomes

$$M = \frac{4\pi}{hc}\left(\frac{e-1}{e}\right) p(o)\,k \tag{154}$$

where p(o) is the incident intensity in watts per unit area, h is Planck's constant, λ the wavelength and k the extinction coefficient. Substituting the appropriate values

$$M = 4 \times 10^{19}\,p(o)\,k \tag{155}$$

where M is the maximum permissible number of photons absorbed per cm^3 per second.

If each photon absorbed produced an electron hole pair, then the number of pairs produced per unit volume, N, would depend on the lifetime of the carriers, τ, in the medium. Therefore

$$N = 4 \times 10^{19} \, p(o) \, k \, \tau \tag{156}$$

The intensity of the visible monochromatic radiation used for the measurement was of the order of 10^{-2} watts per cm . The lifetime of the carriers can be assumed to be of the order of 10^{-6} seconds[16], and the value of k found experimentally to be of the order of unity. The value of N is then calculated to be 4×10^{11} electron-hole pairs per cm^3 which is small when compared to silicon which is normally doped above 10^{15} per cm^3.

The intensity of light used in the experiment was low enough so as not to disturb the measurement. It should be realized, however, that very intense light such as that obtained from lasers have large electric fields, causing population increases and non-linearities which will affect the measurement.

CHAPTER 4

RESULTS

4.1 Comparison of Absorption Model

The absorption coefficients as obtained from measured data for two silicon wafers and the resulting conductivity of one wafer (using the other as a reference) is presented in this section. The wafers are p-type (100) oriented silicon of 15 mil thickness with nominal resistivities (as measured by four point probe) of 0.005 and 50 ohm-cm. The surfaces of the wafers are highly polished and coated with an oxide of about 50 Å. This oxide film will cause a measured absorption coefficient which is too large by about 94% (see table 5). The film together with contaminants and trapped charge in the oxide-silicon interface could be the reason for the absence of a noticeable slope change in the curve. The slope change should occur at the onset of direct transitions (2.6 ev). The effect of the equal surface films will cause equal degradation of the absorption coefficients and produce equal shifts in the absorption curves. Therefore, the relationship of section 2.5 (c) are applicable and the conductivity of one sample can be determined from the shift between the curves. For the sake of brevity, only the two samples of 0.005 and 50 ohm cm silicon will be used throughout the main text of the thesis. Additional data and calculations for six other silicon wafers in which the surfaces are carefully cleaned and etched are presented in Appendix B. A very pronounced slope change is evident in all these curves at about 2.5 ev.

The values of α for the semi-classical model are given in table 2 and those for the quantum mechanical model by tables 3 and 4. The absorption curves for both of these models are compared to the experimental

TABLE 1

EXPERIMENTAL RESULTS

		50 ohm-cm					0.005 ohm-cm				
λ (Å)	hν (ev)	K	θ_p	n_r	k	α (10^5 cm^{-1})	K	θ_p	n_r	k	α (10^5 cm^{-1})
4250	2.92	.217	78°43'	4.82	1.04	3.10	.296	79°19'	5.03	1.49	4.41
4500	2.76	.212	78° 7'	4.56	0.96	2.70	.321	78° 3'	4.41	1.43	4.01
4750	2.62	.179	77°35'	4.35	0.78	2.06	.283	77°25'	4.21	1.19	3.15
5000	2.48	.154	76°43'	4.08	0.63	1.58	.261	77°10'	4.14	1.08	2.71
5500	2.25	.125	76°18'	3.95	0.49	1.13	.212	76°23'	3.93	0.83	1.90
6000	2.07	.103	75°50'	3.80	0.39	0.82	.160	75°40'	3.74	0.60	1.25

curves. The experimental values of α and n_r calculated by using (102) and (105), the polarizing angle θ_p, and the value k obtained by (104) are given in table 1. The intensities of the reflected rays are measured as voltages and are proportional to the square of the amplitude. The values for α and n_r using the semi-classical model (table 2) are for the damping constant δ which gives the best fit to the measured α curve (see figure 15). The values of n_v and k for best fit were obtained by a computer program of (58) and (59) where $\Psi_o = 0.78$ and $E_o = 7.0$. The value of E_o was obtained using (58) and (59) to agree with the refractive index peak obtained from the results of Philipp and Taft [34] .

The quantum mechanical model yields theoretical values of α for indirect and direct transitions which are given in tables 3 and 4 respectively. The value of the phonon energy E_p for indirect transitions has been shown [70] to be about 0.05 ev at room temperature.

The term α_a becomes negligible in (79) for $h\nu$ slightly above the indirect gap, consequently, when Ef is considered as 1.05 ev, (79) becomes

$$\alpha e = A' \ (h\nu - 1.1)^2 \qquad (157)$$

so that absorption is essentially due to phonon emission. From the slope of the curves given [70] , the value of A' for intrinsic silicon can be found to be

TABLE 2

	$\delta = 0.040$		$\delta = 0.070$	
$h\nu$ (ev)	α (10^5 cm^{-1})	n_r	α (10^5 cm^{-1})	n_r
2.1	0.79	4.27	1.34	4.11
2.2	0.96	4.39	1.63	4.18
2.3	1.18	4.53	1.99	4.26
2.4	1.46	4.68	2.47	4.32
2.5	1.84	4.85	3.05	4.37
2.6	2.35	5.04	3.89	4.38
2.7	3.09	5.23	5.03	4.30
2.8	4.20	5.40	6.92	3.98
2.9	6.01	5.44		
3.0	9.74	4.95		

The absorption coefficient α as obtained from the semi-classical model using equations (27), (58) and (59).

TABLE 3

$h\nu$ (ev)	$(h\nu - 1.1)$ ev	α_e (cm^{-1})
1.2	0.1	33
1.3	0.2	131
1.4	0.3	294
1.5	0.4	522
1.6	0.5	816
1.7	0.6	1,175
1.8	0.7	1,600
1.9	0.8	2,090
2.0	0.9	2,645
2.2	1.1	3,950
2.4	1.3	5,518
2.6	1.5	7,346
2.8	1.7	9,436
3.0	1.9	11,786
3.2	2.1	14,398

Quantum mechanical results for the absorption coefficient for indirect transitions assuming intrinsic silicon. A further assumption is that all electron states are initially unoccupied and all hole states are filled.

TABLE 4

$h\nu$ (ev)	$(h\nu - 2.50)$ (ev)	α_{da} (10^4 cm^{-1})
2.51	0.01	0.17
2.52	0.02	0.25
2.54	0.04	0.35
2.60	0.10	0.55
2.70	0.20	0.78
2.80	0.30	0.95
2.90	0.40	1.10
3.00	0.50	1.23
3.10	0.60	1.35
3.20	0.70	1.46

Quantum mechanical results for the absorption coefficient for direct transitions in intrinsic silicon assuming initially unoccupied electron states and filled hole states.

$$\alpha_e = 3265 \, (h\nu - 1.1)^2 \quad (\text{cm}^{-1}) \tag{158}$$

The absorption coefficient for direct allowed transitions can be obtained from equation (75) which applies when the photon energy is near and greater then the direct band gap. Assuming that the electron and hole masses are the same and equal to half the free electron mass, then for an $n_r \simeq 5$, and $E_{gd} = 2.50$ ev

$$\alpha_{da} = 1.74 \times 10^4 \quad (h\nu - 2.50)^{1/2} \quad (\text{cm}^{-1}) \tag{159}$$

The results for the absorption coefficient as a function of photon energy is given in table 3 for equation (158) and in table 4 for equation (159).

Figure 15 compares the absorption coefficient calculated by the semi-classical model with the measured absorption coefficient obtained experimentally. The semi-classical model which may account for dissipative processes of absorption by the crystal lattice, agrees with the experimental curves for the lower values of photon energies. There is a noticeable departure from the experimental curves at higher energies. The value of δ which gives the best fit for the absorption coefficient, however, does not give the best fit for n_r as can be seen in figure 16. The inconsistency appears to be due to the choice of ψ_o and E_o. The vertical shift in the curve of figure 16 is caused by an

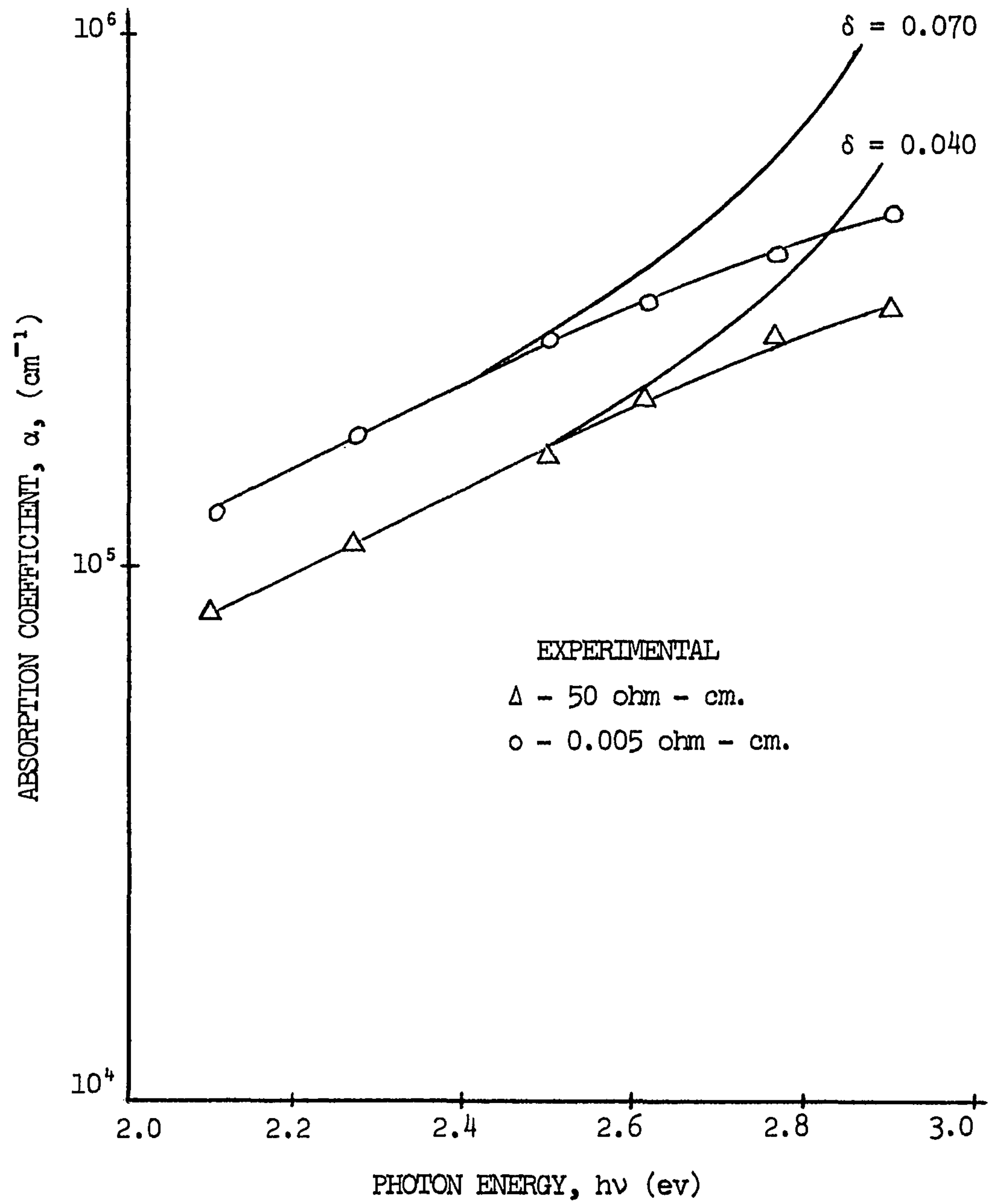

Figure 15.—Comparison between the semi-classical and measured absorption coefficients.

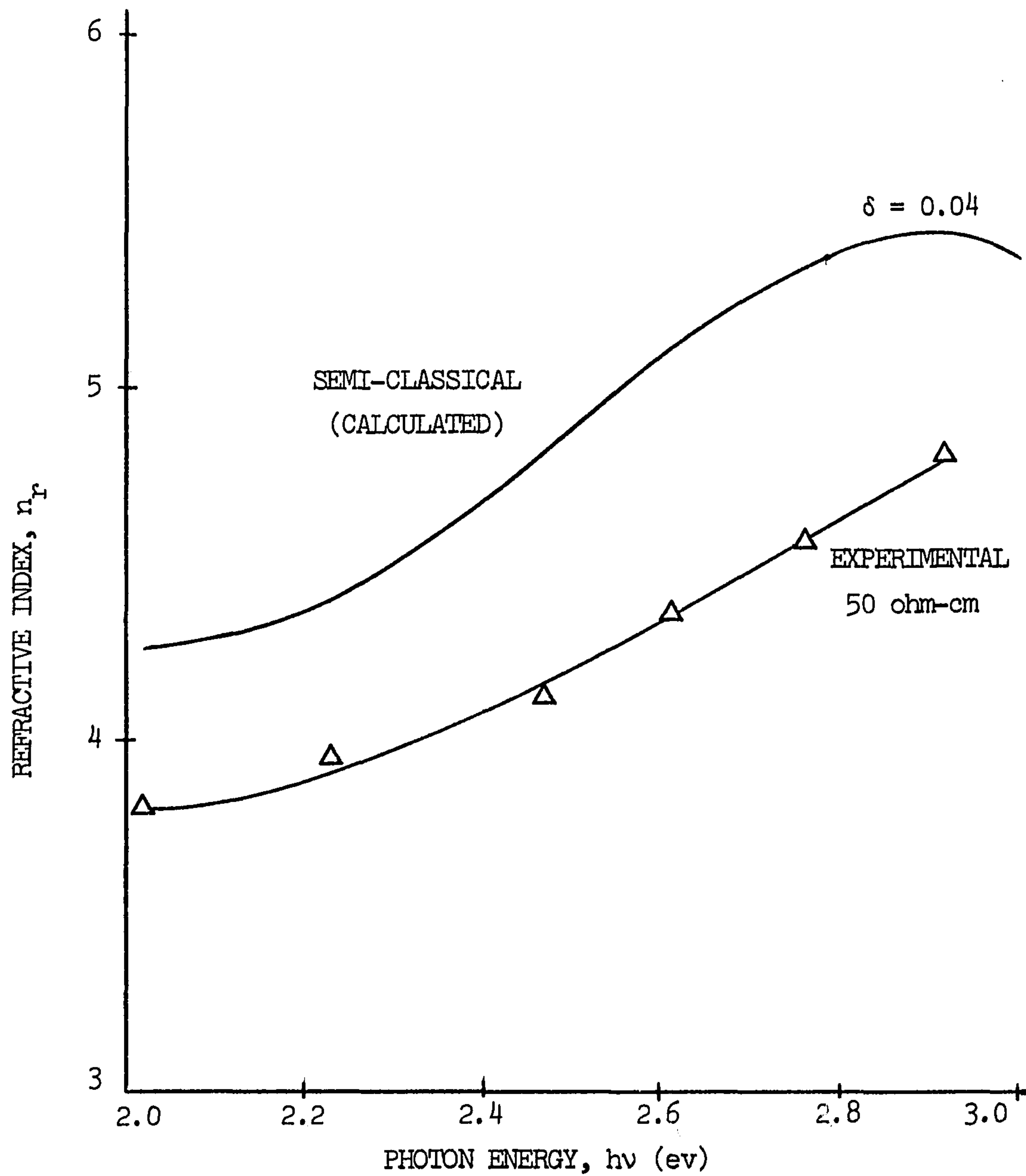

Figure 16.—Comparison between the semi-classical and measured refractive indices for nominal 50 ohm-cm p-type silicon.

error in the choice of ψ_o, whereas, the difference in the peaks is a result of the choice for E. The actual percent variation of the experimental value of n_r is small when compared to the corresponding percent variation in k (see Table 1). From equations (25) and (27), then, it is apparent that the experimental optical conductivity, σ varies very nearly as the absorption coefficient α, consequently, in further discussion it is only necessary to consider the absorption coefficient.

The values of the absorption coefficient obtained experimentally are compared with results of the quantum mechanical model given by tables 3 and 4. The curve in figure 17 shows the results of the experimental absorption coefficient for 50 ohm-cm silicon, which is compared with an ideal quantum mechanical model of near intrinsic silicon. Although the curves are similar, the absorption coefficient for the experimental curve is an order of magnitude larger than the ideal quantum mechanical predictions.

4.2 Dependence of Absorption on Radiation Energy

The absorption characteristics of a semiconductor, in general, are dependent on the number of electron and hole states which are available. This has been discussed in section (2.4) as the anomalous absorption explained by Burstein [72] and Moss [73]. The calculated effect of available states in the conduction band on the absorption in germanium at 4.2°K has been given by Pankove and Aigrain [76]. The calculated effect indicates that the extrapolated band gap

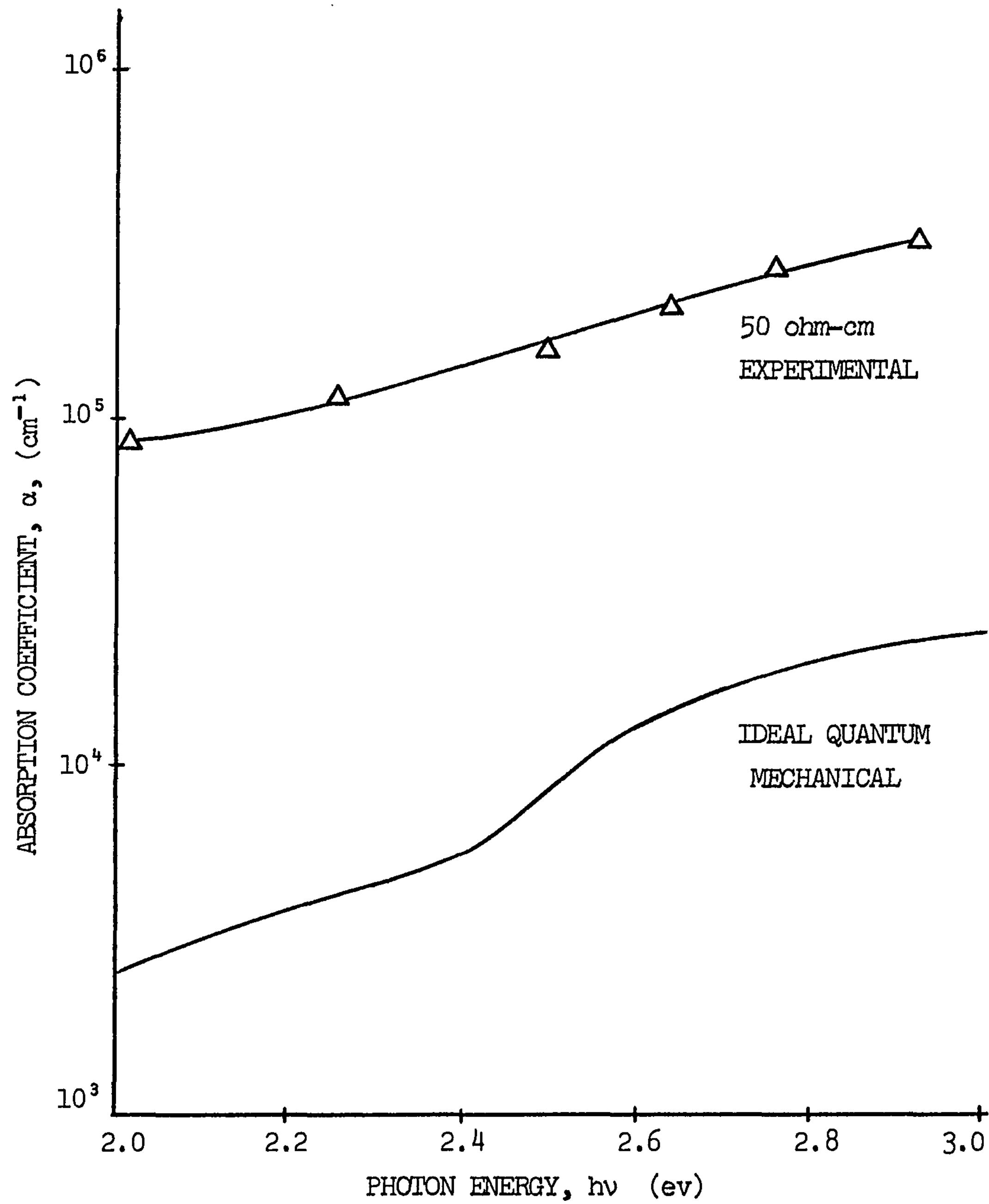

Figure 17.—Comparison between the experimental and ideal absorption coefficient for silicon.

increases with doping at 4.2°K. Experimental evidence [76], [78], however, has shown that the extrapolated band gap for germanium decreases with doping at 4.2°K. This indicates that the anomalous effect is negligible in indirect band gap materials such as germanium.

The experimental data obtained in this study for p-type silicon also shows that the extrapolated band gap decreases with doping at room temperature. The anomalous effect is also not noticeable for silicon which is also considered an indirect band gap semiconductor. Semiconductors in which the indirect process is predominant, apparently mask the anomalous effect and consequently the effect is not observed. The effect is significant because its tends to decrease the absorption as the doping increases. Therefore, it must be considered as part of the absorption process when the data is analyzed.

The absorption curves for 0.005 ohm-cm and 50 ohm-cm p-type silicon are shown in figure 18. The absorption coefficient, α, is plotted versus the quantity, $(h\nu - E_{ge})$, where E_{ge} will be defined as the effective band gap. The values of the indirect band gap (≈ 1.1ev) and the direct band gap (≈ 2.6ev) are known for intrinsic silicon. The corresponding absorption characteristics vary as the square of the energy above the indirect gap, E_{gi}, and the one half power of the energy above the direct gap, E_{gd}. One possibility is to consider that the straight line extrapolated value for the experimental curve (for energies in the range of two to three electron volts) should have a value between E_{gi} and E_{gd}. Another choice for E_{ge} is to consider that

the process of absorption is predominantly due to an indirect process, thereby making it difficult to discern the effect due to a direct process. In this case, it can be assumed that $E_{ge} = E_{gi}$. The two curves shown in figure 18 are plotted for $E_{ge} = E_{gi} = 1.1$ ev for both materials. The curves both have a slope of approximately two which indicates that the absorption process is predominantly indirect. It is reasonable to assume that the direct band gap for the 50 ohm-cm silicon is 1.1 ev because it is relatively lightly doped. The 0.005 ohm-cm material will have an indirect band gap which is less, because of band shrinkage. It is not possible, however, to determine the band shrinkage unless data is taken in the infra-red. Also, anomalous absorption may play an important role by compensating for the band shrinkage. The curves in figure 19 shows how the slope varies when E_{ge} has the values of 1.1 ev and 1.5 ev. The slopes are 2.0 and 1.2 respectively. A larger value for E_{ge} will result in a smaller slope.

4.3 Low Frequency Conductivity

The value of the low frequency conductivity of silicon can be inferred from its absorption characteristics. This is accomplished by the comparison of the absorption coefficients for two different conductivities, one of which is used as the reference. The general relationship which exists between the two conductivities has been presented in the theory in section 2.5 (c) by equation (140). The specific case in which both samples are doped so that simplifying assumptions can be made is given by equation (141). The samples studied in this thesis are doped sufficiently so that equation (141)

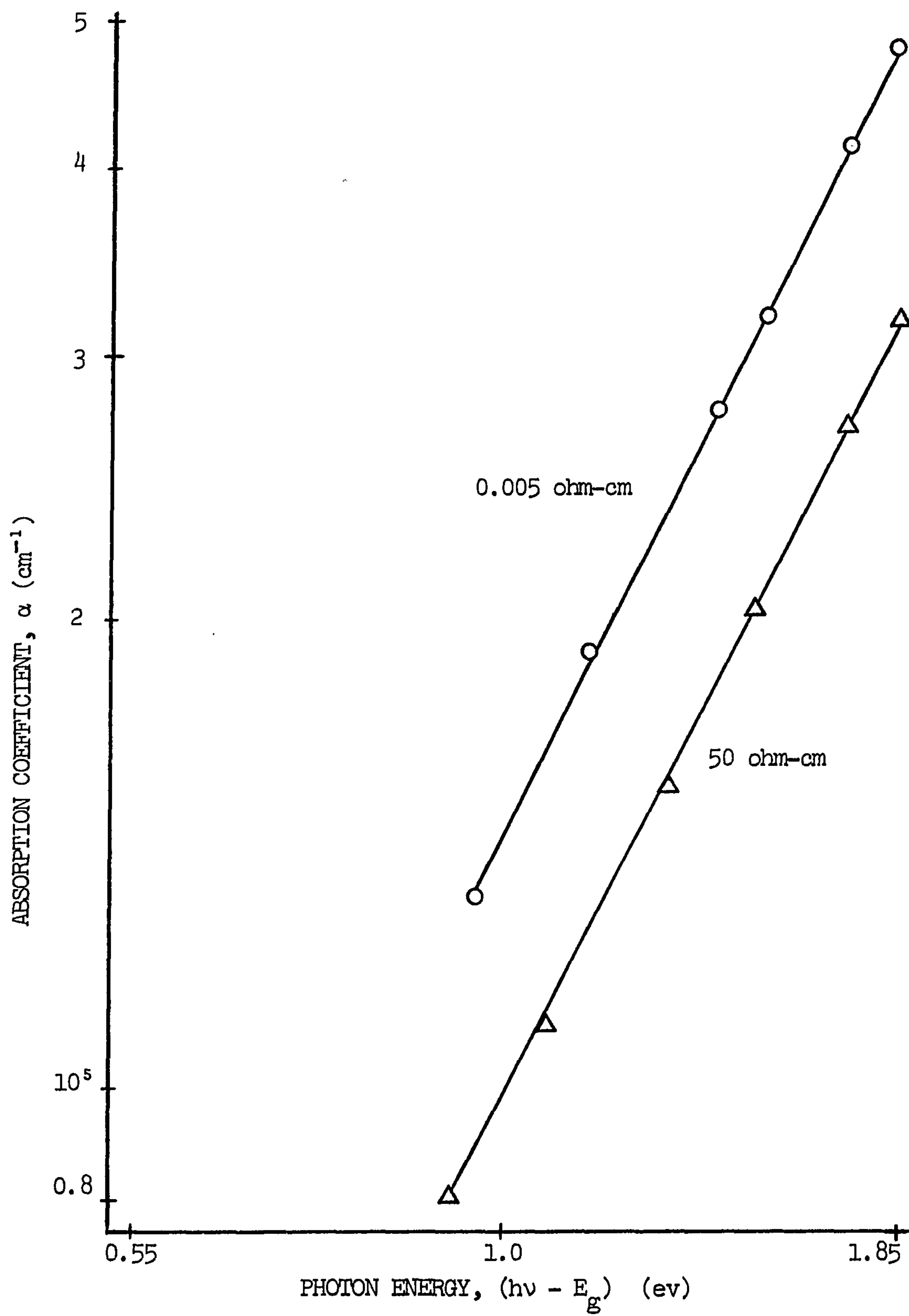

Figure 18.—Absorption characteristics for silicon when E_g = 1.1 ev.

holds. The absorption characteristics for two p-type, nominal conductivity 50 ohm-cm and 0.005 ohm-cm, are shown in figure 20. The logarithm-logarithm plot is used in figure 20 and this appears to give the best fit for a straight line relationship. It appears that the slopes are about the same, although by measurement the 50 ohm-cm has a slope of 3.8, and the 0.005 ohm-cm a slope of 3.5. A direct interpolation of these curves to the vicinity of the band gap, however, will not yield the absorption coefficient for low frequencies. The absorption coefficient is a complex parameter which is frequency dependent and is of the form

$$\alpha = \alpha_o (\nu) + \alpha' (\nu) \tag{160}$$

where $\alpha_o (\nu)$ is the absorption coefficient below the absorption edge (band gap). Free carrier absorption becomes important near but below the band edge (see 2.2(b)), and then eventually $\alpha_o (\nu)$ becomes relatively constant. The term $\alpha'(\nu)$ has a value of zero when $h\nu \leq E_g$, otherwise, its value is essentially determined by an expression which has the same form as given by equation (90) namely

$$\alpha' (\nu) = A (h\nu - E_g)^n \tag{161}$$

The low frequency absorption coefficient can be measured for silicon

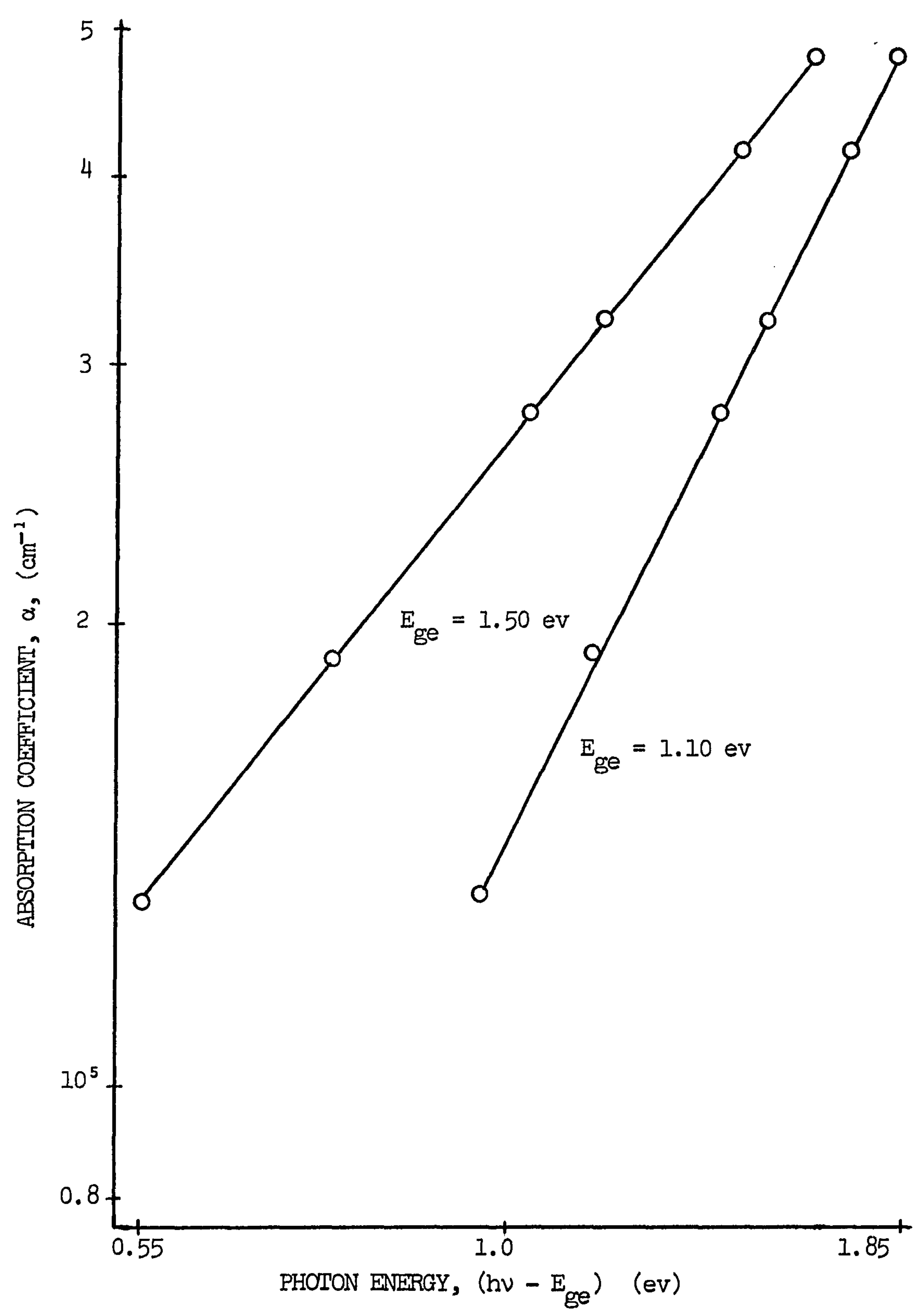

Figure 19.—Absorption characteristics for 0.005 ohm-cm silicon.

if the radiation is 12000 Å or greater. These wavelengths are in the infra-red region and have not been explored in this study. It is therefore not possible to determine either the absorption coefficient α_o (ν) or the band gap of silicon. The band gap for intrinsic silicon at different temperatures, however, is known with a reasonable degree of accuracy. It is also known that there is an effective shrinkage of the band gap with doping,

The curves plotted in figure 20 are significant because they indicate a shift in energy between the two curves. The energy shift is caused by an effective band shrinkage and the shift in the Fermi level. Both of these quantities determine the carrier density which in turn has an effect on the absorption coefficient. The energy shift, ΔE_d, measured as the horizontal difference between the two curves is found to be approximately 0.25 ev. The kt energy at room temperature is 0.26 ev and the mobility of holes in the p materials are assumed to be equal, so that $\mu_{p2} = \mu_{p1}$. This assumption however is valid if one sample is doped within an order of magnitude of the other. When this assumption is made, then equation (141) and the conductivity σ, known to have a nominal value of 0.02 mho/cm, yields a calculated value of 300 mho/cm for σ_2. The nominal value for σ, as measured by a four point probe is given as 200 mho/cm. The discrepancy can be resolved by considering that the mobilities μ_{p1} and μ_{p2} are not equal. This is evident since the conductivities are not within an order of magnitude, consequently, neither are their majority carriers. The mobility μ_{p2} corresponding to the higher

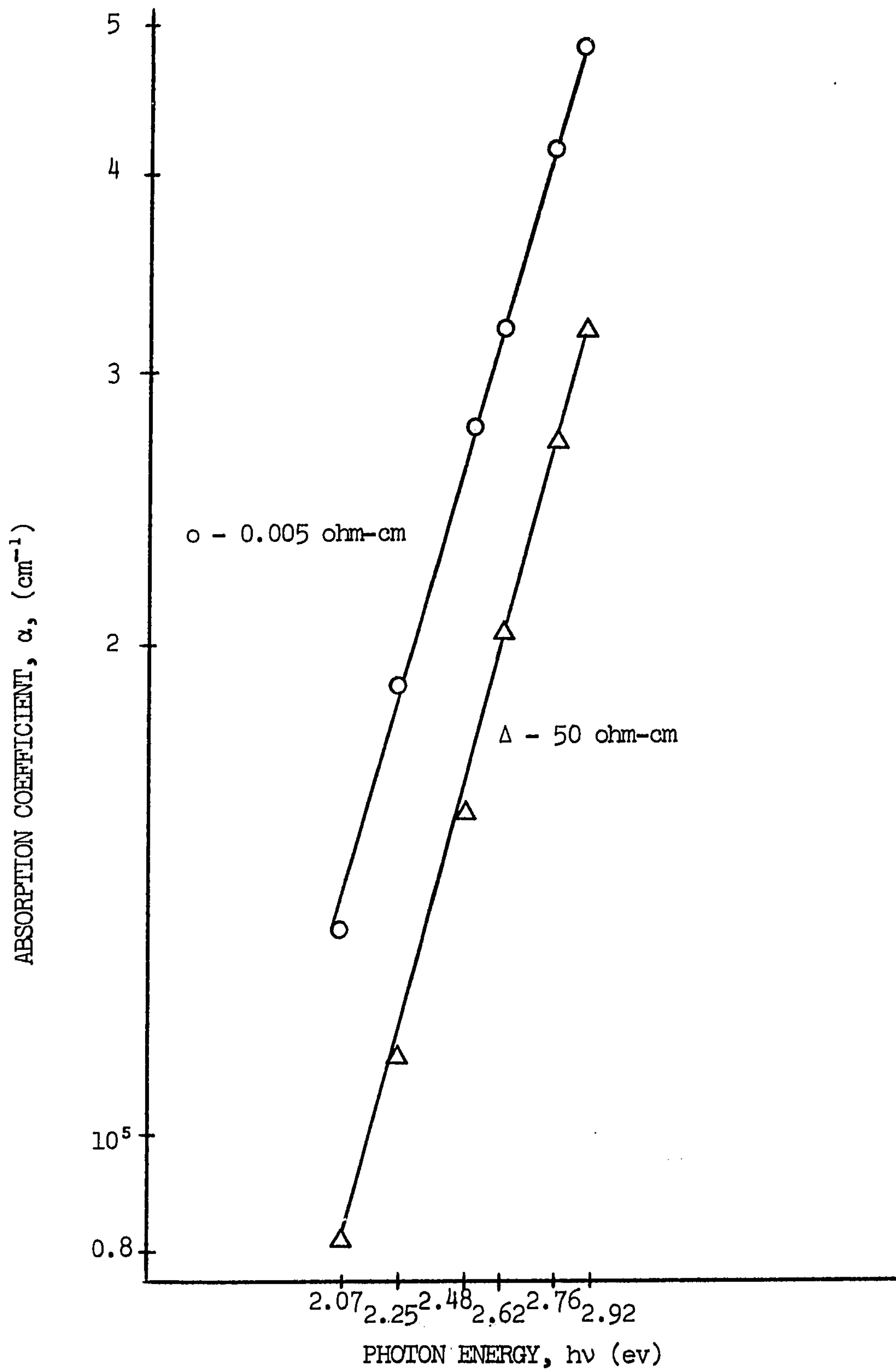

Figure 20.—Experimental absorption coefficient for p-type silicon.

conductivity material is less than the mobility μ_{p1}. The drift mobility for holes, μ_{p1}, in p-type 0.02 mho/cm silicon is about 500 cm^2 - $volt^{-1}$ - sec^{-1} and can be extrapolated to a μ_{p2} of 350 cm^2 - $volt^{-1}$- sec^{-1} for conductivities greater than 1 mho/cm [48]. Then if equation (141) is used, a value of 210 mho/cm is found for σ_2 which is in very good agreement with the conductivity (200 mho/cm) as measured by the four point probe. The results for six additional (111) p type silicon samples (surfaces etched) illustrating the important role played by the mobility is given in Appendix B.

The value of the conductivity σ_2 as has been shown is determined from the displacement, ΔE_d, between the straight lime plots illustrated in figure 20. The conductivity σ_2 is independent of the radiation as is evident by close inspection of the plot. The ruled measurement of ΔE_d at a lower absorption is greater than that obtained at a higher absorption. This results in a ΔE_d in energy units of electron volts (ev) which is independent of the absorption.

CHAPTER 5

DISCUSSION

The absorption coefficient, α, has been shown to be a sensitive function of the doping in the semiconductor silicon. The variation of α with radiation energy has been investigated in this study. The absorption coefficient is defined as a general relationship by equation (27) and the related conductivity by equation (25). Using (25) and (27), the absorption coefficient in terms of the conductivity, σ, is

$$\alpha = \frac{120 \pi \sigma}{n_r}$$

The conductivity, σ, is the value measured at the frequency of the radiation, which is in the visible range for this study. The value of σ in this region is greater than the low frequency conductivity by several orders of magnitude. In this visible region it is commonly referred to as the optical conductivity.

The Theory and Results have been presented in terms of the absorption coefficient α rather than the optical conductivity, σ, because α appears to have more physical meaning than σ. The value of σ, however, is readily obtained from α because n_r has been measured.

With the absorption coefficient defined in general, from (25) as,

$$\alpha = \frac{4\pi k}{\lambda}$$

it is necessary that k be measured so that the experimental value of α can be compared with possible physical models.

The semi-classical model was the first model chosen, because it appeared to be the one which is most fundamental. Also, the similar but modified model for free carrier absorption has been successful in explaining absorption just below the absorption edge. The semi-classical model considers that the charge carriers are bound elastically to the atoms, and are forced to oscillate when subjected to a radiation field. The restoring force between the charge carriers and the atoms are assumed to follow Hooke's law, and the dissipation is in part accounted for by a damping coefficient. The model has been modified from the Clausius-Moscotti [51], [52], and Lorentz-Lorenz [53], [54] form, by replacing the dielectric constant and the refractive index by complex quantities. The resulting equations for n_r and k are given by equations (66) and (67). The values of n_r and α based on calculations using these equations for two different values of the damping constant, δ, are given in table 2. The values of δ have been chosen so as to give the best fit to the experimental α given in table 1. The comparison between the curves shown in figure 15 shows that as expected, the larger damping constant corresponds to the larger conductivity sample.

The semi-classical characteristics also have some other interesting properties. The value of n_r asymptotically approaches the accepted value of the refractive index (3.42) as the wavelength of the radiation increases. Equations (66) and (67) also show that n_r approaches a peak and then eventually will reach a value of unity for decreasing wavelengths. It has been shown by Philipp and Taft [34] that the peak value of n_r for silicon is 7.0 and occurs at 3.3 ev. The comparison between the semi-classical and measured n_r given in figure 14 shows a similarity in the shape of the two curves. The displacement between the two curves has been explained in section 4.1 of the Results.

The equations for the semi-classical model also shows that the absorption coefficient will peak (although not shown in figure 15) and then approach a small value with decreasing wavelength. The value of α also decreases with increasing wavelength, which again agrees with experiment [34]. The decrease, however, is a linear change and not an abrupt change, as is observed experimentally. The sudden increase in the absorption coefficient which takes place at the absorption edge (band gap) in semiconductors is caused by the quantum effect. Below this value the absorption is small as determined experimentally [34]. It is below this edge where the semi-classical model gives an absorption coefficient which is too large when compared to the experimental results. The semi-classical model can therefore not be considered to be valid in this region. Below the absorption edge, however, the modified semi-classical model in

which the elastic restoring force is eliminated, (see section 2.2(b)) results in a free carrier absorption model, which is in good agreement with experiment.

The region above the band gap energy (absorption edge) is physically best described by a quantum mechanical model. The absorption coefficient curve, derived from the quantum mechanical model, is in better agreement with the experimental curve than that obtained by the semi-classical model. The ideal quantum model assumes that the value of the absorption coefficient is zero below the absorption edge. This is in reality not true, because of dissipation of energy by other non-quantum effects, such as processes involving inelastic collisions. Inelastic processes by charge carriers for energies above the band gap also take place in real materials, consequently causing an increase in the absorption coefficient. This should not however, in general, be expected to result in an increase in the measured absorption coefficient, because of other compensating effects such as the anomalous effect [72], [73]. When the anomalous effect is negligible as it is for silicon, then the measured absorption coefficient will be larger than that assumed by the ideal quantum mechanical model.

The ideal quantum model for band gap materials includes transitions which are allowed and those which are forbidden. In addition, transitions can be direct or indirect. The ideal quantum mechanical curve for allowed transitions is shown in figure 17. This composite curve for silicon consists of an indirect transition

for energies above 1.1 ev, and a direct transition for energies greater than about 2.6 ev. It is assumed that there is no inherent absorption below the indirect band gap. Because the anomalous effect is negligible for indirect processes, it can be assumed that the values of the quantum absorption curve should be greater than those shown. The S shape curve is caused by the onset of direct transitions which occur at about 2.6 ev. The curve (indirect transitions) to about 2.6 ev varies as the square of the radiation energy in excess of 1.1 ev, whereas for energies greater than 2.6 ev, the value of α is determined by direct and indirect processes.

The experimental data for the absorption coefficient given in table 1 for 50 ohm-cm and 0.005 ohm-cm is plotted in figure 15. The curves show that the absorption coefficient does increase with the doping concentration, indicating that there is no apparent anomalous effect. The increase in the absorption coefficient with the radiation can be explained by considering equation (160)

$$\alpha = \alpha_o (\nu) + A (h\nu - E_g)^n$$

There are two possibilities which must be investigated when considering this expression. Either the inherent absorption term $\alpha_o (\nu)$ is negligible when compared to the second term, or it is appreciable and must be taken into account.

When the absorption term α_o (ν) is set equal to zero, and the absorption coefficient for 50 ohm-cm is taken from table 1 as α_1 = 1.90×10^5 cm^{-1} for $h\nu_1$ = 2.25 ev and α_2 = 3.15×10^5 cm^{-1} for $h\nu_2$ = 2.62 ev, the value of n is found to be equal to 2.16 if E_g = 1.10 ev. When E_g is considered to be an extrapolated effective value (see section 4.2) and is taken as E_g = 1.50 ev, then the value of n is found to be equal to 1.48. The corresponding values of n for the 0.005 ohm-cm sample were found to be 1.83 and 1.25 for respective values of E_g of 1.1 ev and 1.5 ev.

When the indirect band gap is chosen for E_g, the value of n is 2.16 for the 50 ohm-cm sample and 1.83 for the 0.005 ohm-cm material. The higher conductivity material has a smaller band gap caused by band shrinkage, and will result in a greater n value. Calculations show that n = 2.0 when E_g is assumed to be 1.0 ev for the 0.005 ohm-cm sample.

The results obtained for n are significantly different when the value of α_o (ν) is not negligible. When the following set of equations are solved for n,

$$\alpha_k = \alpha_o + A\ (h\nu_k - E_g)^n$$

where α_1 = 1.13×10^5 cm^{-1}, $h\nu_1$ = 2.25 ev; α_2 = 2.06×10^5 cm^{-1}, $h\nu_2$ = 2.62 ev; α_3 = 1.58×10^5 cm^{-1}, $h\nu_3$ = 2.48 ev; the value of n

can be either 0.5 or 2.2 for the 50 ohm-cm sample.

The result of 0.49 for n implies that the absorption coefficient is due to a direct transition. This is not in agreement with the curves of figures 18 and 19. In particular, the 50 ohm-cm material is very lightly doped so that its inherent absorption α_o (ν) can be considered negligible. Also the indirect band gap can be considered to be 1.10 ev for the 50 ohm-cm material. The slope, n, is found to be 2.0, and even for a curve extrapolated effective band gap of E_{ge} = 1.5, the value of n = 1.65. Further, transitions which are predominantly direct, may cause an anomalous effect which has not been observed.

From the results and the discussion pertaining to the silicon samples it appears that the value of n can have values ranging from about 1/2 to 2. However, the results seem to favor the value for n = 2. This can be verified experimentally by further investigation of the absorption at lower energies. The direct band gap occurs at about 2.6 ev and data may have to be taken at energies significantly above this value in order to determine its slope. The highest energy of the radiation used in this study was 2.92 ev; it was limited by the overall response of the experimental system.

The absorption coefficient for the 50 ohm-cm sample is compared with that of the ideal quantum model. The two curves are shown in figure 17. The experimental curve is about one order of magnitude greater for all wavelengths. It has already been mentioned that the

quantum model neglects inherent absorption. When the inherent absorption is considered, the quantum mechanical curve will be increased by a constant amount. The effect on the log-linear plot is an increase in absorption at all wavelengths and a flattening of the S shape. The flattening of the S shape results in a curve which is in better agreement with the experimental curve.

The argument which strongly favored indirect transitions ($n = 2$) was based on the assumption that the inherent absorption, $\alpha_o(\nu)$, was small when compared to the experimental curve, but not small when compared to the quantum model. Consequently an amount, $\alpha_o(\nu)$, must be added to the ideal quantum curve, but can not be too large. Therefore, it appears that some other factors must be considered which can account for a lower experimental curve.

A surface film which may be present on a silicon wafer will increase the measured intensity of the reflected beam. This will result in an increase in the calculated absorption. Because it is reasonable to assume that a surface layer can exist, it is also valid to expect that the true absorption should be less than that shown by figure 17. The effect of a surface film has been presented in section 2.5 (b) of the theory. The expression for the reflectance of the component of the electric field parallel to the plane of incidence, r_p, is given by equation (121). This expression includes the effect of a surface layer of thickness, d. This expression which gives the reflectance, r_{po}, in which it is assumed that there is no surface layer, is given by equation (122).

The effects of the surface layer can be determined by considering the change the absorption caused by surface layers of different thicknesses. The change is given by

$$\frac{\Delta\alpha}{\alpha_o} = \frac{\alpha_d - \alpha_o}{\alpha_o}$$

in which α_d is the total absorption due to the silicon wafer and its surface oxide layer, d. The value α_o is the absorption due to the silicon wafer alone. Equation (122) is used to find r_{po} at the polarizing angle, θ_p, of the silicon wafer. A polarizing angle of 80° measured at a wavelength of 4000 Å results in an r_{po} of 0.093% and a θ_p of 75.8° at 6000 Å yields an r_{po} of 0.719%. The absorption at the two wavelengths then can be found from (27), (104) and (105). The absorption caused by a silicon dioxide layer of refractive index 1.8 on a silicon wafer, is determined by finding r_p at 4000 Å and then at 6000 Å. Because the polarizing angles are large, the value of r_s can be considered to be approximately equal to unity (see figure 5). Then, it follows that $R_s \simeq 1$, because E_s and E_p are both equal to unity, consequently, α_d and α_o, can be readily found from (104).

The variation in the absorption coefficient of a silicon wafer caused by a surface silicon dioxide layer of 10 Å and 20 Å is given in table 5. The calculations show that a maximum error of 20% in

the absorption coefficient occurs at the shortest wavelength when the oxide layer is 20 Å thick. The ratio $\Delta\alpha/\alpha_o$ was calculated using K and assuming that n_r in (103) is the same for the oxide as for the silicon. An effective value for n_r which should be used will result in a smaller absorption and an error less than those shown in table 5. Therefore, the values shown in table 5 are maximum for their respective oxide layers.

The purpose of the previous discussion on surface layers was to show that they can cause errors in the absorption coefficient. In fact, it results in a measured value of α which is too large. A 20 Å silicon dioxide layer will therefore result in an absorption coefficient which is 20% too large at 4000 Å (3.10 ev) and 16.8% too large at 6000 Å (2.07 ev). Although care was taken in preparing the surfaces, it is reasonable to assume that in practice, a 20 Å layer can be formed at room temperature.

The true absorption coefficient for the 50 ohm-cm silicon is therefore smaller for all wavelengths than those shown in figure 17. If the values of the oxide thickness and the inherent absorption, α_o (ν) (infra-red wavelengths) were known, the experimental curve will be found to be in very good agreement with the quantum mechanical curve.

It has been shown in section 4.3, that the low frequency conductivity of silicon can be determined from its absorption of visible radiation. The absorption curve must be compared to the absorption

TABLE 5

EFFECT OF A SURFACE LAYER

$\frac{\Delta\alpha}{\alpha_o}$ (%)	d (Å)	λ (Å)	θ_p (DEGREES)	K	r_p (%)
0	0	6000	75.83	0.0610	0.093
4.3	10.0	6000	75.83	0.0636	0.101
16.8	20.0	6000	75.83	0.0713	0.127
0	0	4000	80.00	0.1709	0.719
5.9	10.0	4000	80.00	0.1804	0.801
20.0	20.0	4000	80.00	0.2064	1.043
94.2	50.0	4000	80.00	0.3350	2.662

curve for a silicon sample of known conductivity. When the general case is considered, it is necessary that equation (140) be used. The minority carrier densities and minority mobilities must then be known. These quantities, however, may not be known unless the conductivity is known. But, if the conductivity σ, is used as the known value, and it is intrinsic, then the value $\Delta E_{a1} = 0$. When both samples are silicon, then $n_{i1} = n_{i2} = n_i$ and equation (140) becomes

$$\frac{\sigma_2}{\sigma_1} = \frac{\mu_{p2}\, e^{\Delta E_{d/kt}}}{(\mu_{p1} + \mu_{n1})} + \frac{\mu_{n2} \quad n_i}{(\mu_{p1} + \mu_{n1})\; p} \qquad (140a)$$

The values of μ_{n1} and μ_{p1} are known for the intrinsic material to be 1500 and 500 cm^2 - $volt^{-1}$ - sec^{-1} respectively. The value of n_i for silicon at room temperature is also known to be 1.6×10^{10} cm^{-3}.

The low frequency conductivity, σ_2 can be found by first considering that

$$\frac{\sigma_2}{\sigma_1} = e^{\Delta E_{d/kt}}$$

The conductivity σ_2 determined by this expression for a known ΔE_d is then used to determine μ_{p2}, μ_{n2}, and p [47], [48]. Using these

values in (140a) then determines the conductivity σ_2 more precisely. Each trial will theoretically give a more accurate value, however, the parameters are not rapidly varying function of the conductivity, so that in practice it is only necessary to use (140a) one time.

The expression for the low frequency conductivity given by equation (140), is dependent on the band shrinkage ΔE_s and the Fermi level shift ΔE. Both ΔE_s and ΔE increase with impurity concentration when the temperature remains constant. An increase in impurity concentration does lead to an increase in absorption.

It has been shown for germanium [76], that α is roughly proportional to doping. This, however, was shown to be valid only over a doping range from 5×10^{18} cm^{-3} to 4×10^{19} cm^{-3}. In fact, there is no proportional ratio when heavily doped germanium is compared with a pure sample. The n_i of a pure germanium sample is 2.5×10^{13} cm^{-3} and its absorption coefficient, α, as measured from curves [76] at 0.78 ev is about 4 cm^{-1}, whereas, α measured at the same energy is about 30 cm^{-1} for a doped sample of 5×10^{18} cm^{-3}. The absorption value, therefore, has increased by only about an order of magnitude, whereas the doping has increased by five orders of magnitude. The same condition exists for silicon as is shown by the results of this study. This is shown in figure 18 by the two curves for 0.005 ohm-cm and 50 ohm-cm, p-doped silicon. The conductivities differ by four orders of magnitude whereas the ratio of the absorption coefficients are about 1.5. There appears to be no fixed relationship between the absorption coefficient and the impurity concentration

for germanium and silicon, when a broad range of doping is considered.

It has been postulated in this thesis that a simple relationship does exist between the absorption coefficient, and the energy shift, ΔE_d, between the curves of figure 20. The energy shift, consists of both ΔE and ΔE_s which are both related to the impurity concentration. The results of section 4.3 are consistent with the theory given in section 2.5 (c).

There is a tendency for the curves of figure 20 to get closer together at the higher energies. This implies, as expected, that the energy shift ΔE_d is independent of radiation energy, $h\nu$. The tendency for this convergence can best be explained by considering equations (160) and (161) for two different conductivities. A plot of α versus $h\nu$ on a logarithm - logarithm plot, will indicate that the higher conductivity sample changes more slowly than the other sample. However the higher conductivity material will always have the higher absorption although the vertical difference in the absorption although the vertical difference in the absorption coefficient is constant. Consequently, the curve gets closer together at the higher energies.

The inherent absorption coefficient, α_o (ν) of the higher conductivity material can be assumed to be much greater than that of the 50 ohm-cm sample. Therefore, the vertical difference between the curves of figure 20, can be considered to be equal to the value of α_o (ν) for the 0.005 ohm-cm sample. The value of α_o (ν) will then

be about 10^5 cm^{-1}, indicating that the 0.005 ohm-cm curve intercepts the energy axis at about 1.9 ev. This makes it impossible to determine the direct band gap by an intercept method, because, $\alpha_o(\nu)$ is almost constant over a wide range of energies (approximately 1.0 ev). The effect of an energy gap, however, is not obscured when measured by energies in the visible region. Verification of the exact variation of the value of $\alpha_o(\nu)$, can be determined only by absorption data for energies up to and below the direct gap of about 1.1 ev.

Although the increase in carriers due to the photon flux intensity used in this study, has been shown in section 3.3 to be negligible, it should be realized that large increases in intensity can cause errors in the measurement of the absorption coefficient.

The main sources of error in the measurement of the absorption coefficient is due to the surface oxide layer, and has already been considered in detail in this section. However, it should be realized that the values for the resistivities of the samples were obtained by the four point probe method. The method, although commonly employed, can not be considered to give measured values to much better than ± 25% for the samples used in the study.

Conclusion

The data and calculations presented in the body of the text and in the Appendices indicates that the absorption follows the expected relationships. These relationships which assume a quantum mechanical model of absorption, predict that the absorption should vary as the square of the photon energy which is in excess of the indirect gat, and as the one half power of the photon energy in excess of the direct gap. The curves in Appendix B confirm these predictions. These curves also indicate that direct transitions occur consistently at 2.48 ev implying that this is the energy for the direct gap.

The hypothesis that the absorption is due to an intrinsic quantum mechanical effect and proportional to the carrier density is also verified by the experimental results. The horizontal energy shift between the curves shows that these displacements shift to the left as the conductivity increases. The measured conductivities as determined by these shifts in energies and the expressions derived in the Theory and Appendix A, indicate reasonable agreement with measurements obtained by the four point probe (See Table 4B).

The most apparent advantage of the optical method presented in this study is that it has the potential to be adaptable into a system of rapid scanning. The scanning can be utilized either in production processing of materials or as a research tool. The spot size of the photon beam can be adjusted and made small enough so that changes in conductivity over a small contour can be measured. It is true, however, that the

resolution and accuracy of the apparatus must be better than that used in this study if very small changes in resistivity values are to be obtained.

The optical method also eliminates the errors caused by contact methods and perhaps more significantly is independent of the geometry. Further, it can be readily employed to make measurements on materials at all temperatures, which is not always possible or at least is sometimes objectionable when contacts are used.

REFERENCES

1. G. L. Pearson and J. Bardeen, Phys. Rev. 75, 865-883 (1949).

2. F. J. Morin and J. P. Maita, Phys. Rev. 96, 28-35 (1954).

3. Holm, R., Electric Contacts (Eng. trans.), Hugo Gebers Forlag, Stockholm, 1946.

4. J. Bardeen, Theory of relation between hole concentration and characteristics of germanium point contacts, Bell Sys. Tech. Jour., vol. 29, pp. 469-495; October, 1950.

5. W. Shockley, Electrons and Holes in Semiconductors, Van Nostrand, New York, 1950, Chapter 3.

6. W. Schottky, Zeits F. Physik, 118, 539 (1942).

7. N. F. Mott and R. W. Gurney, Electronic Processes in Ionic Crystals, Oxford University Press, London, 1940.

8. W. E. Meyerhof, Contact Potential Difference in Silicon Crystal Rectifiers, Phys. Rev., vol. 71, pp. 727-735, May 15, 1947.

9. I. Tamm, Uber eine mogliche Art der Elektronenbindung an Kristallober flachen, Physik, Z. Sowjetunion, vol. 1, pp. 733-746, June, 1932.

10. J. Bardeen, Surface States and Rectification at a Metal Semiconductor Contact, Phys. Rev., vol. 71, pp. 717-727, May 15, 1947.

11. W. H. Brattain and J. Bardeen, Surface Properties of Germanium, Bell System Tech. J., vol. 32, pp. 1-41, Jan., 1953.

12. J. Bardeen and S. R. Morrison, Surface Barriers and Surface Conductance, Physics, vol. 20, pp. 873-884, November, 1954.

13. J. Bardeen, R. E. Coovert, S. R. Morrison, J. R. Schrieffer and R. Sun, Surface Conductance and the Field Effect on Germanium, Phys. Rev., vol. 104, pp. 47-51, October 1, 1956.

14. W. Shockley and G. L. Pearson, Phys. Rev., 74, 232 (1948).

15. R. N. Hall, Phys. Rev., vol. 87, p. 387, July 15, 1952.

16. E. M. Pell, G. M. Roe, J. Appl. Phys., vol. 27, p. 769, July, 1956.

17. Valdes, L., Resistivity Measurements on Germanium for Transistors, Proc. I. R. E., 42. Feb., 1954, p. 420.

18. E. E. Gardner and P. A. Schumann, Jr., Solid State Electronics, 8, 165 (1965).

19. J. Shields, J. Electron. Control 4, 544 (1958).

20. Z. S. Gribnikov, Sov. Phys. Solid-State 2, 782 (1960).

21. G. Conrad and S. Fine, Proc. Instrn. Elect. Electron. Engers. 51, 405 (1963).

22. E. E. Gardner, J. F. Hallenback, Jr., and P. A. Schumann, Jr., Solid State Electronics, 6, 311 (1963).

23. H. A. Lorentz, Theory of Electronics (Teubner, Leipzig, 1906).

24. P. Drude, The Theory of Optics (Longmans, Green and Company), New York, 1902.

25. C. Zener, Nature, 132, 968 (1933).

26. R. B. Barnes and M. Czerny, Phys. Rev. 38, 338 (1931).

27. P. Drude, op.cit.

28. B. Tousey, J. Opt. Soc. Am. 29, 235 (1939).

29. D. Avery, Proc. Phys. Soc. (London) B65, 425 (1952).

30. H. M. O'Bryan, J. Opt. Soc. Am. 26, 122 (1936).

31. W. H. Brattain and H. B. Briggs, Phys. Rev., 75, 1705 (1949).

32. R. J. Archer, Phys. Rev., 110, 354, (1958).

33. H. R. Philipp and E. A. Taft, Phys. Rev., 113, 1002 (1959).

34. H. R. Philipp and E. A. Taft, Phys. Rev., 120, 37 (1960).

35. W. C. Dash and R. Newman, Phys. Rev., 99, 1151 (1955).

36. R. W. Ditchburn, J. Opt. Soc. Am. 45, 743 (1955).

37. R. M. Emberson, J. Opt. Soc. Am. 26, 443 (1936).

38. P. A. Schumann, Jr., W. A. Keenan, A. H. Tong, H. H. Gegenwarth, and C. P. Schneider, J. Electrochem. Soc. Solid State Science, 118, 145 (1971).

39. P. A. Schumann, Jr., and R. P. Phillips, Solid State Electron., 10, 943 (1967).

40. W. A. Keenan, C. J. Liu, and C. P. Schneider, J. Electro-chem. Soc., Solid State Science and Technology, 119, 522, (1972).

41. H. A. Kramers, Atti Congr. Fis., Como (1927), p. 545.

42. R. Kronig, J. Opt. Soc. Am. 12, 547 (1926).

43. H. Bode, Network Analysis and Feedback Amplifier Design (D. Van Nostrand Company, Inc., Princeton, New Jersey, 1945).

44. T. S. Robinson, Proc. Phys. Soc. (London) B65, 910 (1952).

45. W. Shockley, Bell System Tech. J. (1951), 30, 990.

46. J. Electron, (1956), 2, 145.

47. M. B. Prince, Phys. Rev. 92, 681 (1953).

48. M. B. Prince, Phys. Rev. 93, 1204 (1954).

49. L. Cauchy, Bull. des. sc. math., 14 (1830), 9.

50. L. Cauchy, Sur la dispersion de la lumière (Nouv. exerc. de math, 1836).

51. Clausius, R., Mechanische Wärmetheorie, 2, (Braunschweig, 2nd ed. 1879), p. 62.

52. Mossotti, O. F., Mem. Soc. Sci. Modena, 14 (1850), p. 49.

53. H. A. Lorentz, Wiedem. Ann., 9 (1880), 641.

54. L. Lorenz, Wiedem. Ann., 11 (1881), 70.

55. P. Debye, Polar Molecules, Chemical Catalog Co., New York, 1929, Chap. V.

56. F. Seitz, The Modern Theory of Solids, (McGraw-Hill Book Company, Inc., New York, 1940), pp. 638-642.

57. H. Y. Fan, M. L. Shepherd and W. Spitzer, Proceedings of Atlantic City Photoconductivity Conference, (John Wiley and Sons, and Chapman and Hall, 1956), p. 184.

58. F. Herman, Phys. Rev., 88, 1210 (1952); 93, 1214 (1954); Physica, 20, 801 (1954).

59. M. Cardona and F. H. Pollack, Phys. Rev., 142, 530, (1966).

60. F. Herman, Proc. Inst. Radio Engrs., 43, 1703 (1955).

61. M. M. Cohen, Introduction to the Quantum Theory of Semiconductors, Gordon and Breach Science Publishers, 1972, p. 154.

62. J. G. Dorfman, C. R. Acad. Sci. U. R. S. S., 81, 765, (1951).

63. R. B. Dingle, Proc. Roy. Soc. A, 212, 38, (1952).

64. W. Shockley, Phys. Rev., 90, 491, (1953).

65. G. Dresselhaus, A. F. Kip and C. Kittel, Phys. Rev., 92, 827, (1953).

66. E. Fermi, Nuclear Physics, University of Chicago Press, Chicago (1950), p. 142.

67. J. Bardeen, F. J. Blatt, and L. H. Hall, Proceedings of Atlantic City Photoconductivity Conference, (John Wiley and Sons, and Chapman and Hall, 1956), p. 146.

68. Ibid.

69. Ibid.

70. G. G. MacFarlane and V. Roberts, Phys. Rev., 97, 1714 (1955); ibid, 98, 1865, (1955).

71. M. Tanenbaum and H. B. Briggs, Phys. Rev., 91, 1561 (1953).

72. E. Burstein, Phys. Rev., 93, 632 (1954).

73. T. S. Moss, Proc. Phys. Soc. B, 76, 775 (1954).

74. C. Hass, Phys. Rev., 125, 1965 (1962).

75. S. M. Ryvkin, Physica Status Solidi, 11, 285 (1965).

76. J. I. Pankove and P. Aigrain, Phys. Rev., 126, 956 (1962).

77. Ibid.

78. J. I. Pankove, Progress in Semiconductors, 9, 48 (1965); ed. A. F. Gibson and R. E. Burgess, Heywood and Company.

79. M. Born and E. Wolf, Principles of Optics, Pergamon Press, 1959, p. 615.

80. O. S. Heavens, Optical Properties of Thin Solid Films, Butterworth Scientific Publications, London, 1955, pp. 55-56.

81. R. Messner, Zeiss Nachr, 4 (H9), 253, (1943).

82. K. Hammer, Z. Tech. Phys., 24, 169, (1943).

APPENDIX A

General Analysis Of Electrical Conductivity From The Absorptim Characteristics.

It has been shown in section 2.5 (c) that the electrical conductivity of a semiconductor sample can be determined from the absorption curve of the material. It must, however, be compared to the absorption curve of a semiconductor of known conductivity. The sample of known conductivity is measured by an accepted method such as the four point probe which is perhaps the most reliable of existing direct contact measuring methods. The four point probe does, however, have some disadvantages and measurements can vary significantly even when repeated measurements are taken by the same operator. Extreme precautions in the shielding of semiconductor samples and the four point probe apparatus is necessary in order to obtain consistent readings.

When the conductivity of the sample corresponding to the reference curve is known, the conductivity of any other sample can be determined if its absorption curve is compared to the reference curve. The shift between the curves represents a change in the apparent band gap which can be inferred from (135) to be caused by band shrinkage and the shift in Fermi level. When the same type semiconductor are used, then the expression given by (140) is used to find the unknown conductivity. This is, however, valid only when both semiconductors are non-degenerate. When the samples are of the same material, then the simpler expression given by (141) can be used. The term ΔEd represents the displacement between curves and should be measured at energies below the energy of direct transitions ($\approx$2.5 ev).

When a semiconductor sample becomes degenerate, the assumption of (129) cn no longer be made so that equation (130) is not valid. The expression for p must then be evaluated for the degenerate case.

The expression for p is given from (125) as

$$p = \int_{-\infty}^{E_V} c(E_V - E)^{\frac{1}{2}} \frac{e^{\frac{E-E_F}{KT}} dE}{1+e^{\frac{E-E_F}{KT}}} \tag{1A}$$

when $x = \frac{E_V - E}{KT}$, $\delta = \frac{E_V - E_F}{KT}$

and $c' = c\ (KT)^{3/2}$ then (1A) becomes

$$p = c' \int_{o}^{\infty} \frac{x^{\frac{1}{2}}\ dx}{1+e^{\ x-\delta}} \tag{2A}$$

When the semiconductor is normal (lightly doped), then the value of the integral in (2A) is the $\Gamma\ (3/2)$ so that p becomes the Boltzman approximation,

$$p_n = c'\ 2/3\ \ \delta_n^{\ 3/2} \tag{3A}$$

Under conditions of heavy doping so that a degenerate condition exists ($\delta > o$), it can be seen that the denominator (2A) is essentially unity until x approaches δ. For values of x greater than δ, the denominator increases much more rapidly than the numerator so that the contribution to the integral becomes negligible for $x > > \delta$ and the integral rapidly converges. Consequently, a reasonable approximation for equation (2A) under conditions of degeneracy is

$$p_d = c' \int_0^{\delta_d} x^{1/2}\,dx = c'\ {}^{2}/_{3}\ (\delta_d)^{3/2} \qquad (4A)$$

Using the expression in (3A) and (4A) and applying them to the ratio of two conductivities, one of which is degenerate (δ_2) , then

$$\frac{\sigma_2}{\sigma_1} \simeq \frac{\mu p_2\ P_2}{\mu p_1\ P_1} = \frac{\mu p_2\ C'\ {}^{2}/_{3}\ (\delta_2)^{3/2}}{\mu p_1\ C' \frac{\sqrt{\pi}}{2}\ e^{\delta_1}} \qquad (5A)$$

$$\frac{\sigma 2}{\sigma 1} = \frac{\mu p2}{\mu p1} \frac{4\ (\delta 2)^{3/2}}{3\sqrt{\pi}\ e^{\delta 1}}$$

The expression (5A) will give the true conductivity for μ_2. However, the Boltzmann approximation was used for P_2 in the measurement of the energy shift ΔE_D, therefore the measured conductivity ratio is

$$\frac{\sigma 2'}{\sigma 1'} = \frac{\mu p2\ C' \frac{\sqrt{\pi}}{2}\ e^{\delta 2}}{\mu p_1\ C' \frac{\sqrt{\pi}}{2}\ e^{\delta 1}} = \frac{\mu p2}{\mu p1}\ e^{\Delta E_D / KT} \qquad (6A)$$

Consequently, the true conductivity ratio in terms of measured parameters becomes

$$\frac{\sigma_2}{\sigma 1} = \frac{\sigma 2'}{\sigma 1'} \frac{C'\ {}^{2}/_{3}\ (\delta_2)^{3/2}}{C' \frac{\sqrt{\pi}}{2}\ e^{\delta 2}} \qquad (7A)$$

$$\frac{\sigma_2}{\sigma_1} = \frac{4}{3\sqrt{\pi}} \frac{\mu p2}{\mu p1} \frac{(\delta_2)^{3/2}}{e^{\delta 2}}\ e^{\Delta E_D / K_T}$$

APPENDIX B

Experimental Data and Conductivity Determination of Semiconductors With Clean Surfaces

The values of the absorption coefficients as calculated from measured data, the absorption curves, and the resulting associated electrical conductivities for six clean silicon samples are presented in this appendix.

The six silicon p-type (111) wafers of 20 mil thickness were obtained from the Montsanto Corporation. The wafers were measured by them and then again independently by the Radio Corporation of America with significant differences of up to 70% in the measured values. The measurements were made by four point probe by both companies under the same test conditions. The values of conductivities as obtained optically are compared with the two four point probe measurements and are presented in Table 3B.

The surfaces of the six highly polished wafers were carefully prepared so as to remove contaminants and oxide layers. Each sample was first given a detergent both of distilled water and alconox for 20 minutes. It was then rinsed well in a distilled water bath and blot dried with lens tissue. A 10 minute etch in a 15 to 1 distilled water to hydroflouric acid solution was then followed by several distilled water baths and finally dried by lint free lens tissue. The optical measurements were begun within 5 minutes after the wafer had been dried. The process consisting of the etch and the optical measurements was completed on each wafer before the process was repeated on the next wafer.

The values of the absorption coefficients for the clean surfaces as determined from the measured optical constants (see Section 2.5 (a)) are given in Table 1B. Measurements on the wafers prior to cleaning were also taken, but the results are not included in this Appendix because the surface condition was not known. The wafers had shelf lives ranging from three months to three years with exposure to differing environments. In all cases, the absorption curve was lower after the surface preparation, but the decrease varying significantly from one wafer to the other with decreases by as much as 50%.

The cleaned surfaces served as a basis of comparison for the six wafers. The absorption coefficients given in Table 1B indicate that the values increase as the nominal resistivity (measured by Montsanto) decreases. This is in accordance with theoretical predictions.

The values of the absorption coefficient as a function of photon energy are plotted for each wafer and the results are given in figures 1B, 2B, and 3B. In all of the six curves, there is a noticeable change in slope at a photon energy, $h\nu$ of 2.48 ev which agrees with the energy necessary for the onset of direct transition. This slope change was not observed for the two samples (0.005 and 50 ohm-cm) in the main text of the thesis, because of the surface oxides. However, further calculations to determine the electrical conductivity were unaffected because of the equal surface oxide films.

The graph of Figure 1B shows the absorption curve for the sample known to be 95 ohm-cm (by four point probe) and used as a reference. Comparison between the reference curve and the 0.063 ohm-cm (nominal resistivity by Montsanto using the four point probe) results in a value of 0.07 ohm-cm as shown in Table 3B. Resistivities of the other four silicon samples as obtained by comparison to the reference curve

(95 ohm-cm) are also given in Table 3B. The calculations are made using equation (141) which applies for all the silicon wafers except the value of 0.01 ohm-cm resistivity. The 0.01 ohm-cm sample was found to be degenerate (see Table 3B and Figure 4B) so that equation (7A) derived in Appendix A is applicable. The values of the mobilities at room temperature are readily available from any standard semiconductor handbook. Some values covering the resistivity range of the samples are given in Table 2B. The mobilities are selected so that they correspond to the nominal resistivities. The displacement between the reference curve (95 ohm-cm) and the unknown curve is given by ΔE_D and is taken in the region where the transitions are indirect. The reason for selecting this region is that the experimental curve for photon energies between 1.98 ev and 2.48 ev closely follows the square low predicted theoretically. Energies above 2.48 ev involve the addition of both direct and indirect contributions. This results in the sum of an absorption coefficient which follows a one half power law and one which obeys the square law (see 2.3 (c), (d) and figure 17). The increase in α for energies above but near the direct gap is very large (see equation (159)). This makes it difficult to determine the exact relationship of this part of the curve.

The calculations show that the optical method is in reasonable agreement with measurements taken by the four point probe. There is some degree of error which can be attributed to system error and surface effects. Table 4B presents the comparison of the results using the optical method and the four point probe.

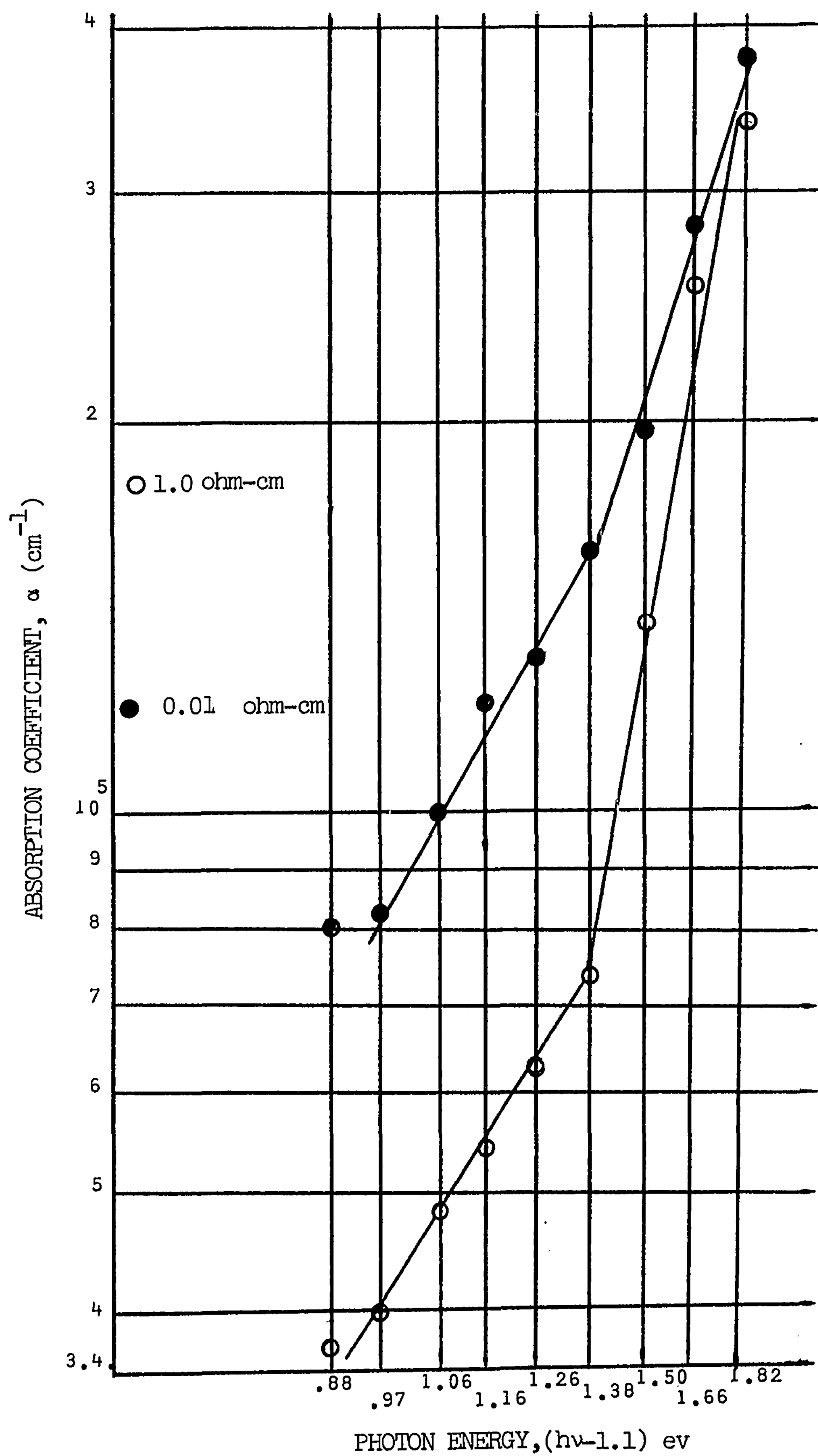

Figure 1B Absorption curves for Nominal Resistivties of 1.0 ohm-cm and 0.01 ohm cm.

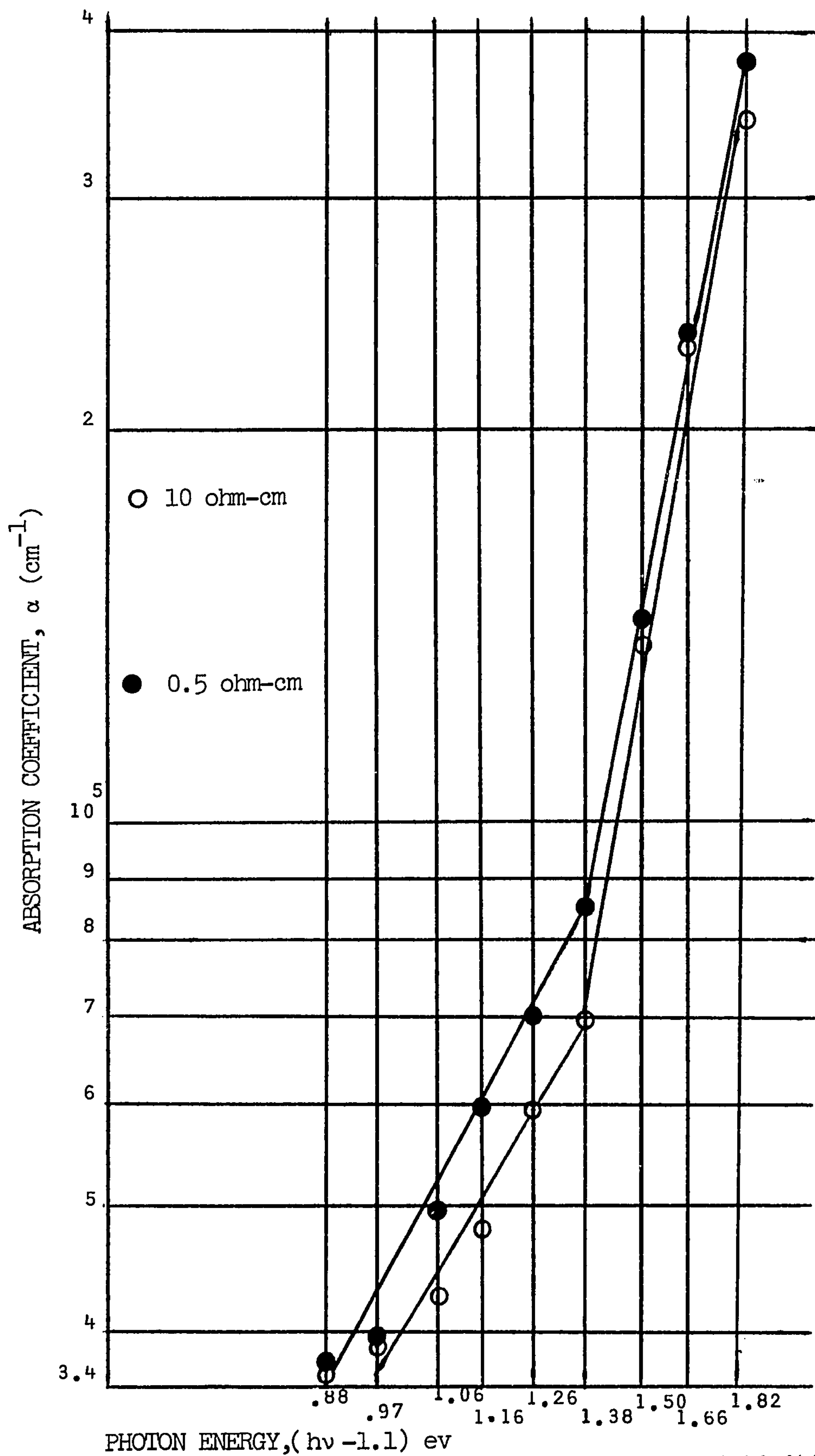

Figure 2B Absorption curves for Nominal Resistivities of 10 ohm-cm and 0.50 ohm-cm.

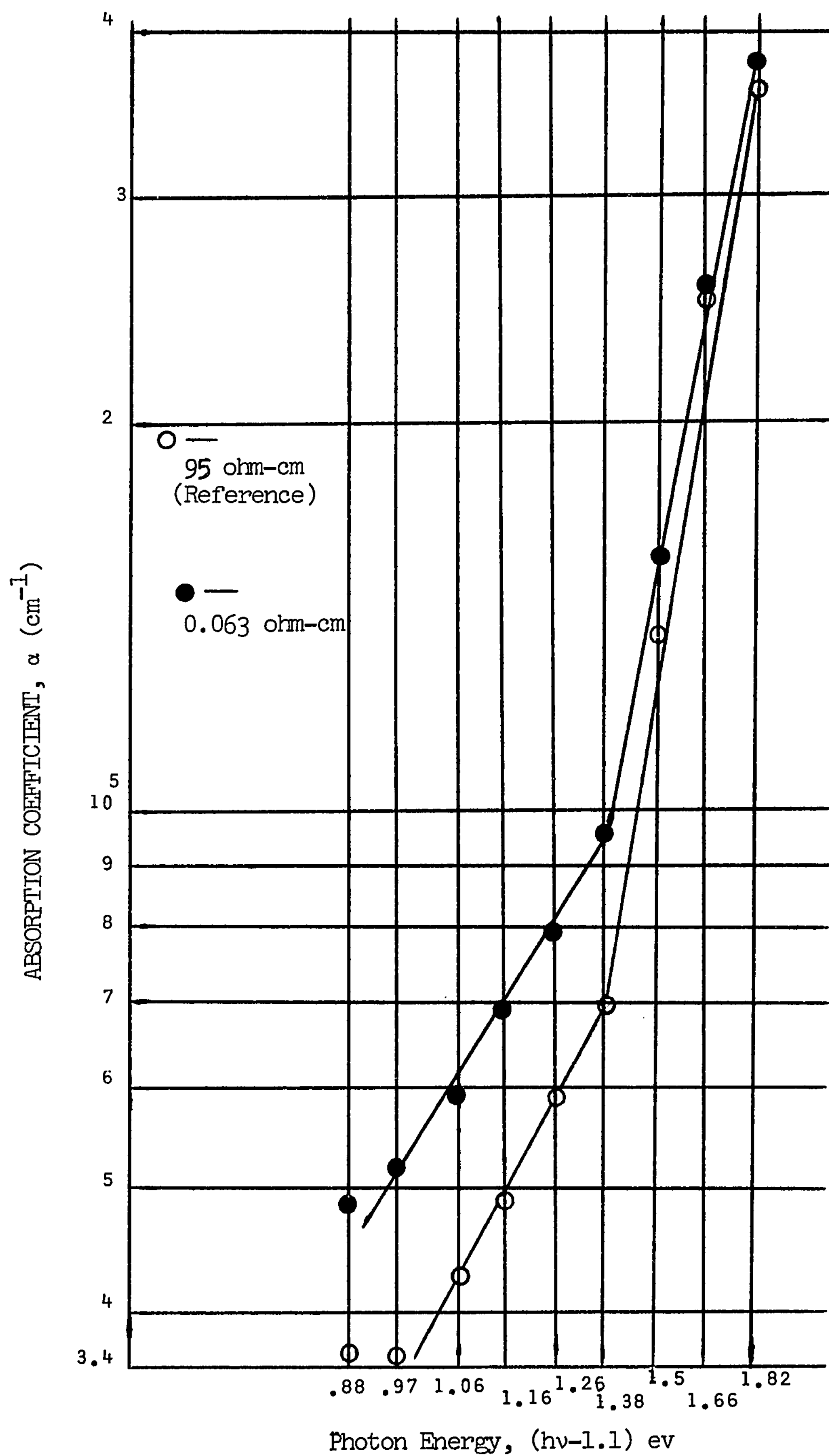

Figure 3B Absorption curves for Nominal Resistivities of 95 ohm-cm and 0.063 ohm cm.

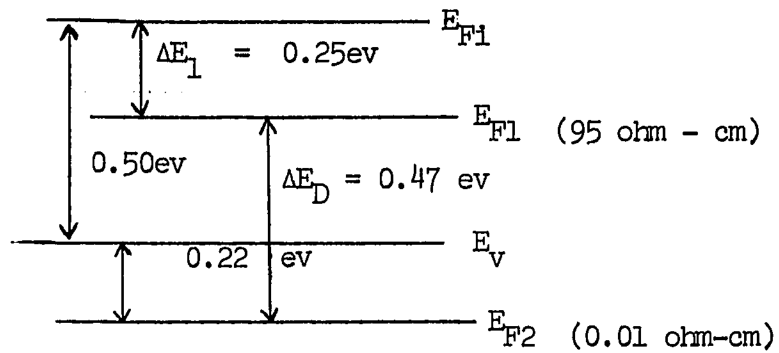

FIGURE 4B Energy band diagram for silicon assuming some band shrinkage in the degenerate case (E_G = 1.0 ev). The value of $\delta = \frac{.22}{KT} \simeq 9$ at room temperature. The value of ΔE, is found using equation (132).

TABLE 1B

	Nominal Resistiuity (ohm-cm)					
	95	10	1.0	0.5	.063	.01
$h\nu$-1.1 (ev)	Absorption Coefficient, α (10^4 cm^{-1})					
.88	3.6	3.6	3.6	3.6	4.9	8.1
.97	3.5	3.8	3.8	3.8	5.1	8.4
1.06	4.3	4.4	4.5	4.9	5.8	11.2
1.16	4.7	4.7	5.2	5.9	6.8	13.4
1.26	5.9	5.9	6.1	7.0	7.9	14.5
1.38	7.1	6.9	7.2	8.3	9.3	15.8
1.51	12.4	12.7	12.6	12.4	14.9	20.4
1.66	24.3	22.3	24.7	23.0	24.1	28.7
1.82	33.7	32.7	33.1	36.6	35.8	35.6

TABLE 2B

ρ(ohm-cm)	N_A (cm^{-3})	μp (cm^2-v^{-1} s^{-1})
100	10^{14}	500
10	10^{15}	450
1	2×10^{16}	350
0.1	4×10^{17}	200
0.01	10^{19}	50

TABLE 3B

ΔE_D (ev) (a)	ρ(ohm-cm) calculated (b) optical method	ρ(ohm-cm) Nominal Resistivity
.01	52	10
.09	3.2	1.0
.12	1.1	.5
.22	.07	.063
.47	.006	.01

(a) ΔE_D is the displacement from the reference curve (95 ohm-cm) to the unknown resistivity curve.

(b) The value of KT is taken as 0.025 ev.

TABLE 4B

Four Point Probe		Optical Method
Monsanto	RCA	
ρ (ohm-cm)	ρ (ohm-cm)	ρ (ohm-cm)
95	60	95
10	9.7	52
1.0	.89	3.2
0.5	.37	1.1
0.063	.064	.07
0.01	.017	.006